

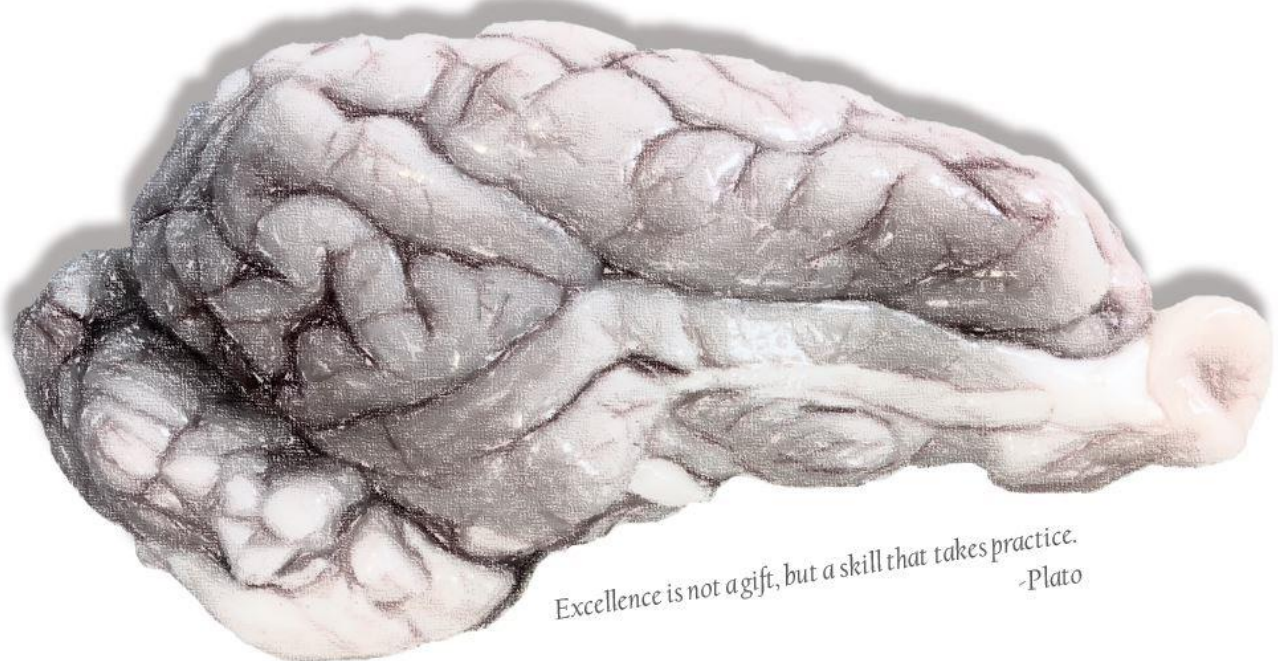


PhD Thesis

Lene Lundgaard Donovan, M.Sc.

Epigenetic and pharmacological investigations of the pig brain

In vivo and *in vitro* studies of
[¹¹C]Martinostat and psilocybin



Excellence is not a gift, but a skill that takes practice.
-Plato

Ph.D. Thesis

Epigenetic and pharmacological investigations of the pig brain

In vivo and *in vitro* studies of [¹¹C]Martinostat and psilocybin

by

Lene Lundgaard Donovan, M.Sc.

Neurobiology Research Unit
Copenhagen University Hospital Rigshospitalet

Faculty of Health and Medical Sciences
University of Copenhagen

For Ellinor & Frederik
Winners never quit
Quitters never win

Title: Epigenetic and pharmacological investigations of the pig brain
In vivo and *in vitro* studies of [¹¹C]Martinostat and psilocybin

Author: Lene Lundgaard Donovan

Department: Neurobiology Research Unit, Department of Neurology
Copenhagen University Hospital Rigshospitalet, Denmark

Institution: Faculty of Health and Medical Sciences
University of Copenhagen, Denmark

Date of submission: March 1st 2020

Date of defense: September 11th 2020

Principal supervisor: Professor Gitte Moos Knudsen
Copenhagen University Hospital Rigshospitalet, Denmark

Co-supervisors: Associate Professor Jacob M Hooker
Massachusetts General Hospital, Massachusetts, USA

Hanne D Hansen, PhD
Copenhagen University Hospital Rigshospitalet, Denmark

Review committee: Associate Professor Birgitte R Kornum (chairperson)
Department of Neuroscience
University of Copenhagen, Denmark

Associate Professor Anne M Landau
Department of Nuclear Medicine and PET
Aarhus University, Denmark

Professor Charles D Nichols
Department of Pharmacology and Experimental Therapeutics,
Louisiana State University, New Orleans, USA



PREFACE

The present PhD thesis represents the outcome of a 3-year PhD programme at the Graduate School of Neuroscience, University of Copenhagen, made financially possible by a PhD scholar stipend from the Lundbeck Foundation. The work was carried out in October 2015 – January 2016, October 2016 – December 2017 and September 2018 – February 2020 primarily at the Neurobiology Research Unit under the supervision of Professor Gitte Moos Knudsen and Dr. Hanne Demant Hansen.

This thesis is based on the following manuscripts, which will followingly be referred to by their roman numerals:

- I. **LL Donovan**, JH Magnussen, A Dyssegaard, S Lehel, JM Hooker, GM Knudsen, HD Hansen. Imaging HDACs *In Vivo*: Cross-Validation of the [¹¹C]Martinostat Radioligand in the Pig Brain. *Mol Imaging Biol* 2020 22(3):569-577.
- II. **LL Donovan**, JV Johansen, NF Ros, E Jaber, K Linnet, S Johansen, B Ozenne, S Issazadeh-Navikas, HD Hansen, GM Knudsen. Effects of a single dose of psilocybin on behaviour, brain 5-HT_{2A} receptor occupancy and gene expression in the pig. *Manuscript in revision*.

TABLE OF CONTENTS

PREFACE.....	5
TABLE OF CONTENTS.....	6
ENGLISH SUMMARY	9
DANSK RESUMÉ.....	11
ACKNOWLEDGEMENTS.....	13
ABBREVIATIONS	15
1. INTRODUCTION.....	17
1.1 The serotonin system	17
1.1.1 The cerebral 5-HT _{2A} R.....	18
1.1.2 The involvement of 5-HT _{2A} R in psychiatric disease	19
1.1.3 Psychedelic agents	20
1.1.4 Psilocybin as a treatment option.....	21
1.2 Epigenetic principles	22
1.2.1 Histone modifications	23
1.2.2. Epigenetics in psychiatric disorders	24
1.2.3. Investigating epigenetics <i>in vivo</i>	24
1.3 Investigating epigenetic changes following psilocybin administration	25
2. AIMS AND HYPOTHESES.....	27
3. METHODS	29
3.1 The pig in biomedical research	29
3.1.1 Establishing a large animal model for administration of psilocybin	29
3.2 Positron Emission Tomography	30
3.2.1 Principles of PET	30
3.2.2 PET data acquisition	32
3.2.3 PET data quantification	32
3.3 Western blotting.....	34
3.3.1 Principles of western blotting	34
3.3.2 Stain Free® wb.....	35
3.4 RNA sequencing	35
3.4.1 Principles of SBS.....	36
3.4.2 RNA sequencing data acquisition.....	36

4. RESULTS & DISCUSSION	39
4.1 Histone deacetylase 1-3 in the pig brain.....	39
4.1.1 Evaluation of the [¹¹ C]Martinostat radioligand in the pig brain	39
4.1.2 Kinetic modelling and simplified quantification of [¹¹ C]Martinostat	40
4.1.3 <i>In vivo/in vitro</i> correlations of HDAC1-3 protein levels	41
4.1.4 VPA as competitor to [¹¹ C]Martinostat.....	42
4.2 <i>In vivo</i> and <i>in vitro</i> effects of psilocybin in pigs	44
4.2.1 Characterization of the porcine behavioural response to psilocybin	45
4.2.2 Ketanserin as inhibitor of psilocybin induced behaviour	46
4.2.3 Cerebral transcriptomic changes following psilocybin exposure	47
4.2.4 A single psilocybin exposure does not alter histone deacetylase 1-2	49
5. LIMITATIONS.....	51
6. CONCLUSIONS AND FUTURE DIRECTIONS	55
7. REFERENCES.....	57
PAPER I	65
PAPER II.....	77
DECLARATIONS OF CO-AUTHORSHIP.....	105

ENGLISH SUMMARY

The serotonergic (5-HT) system is pivotal in modulating behavioural and cognitive functions. Accordingly, dysfunctions of the system have been implicated in the pathophysiology of multiple neuropsychiatric disorders. Recent evidence suggests that use of psilocybin – a classic psychedelic and 5-HT_{2A} receptor agonist – can have long term beneficial effects on mood and behaviour. However, the molecular processes by which psilocybin induces its lasting effects are unknown.

We used pigs as a large animal model to investigate *in vivo* and *in vitro* status of molecular targets.

The aim of the present thesis was to 1) evaluate the positron emission tomography (PET) radioligand [¹¹C]Martinostat, 2) establish the pig as a large animal model of an acute psilocybin-induced psychedelic experience in humans and, 3) investigate molecular mechanisms underlying the sustained effects induced by a single dose of psilocybin.

[¹¹C]Martinostat PET is supposed to visualise histone deacetylase 1-3 (HDAC1-3) proteins *in vivo*, and we determined a wide distribution and slow kinetics of the radioligand in pig brain.

[¹¹C]Martinostat had an excellent signal to noise ratio, and since no brain region was devoid of target, we suggested to use olfactory bulbs as reference region in pigs. We found the Ichise multilinear analysis 1 to be the most accurate kinetic model but also that the standardised uptake value ratio (SUVR) correlated significantly with *in vitro* measured HDAC1-3 protein levels. We used valproic acid to validate HDAC inhibitory activity in the pig brain. We recommended SUVR of [¹¹C]Martinostat as a useful proxy for cerebral HDAC1-3 levels *in vivo*.

We then established a model with psilocybin administration to awake pigs. This involved determination of which dose of psilocybin was associated with plasma psilocin concentrations and cerebral 5-HT_{2A} receptor occupancy in the same order of magnitude as in people with a psilocybin-induced intense psychedelic experience. We also characterized the behavioural response of pigs to psilocybin; it included headshakes, scratching and rubbing behaviour. We found that the transcriptomic profile in prefrontal cortex at 1 day or 1 week post-psilocybin only exhibited subtle changes, without any evidence of synaptic plasticity or epigenetic regulation. However, multiple inflammatory pathways were altered 1 week after psilocybin exposure, in consistency with a prevailing theory of neuroinflammation being critically involved in many psychiatric disorders.

In summary, we provide the first cross-validation of the [¹¹C]Martinostat radioligand and found that the *in vivo* SUVR correlates well with *in vitro* levels of HDAC1-3, making it a useful tool for epigenetic investigations of the living brain. Furthermore, we established and characterized a porcine model of psilocybin administration. Our data did not provide direct evidence for specific molecular mechanisms but suggests that neuroinflammation is an underlying mechanism involved in the sustained effects of psilocybin in humans.

DANSK RESUMÉ

Serotonin (5-HT) systemet spiller en afgørende rolle i reguleringen af psykofysiologiske funktioner, og dysfunktion af 5-HT systemet ses ved adskillige neuropsykiatriske sygdomme, herunder depression. Nyere forskning viser at psilocybin – et psykedelisk stof, hvis nedbrydningsprodukt stimulerer 5-HT_{2A} receptoren – kan have langvarig positiv indvirkning på humør og adfærd hos mennesker. Denne PhD-afhandling tilsigter ved hjælp af forsøg i grise at afklare de underliggende molekulære hjernemekanismer af psilocybins langtidseffekter.

Formålet med denne PhD afhandling var 1) at evaluere sporstoffet [¹¹C]Martinostat med positron emissionstomografi (PET) som mål for hjernens indhold af proteinerne histon deacetylase 1-3 (HDAC1-3), 2) at etablere grisen som en stor dyremodel for at efterligne situationen hos mennesker, der har indtaget psilocybin og, 3) at undersøge hvilke molekulære mekanismer i hjernen, der kan ligge til grund for psilocybins blivende effekter på personlighed. Ved PET fandt vi at [¹¹C]Martinostat blev taget let op af grisehjernen, hvorefter det blev udskilt relativt langsomt. [¹¹C]Martinostat havde et godt signal:baggrundssignal som kunne blokeres i alle hjerneregioner. Med anvendelse af lugtekolberne som referenceregion uden (HDAC1-3), påviste vi at den såkaldte Ichise multilineær model 1 var dén kinetiske model, der gav det bedste fit til data. Ved at validere PET målingerne overfor målinger af HDAC1-3 i det udtagne hjernevæv kunne vi dog vise at en simplere metode, nemlig det såkaldte SUVR, afspejlede HDAC1-3 niveauerne bedre. Vi undersøgte også effekten af valproat på [¹¹C]Martinostat bindingen, og påviste at valproat havde den forventede hæmmende effekt på HDAC aktiviteten i grisehjernen.

Dernæst definerede vi hvilken dosis af psilocybin, der skulle gives til grise for at opnå effekter sammenlignelige med mennesker. Denne dosis blev etableret på baggrund af sammenligninger med hensyn til grisens adfærd efter psilocybin injektion, plasma psilocin koncentration over tid og størrelsen af 5-HT_{2A} receptor-okkupansen i grisens hjerne. Efter indgift af psilocybin udviste grisene karakteristisk adfærd med kraftig rysten af hovedet, kradsen med bag- og forben samt gniden sig imod genstande. Noget overraskende fandt vi kun minimale ændringer i hjernens genekspression, såvel 1 dag som 1 uge efter psilocybin. Vi fandt heller ikke noget holdepunkt for ændret synaptisk plasticitet eller epigenetisk regulering. Generelt sås de inflammatoriske gener dog ændret 1 uge efter psilocybin administration, hvilket er

overensstemmende med opfattelsen af neuroinflammation som en vigtig komponent ved mange neuropsykiatriske sygdomme.

Denne afhandling beskriver således den første validering af [¹¹C]Martinostat PET i grisen og det fastslås at SUVR afspejler HDAC1-3 proteinniveauet i hjernen godt og sporstoffet er dermed et værdifuldt redskab i epigenetiske undersøgelser af den levende hjerne. Derudover etableres og karakteriseres en grisemodel for psilocybin-indtag hos mennesker. De molekylære undersøgelser af hjernen peger på effekter af psilocybin på neuroinflammation som en underliggende mekanisme bag de langvarige effekter af indtag af blot en enkelt dosis af psilocybin hos mennesker.

ACKNOWLEDGEMENTS

My outmost gratitude goes to my principal supervisor Gitte – I would never in my wildest dreams have dared to wish for all the things this PhD has taught me. You've enabled me to do great research, and your ever-positive take on results has inspired me to view things from all angles. Thank you for keeping the calm overview and professionally guiding me through tough times.

To my mentor and friend Hanne – words fall short to describe my gratitude for everything you have done for me. Without you this PhD would not have come about. You have picked me up from the depths of despair, you have pushed me to be better, but you have ever-patiently taught me and answered my questions. Everything you have done has enabled me to grow and develop, and although we are now oceans apart, you are the voice inside my head striving for perfection.

To all the people outside NRU who made this work possible; Karsten, Charlotte, Jannie, Embla, Pia, Anne Mette, Szabolcs, Bente, Christina, Anna, Tomas, Jesper, Jacob – thank you for your generous help, flexibility and understanding. It has been a true pleasure working with all of you.

To the most amazing office companions; Annette, Vibeke, Martin S and Nakul – thank you for making every day special, joyful and something to look forward to. Thank you for your never-failing support, you have preserved my mental health for which I will forever be grateful. May many more discussions on everything between heaven and Earth arise in the future. Awesomeness Inc., this was only the beginning of a life-long journey, I can feel it in my heart.

To my partners in crime; Martin KM and Sanjay – thank you for always having back. Martin you are my human encyclopaedia on psychedelics, your dedication and interest for the field is a true inspiration. I could not have wished for a better clinical counterpart to embark on this journey with and I treasure the friendship we have built. Sanjay, you have been my preclinical support-line throughout all of this and I humbly acknowledge all the help you have given me.

To all the past and present NRU members – thank you for the community you’ve built and invited me into. It has been a true pleasure working with all of you and I thank you for the various support you have given me through the years. A special thanks goes to all past and present PhD’s of NRU, you’ve inspired me and taught me great science from so many different aspects. I will carry a piece of each of you with me on my future endeavours.

To my longstanding friends from real life; Thea, Charlotte, Liv, Maja, Linn, Henriette and families – thank you for forcing me out of the scientific bubble and showing me the pleasures and joys of true friendship.

To all the amazing people who have made Copenhagen my home; Emma, Danielle, Maria, Rosa, Helene, Mie, Louise, Sofie and families – without you this city would have been tedious and unmemorable, because of you this is where I call home and will raise my children. A special thanks goes to Emma for constant sanity checks, and to Rosa and Rasmus – you guys are life/marriage saviours, and I will forever be indebted to your generous help and support, one could not have wished for better friends let alone have them as neighbours.

To my family; Danish as well as Kiwi – thank you for your support and for questioning the value of my work in ways that challenged my views. Special thanks go to Mor and Far for supporting my uprooting and always understanding my desire to venture new grounds. Ellinor and Frederik, you’ve given me the true perspective on life and forced me to prioritize what really matters. Chad, my rock, best friend and husband – congratulations on your personal PhD in parenting and housekeeping, and thank you for your everlasting support, genuine interest and wish to understand what it is I actually do. I love you.

Lene Donovan, Copenhagen March 1st 2020

ABBREVIATIONS

1-TC	1 tissue compartment model
2-TC	2 tissue compartment model
5-HT	5-hydroxytryptamine or serotonin
5-HT _{2A} R	5-hydroxytryptamine 2A receptor
5-HT _{1A} R	5-hydroxytryptamine 1A receptor
5-MeO-DMT	5-methoxy-N,N-dimethyltryptamine
AIC	Akaike information criterion
BP _{ND}	Non-displaceable binding potential
cDNA	Complementary DNA
CNS	Central nervous system
DE	Differential expression
DOI	1-(2,5-dimethoxy-4-iodophenyl)-2-amino-propane
ECT	Electroconvulsive therapy
GSEA	Gene set enrichment analysis
H3ac	Acetylated histone 3
H4ac	Acetylated histone 4
HAT	Histone acetyl transferase
HDAC1-3	Histone deacetylase isoform 1, 2, 3
HRRT	High resolution research tomograph
HTR	Head twitch response
LSD	(5R,8R)-(+)-lysergic acid-N,N-diethylamide
MA1	Ichise multilinear analysis 1
mGluR2	Metabotropic glutamate 2 receptor
MRI	Magnetic resonance imaging
PCA	Principal component analysis
PET	Positron emission tomography
RNAseq	RNA sequencing
ROI	Region of interest
RTqPCR	Reverse transcription quantitative polymerase chain reaction
SAHA	Suberoylanilide hydroxamine
SBS	Sequencing by synthesis
SUV	Standardized uptake value
SUVR	Standardized uptake value ratio
TAC	Time-activity curve
V _{ND}	Non-displaceable distribution volume
VPA	Valproic acid, 2-propylpentanoic acid
V _T	Total distribution volume
Wb	Western blotting



1. INTRODUCTION

1.1 The serotonin system

Serotonin is an evolutionary ancient monoamine found in almost all living organisms on Earth, from plants and fungi to bacteria and mammals. It is found both in the periphery and the central nervous system (CNS) of the human body. The substance was first described in 1937 by Vialli and Erspamer¹, but the name stems from the discovery of a substance in serum which had vasoconstricting properties, hence the duality “sero-tonin”². It is estimated that >90% of serotonin is synthesized in the gut, wherefrom it plays a multitude of roles, e.g. peristalsis, pain or nausea perception³. When it was later found in the mammalian brain, the chemical name of 5-hydroxytryptamine (5-HT) became the preferred scientific nomenclature. In the CNS it acts as a neurotransmitter, influencing a wide variety of biological functions including cognitive processes and behaviour^{4,5}.

The essential amino acid tryptophan forms the basis of 5-HT synthesis (fig.1). Tryptophan hydroxylase requires molecular oxygen to form 5-hydroxytryptophan, which is then converted by amino acid decarboxylase and pyridoxal phosphate to 5-HT⁶. The tryptophan hydroxylase enzyme is the rate-limiting step in the synthesis⁷. The serotonergic neurons of the raphe nuclei in the brain stem express the tryptophan hydroxylase enzyme and from here serotonergic projections covers vast areas of the CNS⁸.

Following release from the presynaptic neuron, 5-HT can interact with a multitude of 5-HT receptors, most of which are located on the postsynaptic terminal (fig.1). There are currently 7 known families of mammalian 5-HT receptors (5-HT₁₋₇R), with a total of 14 distinct subtypes⁴. Except for the 5-HT₃R, which is a

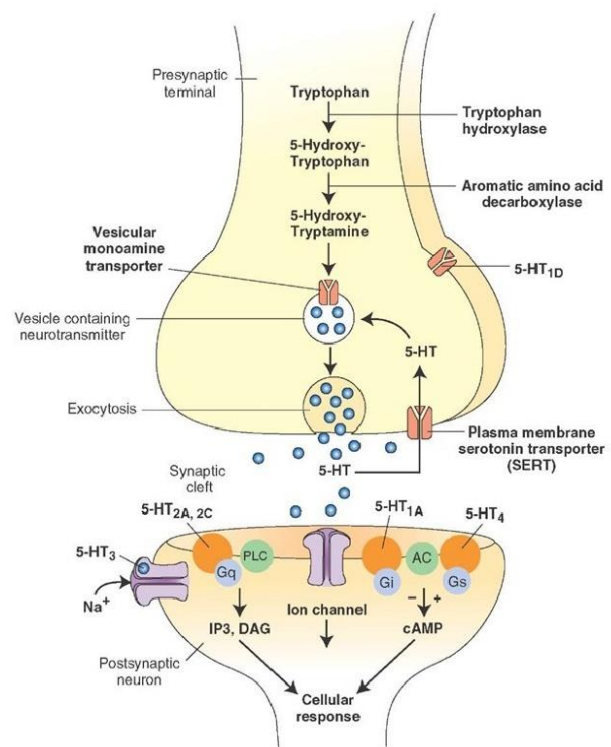


Figure 1 – The serotonin system. Graphical presentation of serotonin synthesis and signalling.¹³¹

ligand-gated ion channel, all 5-HTRs are G-protein coupled receptors, meaning that, upon stimulation by an agonist (e.g. 5-HT) the receptor interacts with a G-protein resulting in various downstream effects. 5-HT₁Rs couple to G_{i/o}, which decreases cAMP; in contrast, 5-HT₄Rs, 5-HT₆Rs and 5-HT₇Rs preferentially couple to G_s which increases cAMP formation upon activation. The 5-HT₂Rs couple to G_{q/11} whereby they, upon activation, increase cytosolic Ca²⁺ concentrations and inositol phosphates. Although 5-HT₅Rs are not new-comers, not much is known about their coupling and function, but they have been suggested to couple to G_{i/o} and inhibit adenylyl cyclase activity⁹.

To regulate the signalling in the synaptic cleft, the serotonin reuptake transporter located on the presynaptic terminal, transports 5-HT back into the presynaptic neuron. Here the neurotransmitter can be stored in vesicles or degraded, which mainly involves the catalyst enzyme monoamine oxidase located on the outer mitochondrial membrane¹⁰.

In the following section, the 5-HT_{2A}R will be described in further detail since this receptor subtype is a major effector site of some pharmacological agents used in the present thesis.

1.1.1 The cerebral 5-HT_{2A}R

In the human brain, the 5-HT_{2A}R is the most abundant excitatory 5-HT receptor and it is crucially involved in a wide variety of executive functions, such as attention, learning and memory¹¹. Macroanatomical studies of the receptor have consistently found it to be most abundant in neocortex, especially the medial- and dorsolateral prefrontal cortices contain high densities of 5-HT_{2A}R¹². Furthermore, subcortical structures, such as the hippocampus and amygdala, also contains 5-HT_{2A}R although to a lesser extent than the cortical regions¹²⁻¹⁴. The microanatomical investigations of the receptor localization has revealed an interesting banded pattern, corresponding to the cytoarchitectural organization of various cortical areas. The receptor is most prominently found on proximal apical dendrites of pyramidal neurons in layer V.¹⁵⁻¹⁷ However, the 5-HT_{2A}R also localizes to multiple other cell types, such as GABAergic interneurons as well as non-pyramidal cells^{4,17}.

Drugs acting on the 5-HT_{2A}R can display functional selectivity by activating various intracellular signalling pathways. The most well-studied 5-HT_{2A}R signalling pathway is through the G_{q/11} proteins, which activates phospholipase C, which in turn promotes the release of diacylglycerol and inositol phosphates, thereby stimulating protein kinase C activity and increasing intracellular Ca²⁺ concentration¹⁸. However, signalling through G_{i/o} proteins can activate

phospholipase A₂, which in turn causes a build-up of intracellular arachidonic acid¹⁹. Furthermore, signaling through calmodulin and JAK/STAT pathways have also been described^{20,21}, demonstrating a complexity of signalling cascades ultimately leading to specific neuronal activation and gene expression changes^{4,21}.

An interesting feature of the 5-HT_{2A}R is the localization of the receptor in multiple cellular compartments, i.e. the plasma membrane and intracellular vesicles²¹. A large fraction of receptors is located intracellularly, where they are thought to serve as a reservoir ready for trafficking to the plasma membrane. Furthermore, a feature of the 5-HT_{2A}R is rapid internalization upon ligand interaction – agonist as well as antagonist^{21,22}, possibly also playing a role in mediating the vast array of downstream effects initiated by receptor activity.

1.1.2 The involvement of 5-HT_{2A}R in psychiatric disease

Since the 5-HT_{2A}R is involved in many functions essential to human behaviour, it also plays a role in a multitude of neurological as well as psychiatric disorders, such as Parkinson's disease, addiction, schizophrenia and depression^{8,11}. The serotonin hypothesis of schizophrenia was posited decades ago, when psychedelic intoxication was believed to bear resemblance to psychotic behaviour. Today, however, psychosis is more seen as a result of dopaminergic hyperfunction²³, rather than serotonin dysregulation. It has been suggested that 5-HT_{2A}R agonism better represents acute-phase schizophrenia, rather than the chronic-state, due to the switch from hyperfrontality to hypofrontality²⁴. Furthermore, up to a third of schizophrenic patients do not respond sufficiently to dopaminergic treatment, whereas atypical antipsychotic medication, which antagonizes both dopamine D₂ and 5-HT_{2A}R, alleviates multiple symptom aspects of schizophrenia²⁵. Although the aetiology of 5-HT_{2A}R in schizophrenia is not fully understood, large reductions of 5-HT_{2A}R densities in frontal cortex have been found in drug-naïve first-episode schizophrenics²⁶, as well as individuals at high risk of developing psychosis²⁷.

The post-World War II pharmacology research also led to the serendipitous discovery of antidepressant effect of antihistaminergic and antitubercular agents. This led to the catecholamine²⁸ and later the monoaminergic hypothesis of depression²⁹, suggesting that monoaminergic deficiency is the cause of major depressive disorder. Numerous molecular neuroimaging studies have investigated the 5-HT_{2A}R levels of depressed patients vs healthy controls, however, the results are inconclusive and vary from increased, unchanged to

decreased receptor levels (reviewed by Savitz³⁰). Interestingly, the personality trait neuroticism, a well-known risk factor of major depression, is positively correlated to 5-HT_{2A}R levels³¹. In human patients, the role of single-nucleotide polymorphisms (SNPs) of the 5-HT_{2A}R gene is a field of intense studies, with researchers attempting to identify the underlying genetic predisposition to depression³². Interestingly though it was recently found that various 5-HT_{2A}R SNPs does not associate with *in vivo* receptor levels measured by positron emission tomography (PET)³³.

1.1.3 Psychedelic agents

In 1957 Humphrey Osmond coined the term 'psychedelics' to describe a group of substances which had 'mind-manifesting' capabilities³⁴. Several decades later, a very extraordinary definition of the compounds was proposed by Dr. Jaffe: "the feature that distinguishes the psychedelic agents from other classes of drug is their capacity reliably to induce states of altered perception, thought, and feeling that are not experienced otherwise except in dreams or at times of religious exaltation."³⁵ Naturally occurring psychedelics have been used in ritual ceremonies or religiously for centuries, but modern psychedelic research was initiated by the synthesis of (5R,8R)-(+)-lysergic acid-N,N-diethylamide (LSD-25, also known as LSD or "acid") in 1938 by Albert Hofmann – although the later extremely famous psychoactive properties were not recognized until 1943³⁶. Serotonin was discovered in the mammalian brain in 1953³⁷, and the chemical scaffold similarities between LSD and serotonin was quickly recognized (fig.2), initiating the modern era of serotonin research³⁷.

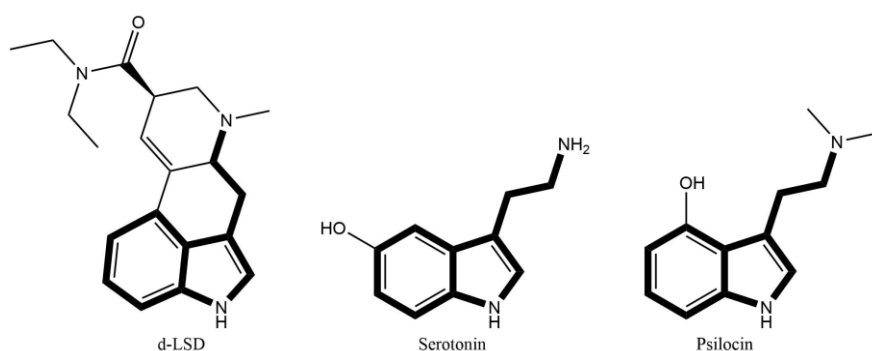


Figure 2: Chemical structures of LSD, serotonin and psilocin.
Bold lines mark similarities between the three compounds.

Psychedelics induce their psychoactive properties by activating the 5-HT_{2A}R – especially the receptors located on cortical pyramidal neurons are critical for the hallucinogenic experience³⁸. Many other substances are capable of inducing hallucinations, e.g. ketamine and opioids, but the primary mode of action of these compounds is not 5-HT_{2A}R activation – a defining feature of psychedelics. The scope of the present thesis will be limited to the so-called classic psychedelic, psilocybin and its active metabolite psilocin (fig.2).

Psilocybin is a naturally occurring psychedelic found in some species of mushrooms, hence the popular name ‘magic mushrooms’. Although it has been used by indigenous populations for millennia, the scientific era of psilocybin coincide with that of LSD and serotonin^{35,39}. Psilocybin is a pro-drug that *in vivo* dephosphorylates to the active compound, psilocin. Psilocin is an agonist at several 5-HT receptors, but most important is the 5-HT_{2A}R as responsible facilitator of the psychedelic experience in humans and 5-HT_{2A}R-mediated behaviour in animals³⁸. From mice studies, there is some evidence that psychedelic 5-HT_{2A}R stimulation mediated effects also involves the metabotropic glutamate 2 receptor (mGluR2)⁴⁰. By means of 5-HT_{2A}R knock-out mice, the cortical pyramidal neurons have been shown to be crucial for psychedelic behaviour as well as specific gene expression profiles³⁸. Induction of *c-fos* gene expression is often used as proxy for neuronal activation, however, *egr2* induction has been proposed to distinguish receptor activation by psychedelic vs non-psychedelic compounds³⁸ but this finding needs to be validated.

1.1.4 Psilocybin as a treatment option

Psilocybin has an interesting pharmacological profile as it is not addictive, generally well tolerated, and produces psychedelic effects for only 4-6 hours after oral administration^{41,42}. Conversely, an intravenous (i.v.) dose produces immediate effects which only lasts ~20 min^{41,43}. In healthy humans, psilocybin has been shown to induce lasting psychological effects. Griffiths and colleagues have on numerous occasions found that personality traits, which are otherwise considered stable in adulthood, change after a single psilocybin exposure⁴⁴⁻⁴⁷.

During the early years of psychedelic research, a vast amount of scientific reports showcased the therapeutic efficacy of these compounds, however, legislative restrictions delayed further explorations for decades³⁵. In recent years, small-numbered clinical trials have documented the efficacy of psilocybin-assisted psychotherapy towards a wide spectre of psychiatric disorders including substance addiction^{48,49}, treatment-resistant depression⁵⁰ and anxiety⁵¹.

The treatment effect of psilocybin is three-fold: single dosage, rapid onset of action, and sustained improvements. This is unparalleled by any known psychiatric pharmaceutical and have left scientists puzzled as to the mechanism of action. A very intriguing feature of psilocybin is the mismatch between the duration of pharmacological receptor activity and the sustained therapeutic effects. In order for a drug to have such long-lasting effects, far after it has been metabolized and excreted by the body, it is likely that plasticity or epigenetic mechanisms play a role.

1.2 Epigenetic principles

The term “epigenetic” was first coined by Waddington in 1942 when he observed phenotypic changes in the fruit fly’s wing development which he attributed to changing genotypic expression⁵². Epigenetics have later been defined as heritable changes which are not caused by altered genotype. However, the heritable aspect has lately been discussed widely, since many epigenetic marks are dynamic and constantly changing in response to external stimuli.

Epigenetic mechanisms can broadly be divided into three categories: DNA methylation, histone modifications and RNA mechanisms (fig.3); having two types of effect: establishing a global chromatin environment or directing DNA-based biological tasks^{53,54}. DNA methylation denotes the addition of a methyl group to a cytosine base, generally viewed as a very stable inhibitor of gene expression. However, emerging evidence suggest DNA methylation is in fact dynamic and can be, depending on the genetic location, either repressive or permissive⁵⁵. DNA methylation is most often located in so-called CpG islands where a cytosine followed by a guanine is more prevalent than average. Histone modifications denote the covalent binding of a wide variety of chemical groups to the N-terminal tails of histone proteins protruding from the nucleosome core (fig.3). Histone modifications will be explored in more detail below. RNA-based epigenetic mechanisms are the effects that non-coding RNAs exert on the chromatin structure, e.g. coordinating other epigenetic mechanisms⁵⁶.

These epigenetic mechanisms work in concert to create overall chromatin environments such as inactivation of an entire chromosome, e.g. X-chromosome silencing in females. They also orchestrate the genetic basis of biology by rendering the genetic code (un)available to effector proteins based on external stimuli⁵⁴.

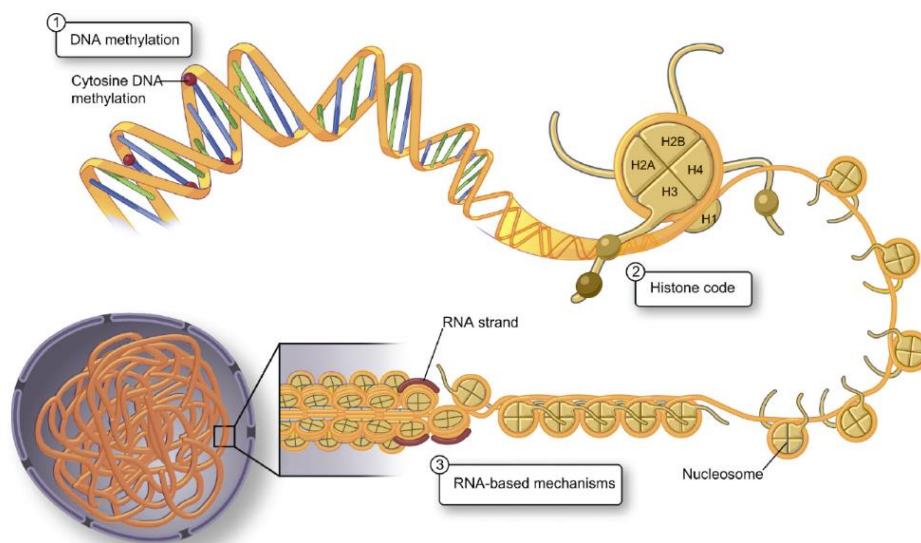


Figure 3 – Stepwise compaction of DNA into the cell nucleus. Chromatin structure indicating epigenetic modifications sites. Modified from ⁵⁷.

1.2.1 Histone modifications

Each cell of the body contains ~2.5m of DNA. To fit inside the cell nucleus, DNA needs to be compacted enormously while maintaining accessibility for the transcriptional machinery. The nucleosome is the answer to both requirements (fig.3). A nucleosome consists of an octamer of 2x four histone proteins (H2A, H2B, H3 and H4) with DNA wrapped around it giving it the microscopic appearance of beads on a string. The N-terminals of the histone proteins protrude from the nucleosome and are subject to vast amounts of chemical modifications. More than 60 modifications have been described, including the well-established acetylation (ac), methylation and phosphorylation^{54,58} – however, the scope of the present thesis will pertain to acetylation only.

Two groups of proteins are responsible for the addition or removal of acetyl groups from lysine residues, namely histone acetyltransferases (HATs) and histone deacetylases (HDACs), respectively (fig.4). HAT proteins can be divided into 3 superfamilies: GNAT, MYST and p300/CBP, all of which transfer an acetyl group from acetyl-CoA to a histone lysine residue⁵⁹. HDACs confine to 4 classes (I-IV) based on sequence homology, and are either zinc- or NAD⁺-dependent for their enzymatic activity⁶⁰. Histone acetylation levels are positively associated with gene transcription whereas decreased acetylation implies a transcriptionally silent region⁵⁹. The covalent addition of an acetyl group to a lysine residue enables transcription by

1) lowering the electrochemical bond between DNA and histone proteins, thereby loosening the chromatin structure and, 2) acting as binding site for bromodomain-containing transcription factors⁵⁹.

In the CNS, histone acetylation status has been associated with various diseases, and pharmaceuticals targeting the HAT/HDACs are currently being tested for therapeutic efficacy⁶⁰⁻⁶². Some well-known drugs, such as valproic acid (VPA) are experiencing a renaissance due to the discovery of their epigenetic modulatory effect. VPA has long been used as an anti-convulsant in epilepsy but since the discovery of its ability to inhibit HDACs, it has been tested as adjuvant treatment in multiple settings⁶³⁻⁶⁵. Although the mechanism of action is unclear, VPA is a pan-inhibitor of class I and IIa HDACs (including HDAC1-3), causing hyperacetylation of histones leading to increased gene expression⁶⁶.

1.2.2. Epigenetics in psychiatric disorders

Epigenetic regulation underlies all transcriptional activity and is believed to be the biological mediator of external stimuli. Therefore, epigenetic alterations is naturally found to play crucial roles in multiple disorders, including psychiatric disorders such as depression where environmental factors are key⁶⁷. Improved treatment outcomes in schizophrenic patients have been reported when atypical antipsychotic medication is given in conjunction with HDAC inhibitors such as VPA^{65,68}. The mGluR2 is a potential mediator of this treatment efficacy. Mice treated with chronic clozapine had decreased gene expression of both 5-HT_{2A}R and mGluR2 due to decreased H3ac established by HDAC2 through a 5-HT_{2A}R-dependent mechanism⁶⁹.

1.2.3. Investigating epigenetics *in vivo*

Although epigenetics is now recognised for its role in multiple disorders, the study of epigenetic changes depended on *in vitro* methodologies applied to tissue samples. Therefore, studies of

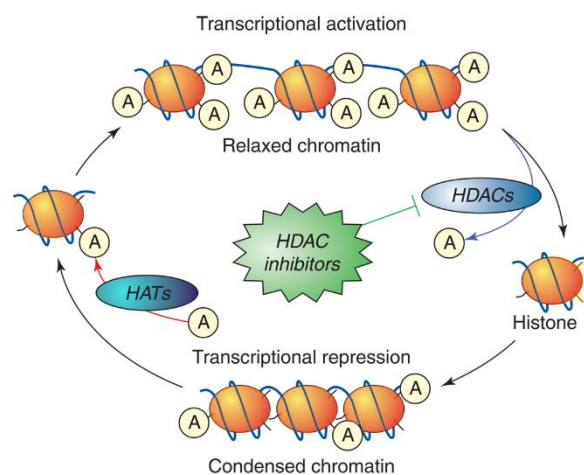


Figure 4 - Histone acetylation. Histone acetyltransferases (HATs) activate transcription by addition of acetyl groups to histone lysine residues. Histone deacetylases (HDACs) repress transcription by removal of acetyl groups. Modified from⁶⁶

epigenetic changes in the CNS was until recently limited to animal models or post-mortem human tissue. Several PET radioligands have been developed with the aim to visualise the cerebral HDAC1-3 protein levels *in vivo*. Some of them have limitations; both [¹⁸F]SAHA and [¹¹C]MS-275 have low blood-brain-barrier penetrance^{70,71}, and [¹⁸F]FAHA is rapidly metabolised⁷². While [¹¹C]Martinostat has good brain penetrance and high affinity for class I HDACs, it also has minimal off-target binding, an important prerequisite for a good PET radioligand^{62,73,74}. [¹¹C]Martinostat imaging has revealed regional as well as sex and age differences in HDAC protein levels in the living human brain^{75,76}. Although the radioligand has been applied in several species and even in patients and controls^{62,74-78}, a direct validation between *in vitro* and *in vivo* findings had not been done. The validation of [¹¹C]Martinostat is part of the present PhD-thesis⁷⁴.

1.3 Investigating epigenetic changes following psilocybin administration

Psilocybin has been shown to induce lasting beneficial effects in both health and disease. However, the mechanisms by which this compound asserts its lasting effects and which molecular processes are involved are unknown. For a drug to have such long-lasting effects, far after it has been metabolized and excreted by the body, suggests that plastic or epigenetic mechanisms may play a role. Therefore, we wanted to investigate the *in vivo* epigenetic modifications induced by a single psilocybin intervention, which lead to secondary lasting effects such as gene expression changes. Understanding how pharmacological interventions influence epigenetic enzymes and their regulation of gene expression can give valuable insight into the neurobiology of psychiatric diseases.

2. AIMS AND HYPOTHESES

The aim of the present thesis was three-fold:

- To evaluate the PET radioligand [¹¹C]Martinostat in the pig brain, including the regional distribution, suitable kinetic modelling and the correlation between *in vivo* and *in vitro* measured HDAC1-3 levels.
- To establish a large animal model for acute psilocybin administration and characterize the porcine reaction to psilocybin, including determining the 5-HT_{2A}R occupancy of the dose eliciting behavioural changes.
- To investigate genetic mechanisms underlying the sustained effects induced by acute psilocybin administration.

The following hypotheses shaped the framework of the present thesis:

1. [¹¹C]Martinostat PET neuroimaging reflects HDAC1-3 *in vitro* levels in the pig brain.
2. An acute dose of VPA affects [¹¹C]Martinostat binding in the pig brain.
3. A large animal model reflecting the intake of a psychedelic dose of psilocybin can be established in the pig.
4. A single dose of psilocybin alters gene expression of epigenetic modulators, synaptic density markers and 5-HT_{2A}R.



3. METHODS

3.1 The pig in biomedical research

The pig is a large animal, high in the evolutionary tree and quite closely related to humans in many ways. The pig has long been used in surgical research, but it also offers a multitude of advantages in neuroscience. For example, the porcine brain is gyrencephalic like the human brain and due to anatomical and physiological similarities the pig is gaining popularity in neuroscience research⁷⁹. In addition, the pig's brain size is substantially larger than that of rodents, providing a better match to the spatial resolution of various *in vivo* imaging techniques, as well as a large amount of tissue for *in vitro* molecular investigations. The large size of the pig also enables multiple blood samples throughout experimental designs which is a substantial advantage in studies with pharmaceuticals or radioligands. Furthermore, the serotonin system has been characterized in the pig brain and has been shown to closely resemble the human brain, both neurochemically and topographically⁸⁰. The distribution of several 5-HT receptors has been shown to be similar to the cerebral human distribution⁸¹⁻⁸³.

In Denmark the pig is readily available since Danish slaughter pigs are bred to grow fast for commercial purposes, with an average weight increase of 5 kg/week, making them an easily sourced and cheap large animal model for research. The Danish slaughter pig is a very controlled cross-breed between three races of pigs; Landrace, Yorkshire and Duroc. Hence, it is not a homogenous well-characterized inbred strain like e.g. Göttingen, but possibly a better representation of the variations observed in a human population. However, due to the high economic implications of Danish slaughter pigs, the breed is very well-defined and controlled. Finally, studies in pigs have fewer ethical restrictions than non-human primates. The use of pigs also does not necessitate reuse of animals for many different experiments, thereby ruling out concerns about carry-over effects from previous testing.

3.1.1 Establishing a large animal model for administration of psilocybin

We aimed to investigate the molecular changes induced by a single exposure to psilocybin, possibly underlying the therapeutic action described in humans. To ensure translatability, we accustomed the pigs to human handling which allowed us to do i.v. injections or blood sampling without anaesthesia.

In a dose escalation study, we established the porcine dose-response relationship to psilocybin. Psilocybin in doses of 0.01, 0.04, 0.08, 0.16 mg/kg was given i.v. and the pig was observed for changes in behaviour, e.g. headshakes, and various parameters such as temperature and skin colour were noted. The lowest dose (0.01 mg/kg) did not induce behavioural changes; doses of 0.04 and 0.08 mg/kg had noticeable effects on behaviour; while 0.16 mg/kg had strong sedative effects. We chose to proceed with 0.08 mg/kg of psilocybin.

To ensure 5-HT_{2A}R engagement of psilocybin in the pig brain, we confirmed the occupancy of psilocybin (0.08 mg/kg) at the 5-HT_{2A}R by PET imaging using [¹¹C]Cimbi-36. During the PET scan blood samples were collected to assess psilocin concentrations and determine the drug half-life.

Aiming at elucidating both sub-acute and sustained molecular effects of psilocybin exposure, we euthanized animals 1 day or 1 week post-psilocybin/saline (fig.5). For practical reasons, we used 1 week post-psilocybin as proxy for lasting molecular changes induced by a single psilocybin exposure. However, multiple human studies report onset of therapeutic action within one week^{49,50}, meaning that molecular imprinting should have taken place before then.

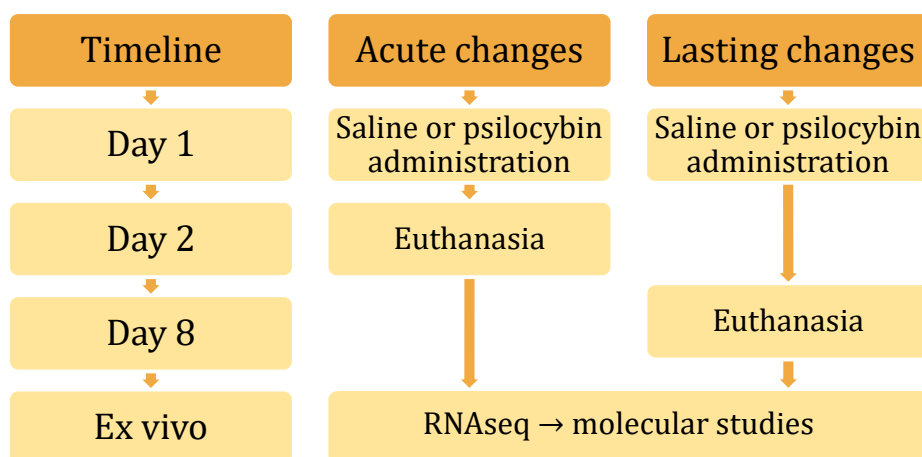


Figure 5 – Study design for investigation of psilocybin effects in pig brain.

3.2 Positron Emission Tomography

3.2.1 Principles of PET

PET imaging is based on the physics principle of positron emitting radioactive decay. Most radioisotopes used for *in vivo* research or clinical purposes have relatively short half-lives, e.g.

carbon-11 ~ 20 min, oxygen-15 ~ 2 min, fluorine-18 ~ 110 min, thereby minimizing the amount of radiation exposure to the subject. When substituting an atom of a ligand or pharmaceutical with an appropriate radio isotope, a radioligand (or radiotracer) is produced. Such radioligands enable examination of e.g. receptor/protein densities, blood flow and glucose metabolism⁸⁴.

When the radionuclide decays it emits a positron which travels from the nuclide and quickly collides with an electron in the environment, thereby undergoing annihilation (fig.6). The process of annihilation emits two photons in opposite directions from the site of collision. These two photons, also known as gamma rays, are high energy (511 keV) rays, enabling them to exit the body of the subject. The actual PET scanner consists of rings of scintillation crystals which detects the gamma rays escaping the subject; each individual detection of gamma rays is called a coincidence. The line of response between the two opposing crystals detecting the coincidence, enables localization of the site of annihilation, which closely resembles the site of decay. Reconstructing the sum of response lines (corrected for absorption, scatter and random coincidences) is used to make a 3-dimensional image of radioactivity concentration as a function of time.

In the present thesis, PET imaging was used to visualize cerebral HDAC1-3 and 5-HT_{2A}R proteins by means of the [¹¹C]Martinostat and [¹¹C]Cimbi-36 radioligands, respectively.

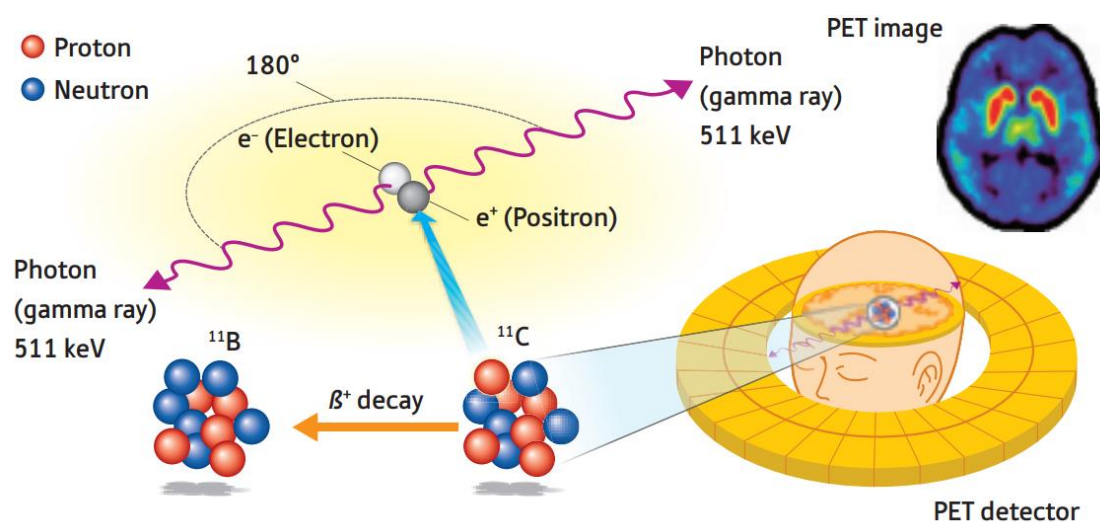


Figure 6: principles of PET imaging exemplified by carbon-11 radio isotope. ⁸⁵

3.2.2 PET data acquisition

We used female Danish Landrace pigs (crossbreed of Landrace, Duroc and Yorkshire) weighing ~20 kg. All experiments were in accordance with the European Commission's Directive 2010/63/EU, in compliance with the ARRIVE Guidelines, and approved by the Danish Council of Animal Ethics (Journal# 2012-15-2934-00156 and later 2016-15-0201-01149).

On the day of experiment, the animal was anesthetized by 0.13 ml/kg Zoletil Veterinary Mixture and maintained by 1.5ml/kg/h propofol. Anaesthesia was maintained by inhalation isoflurane in one non-terminal experiment (psilocybin occupancy study). Intravenous catheters were placed in one ear, two mammary veins and two femoral arteries to facilitate blood sampling, radioligand and/or drug administration, as well as blood pressure measurement. Other vital parameters monitored throughout the PET scan were heart rate, temperature, O₂ and CO₂ saturation. The pig was ventilated by 20% oxygen in air by endotracheal intubation and urine catheter minimized stress and discomfort. Animals were euthanized by i.v. pentobarbital/lidocaine.

All PET scans were performed in a high-resolution research tomograph (HRRT) scanner at Copenhagen University Hospital Rigshospitalet. All radiochemistry was prepared by the PET and Cyclotron Unit, Copenhagen University Hospital Rigshospitalet by carbon-11 methyl iodide for [¹¹C]Martinostat⁶² or methyl triflate for [¹¹C]Cimbi-36⁸⁶.

Prior to radioligand injection, a transmission scan using an internal ¹³⁷Cs source was performed; this was later used for attenuation correction in the reconstruction process. Simultaneous to an i.v. bolus injection of radioligand, PET data acquisition was initiated and lasted 121 min for [¹¹C]Martinostat or 90 min for [¹¹C]Cimbi-36. Throughout the scan manual blood samples were collected and used for whole blood radioactivity measurement as well as radiometabolite determination by means of radio-HPLC⁸⁷. Continuous measurement of whole blood radioactivity was performed during the initial 30 min of the PET scan.

3.2.3 PET data quantification

To delineate regions of interest (ROIs), the reconstructed PET images were co-registered to a magnetic resonance image (MRI) of the pig brain and subsequently fitted to a pig brain atlas in an automated fashion⁸⁸. This produces regional time-activity curves (TACs) of the radioligand (kBq/mL) which is normalized to injected dose and corrected for animal weight (kBq/kg) to yield standardized uptake values (SUV, g/mL).

In order to quantify radioligand binding within a ROI, kinetic modelling was performed. The core concept of kinetic modelling is the ability to describe the regional TACs while distinguishing between various compartments containing radioligand, i.e. freely, specifically and non-specifically bound. These kinetic models use arterial input function, referring to the metabolite corrected radioactivity measured in blood during the PET data acquisition. Some widely used kinetic models are the 1 tissue compartment (1-TC) and 2-TC models^{89,90}, which differentiates the concentration of radioligand into either one or two compartments, respectively – as well as plasma radioactivity⁹¹. The outcome measure of compartmental models is total distribution volume (V_T).

From the computed V_T values, the non-displaceable binding potential (BP_{ND}) can be estimated using the equation $BP_{ND} = \frac{V_T - V_{ND}}{V_{ND}}$, where V_{ND} denotes the non-displaceable distribution volume. V_{ND} can be estimated by a blocking study of the radioligand followed by graphical presentation of the V_T s in the blocked and unblocked condition called a Lassen plot^{92,93}. By linear regression the x intercept estimates the V_{ND} , whereas the slope of the regression line estimates occupancy of the blocking agent. In the present thesis, the Lassen plot was used to estimate V_{ND} of [¹¹C]Martinostat, as well as occupancy of psilocybin at the 5-HT_{2A}R by [¹¹C]Cimbi-36.

A quite different approach to compartmental quantification, is the linearization of the TAC, also known as graphical analysis, e.g. the Logan plot⁹⁴ or Ichise Multilinear Analysis 1 (MA1)⁹⁵. The core of this approach is to convert the model equations to linear plots, where the slope estimates the radioligand binding. However, the initial dynamic part of the TAC is discarded due to the non-linearity, and the t^* refers to the time at which the analysis becomes linear. In our analyses of [¹¹C]Martinostat t^* was thoroughly assessed for each ROI, revealing substantial differences between ROIs and thereby the amount of data that their estimates were based on. In order to assess the goodness-of-fit of the various kinetic models to the [¹¹C]Martinostat data, we used the Akaike information criterion⁹⁶ (AIC).

A crude quantification method suitable for a subset of radioligands with very slow kinetics, is the simple ratio of the SUV at equilibrium in a ROI over a reference region, denoted SUVR. We investigated this approach for the [¹¹C]Martinostat radioligand, since it displayed very slow kinetics and we used the olfactory bulbs as reference region. However, the time at which the

radioligand reached equilibrium varied across brain regions, therefore we denote the time span used for ratio calculation as $SUVR_{x-121}$.

3.3 Western blotting

3.3.1 Principles of western blotting

Western blotting (wb) is a widely used methodology to detect proteins in solution. Proteins are denatured and coated with negatively charged ions which enables separation of proteins according to size by gel electrophoresis (fig.7). Electroblotting stabilizes the proteins onto a membrane where they can be detected by means of consecutive target-antibody complex formation. Final visualization is accomplished by the detection of light emitted from the target-antibody complex. The methodology can be tweaked in several ways and optimization is always recommended to suit the specific starting material, the chosen antibody, etc.

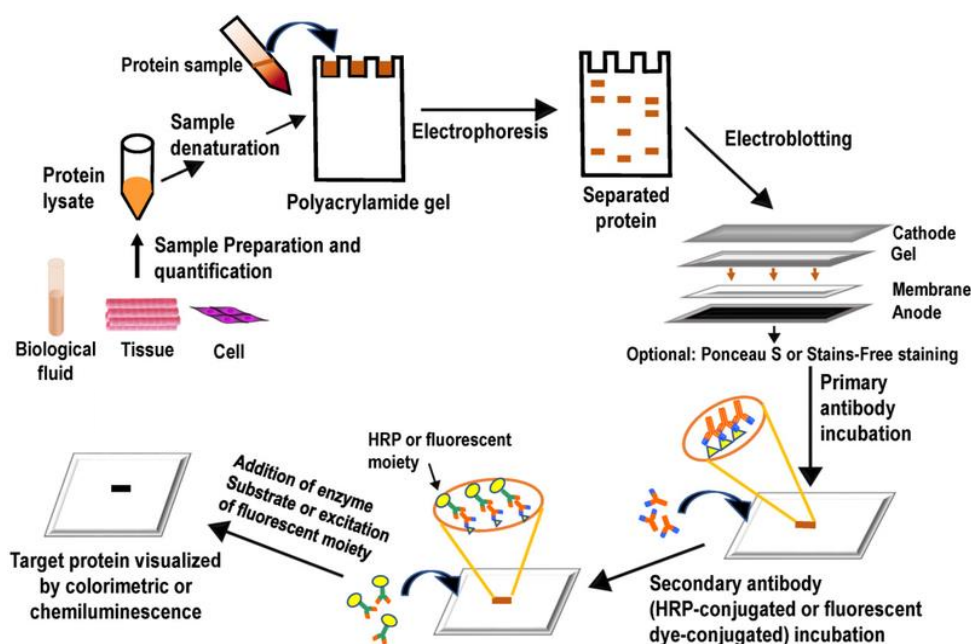


Figure 7 – Principles of western blotting.

Wb is generally considered a semi-quantitative methodology due to the usual implementation of a reference comparison, whether it is a ‘housekeeping’ protein or total protein (as described below). ‘Housekeeping’ denotes the assumption of stability of a given protein across

experimental groups, however, validation of this crucial component is often skipped by researchers. The addition of serial dilutions of known protein, e.g. purified recombinant protein, enables quantification of the target protein.

3.3.2 Stain Free® wb

We employed the Stain-Free® wb modality developed by Bio-Rad Laboratories, Inc⁹⁷. The principle behind the Stain-Free technology is that a proprietary molecule in the gel irreversibly binds to tryptophan residues of proteins when exposed to UV light. The molecule-tryptophan complex enables visualization like the toxic Ponceau S and Coomassie staining of membrane and gel, respectively. Following transfer of proteins to the membrane, a picture of total protein is taken, which is then used as normalization channel in the quantification software.

One aim of the present thesis was to test the correlation between HDAC1-3 protein levels measured *in vivo* by PET scanning to *in vitro* wb measures. HDAC1 is generally considered stably expressed and is proposed as nuclear ‘housekeeping’ protein. Therefore, we employed the Stain-Free® modality to confidently measure small changes in rather stable proteins, hopefully without the bias another presumably stable ‘housekeeping’ protein could introduce. Furthermore, to directly compare the *in vivo* tissue measure to extracted protein levels, we employed a dilution series of known human recombinant protein concentrations together with the formula $\left(\frac{X \text{ nmol HDAC1-3}}{9 \mu\text{g protein}}\right) * \left(\frac{\text{total mg protein extracted}}{\text{total mL tissue used for extraction}}\right)$. By the lowest common denominator-principle, we loaded 9 µg nuclear protein in all the wb used in Paper I – which is accounted for by the first fraction of the formula, whereas the second fraction accounts for the variation in protein extraction efficiency; collectively yielding total HDAC per mL fresh brain tissue – a measure directly comparable to *in vivo* PET measures.

3.4 RNA sequencing

The ability to perform high-throughput sequencing at reasonable cost has revolutionized modern science – and consequently the amount of data constantly created is unfathomable. Several different sequencing techniques exist; however, in the present thesis only the Illumina Sequencing By Synthesis (SBS) technology will be covered. SBS is one of many so-called Next Generation Sequencing techniques, which has advanced the original Sanger sequencing technique. Although the starting material is RNA, and the goal is to sequence RNA molecules in a

given sample mixture, sequencing is only performed on DNA or complementary DNA (cDNA) synthesized by reverse transcription of isolated RNA.

3.4.1 Principles of SBS

The input DNA is fragmented and ligated with specific adaptors in the process of library preparation (fig.8). The adaptor sequences are crucial for appropriate sequencing for two reasons, 1) hybridization of the template DNA to the flow cell and 2) sequencing primer binding sites. The flow cell is a glass slide containing two types of oligonucleotides – it is on this glass slide the sequencing takes place. After hybridization of the sample DNA to the flow cell, by means of the adapter, a polymerase synthesizes the complementary strand of DNA, followed by denaturing and washing away of the initial template strand. To achieve sufficient signal, clusters of clonal templates are generated by bridge amplification (fig.8), ending by the reverse strands being cleaved off and washed away. This ensures a uniform signal from each cluster during sequencing. The sequencing process then starts by sequencing the forward strand, after which the reverse strand follows by reverse transcription. The actual sequencing consists of the addition of a nucleotide coupled to a terminator cap and a fluorescent dye, one colour for each type of nucleotide (fig.8). The terminator cap ensures that only one nucleotide is incorporated in each cycle. After each cycle the flow cell is excited by a laser beam which causes the fluorescence dye to emit its signal. The terminator cap and fluorescence are subsequently cleaved off so another nucleotide can be incorporated in the next cycle.

The consecutive signal from an entire cluster is termed ‘read’. The amount of reads per sample is called ‘sequencing depth’, which is a measure of the coverage of sequencing. The sequencing can be either single end or paired end. In a single end analysis, the template is only sequenced in one direction, whereas the paired end analysis sequences the template from the opposite direction after completion of the initial direction.

The analysis of sequencing data consists of mapping each of the reads to a reference genome, enabling quantification of the initial sample content of any given nucleic acid sequences. The deeper the sequencing, the higher the confidence in the alignment of the read to the reference genome.

3.4.2 RNA sequencing data acquisition

Prefrontal cortex tissue from pigs exposed to psilocybin/saline was used for RNA sequencing (RNAseq).

RNAseq was performed by Admera Health, New Jersey, USA, who performed the RNA extraction, library preparation and sequencing by Illumina SBS technology. Our goal was to

determine gene expression changes following psilocybin treatment, so the extracted total RNA was enriched for mRNA by poly-A selection. The resulting cDNA was analysed to a read length of 150 base pairs by paired-end sequencing to a depth of 20-22 million reads per sample. The reads were aligned to the susScr11 genome assembly guided by an ENSEMBL gene annotation. Gene counts were used for statistical analysis and gene set enrichment analysis (GSEA), which determined functionally related genes collectively altered between treatment groups. Based on the leading edge list of such related genes, we sought to validate the RNAseq results by reverse transcription quantitative polymerase chain reaction (RTqPCR).

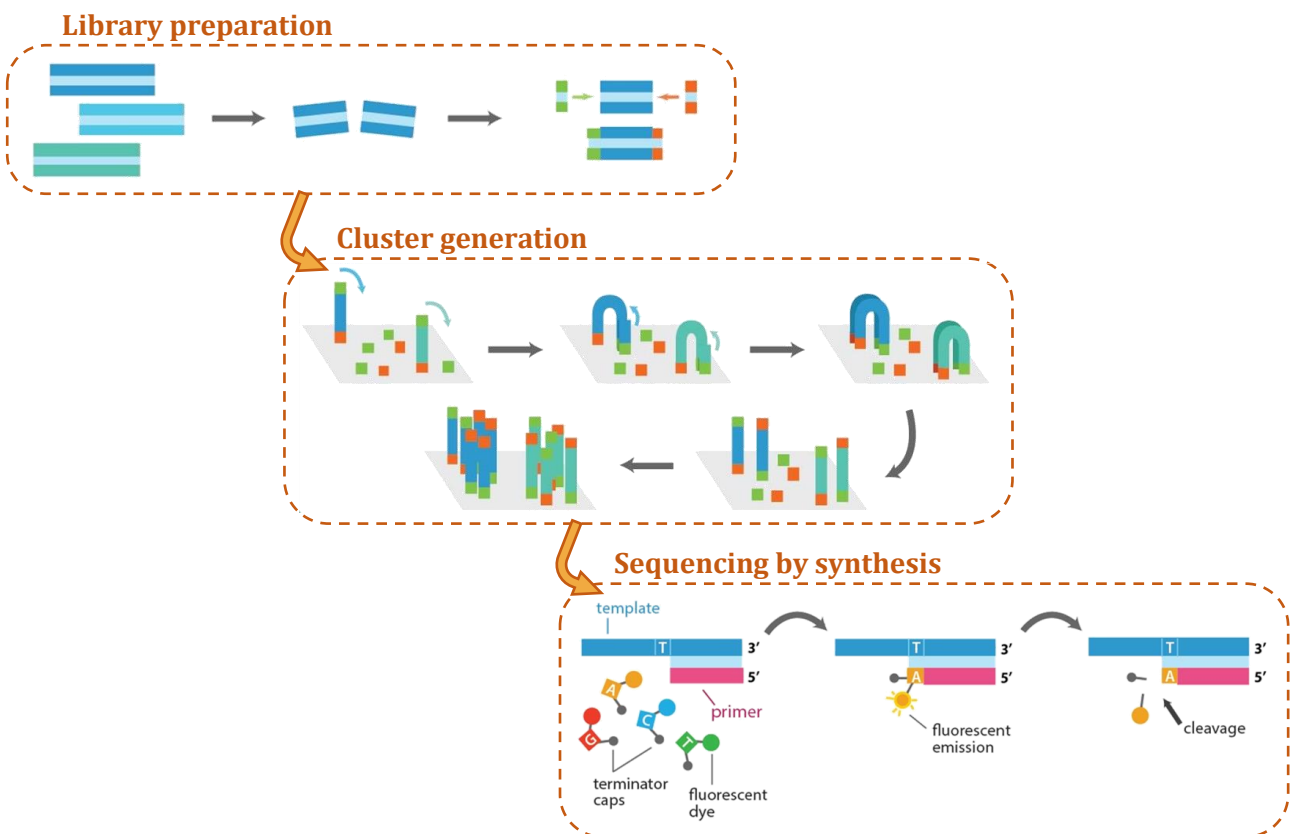


Figure 8 – Principles of Illumina sequencing by synthesis. Modified from⁹⁸

4. RESULTS & DISCUSSION

4.1 Histone deacetylase 1-3 in the pig brain

Epigenetic modifications have been found to play crucial roles in multiple disorders⁶², however, invasive tissue sampling is necessary to investigate the organ-specific epigenetic status. The [¹¹C]Martinostat radioligand enables visualization of the HDAC1-3 proteins in living tissue, however, no direct comparison between *in vivo* [¹¹C]Martinostat binding and *in vitro* measured HDAC1-3 protein levels had been undertaken.

4.1.1 Evaluation of the [¹¹C]Martinostat radioligand in the pig brain

We observed high uptake of the radioligand and slow kinetics across various brain regions (fig.9a). This was in line with previous reports for [¹¹C]Martinostat in non-human primates and humans^{62,76,77}. From a self-block study (fig.9b) employing a dose of 0.5 mg/kg unlabelled Martinostat i.v., we determined 89% occupancy when the derived V_T s were used in a Lassen plot (fig.9c). From the Lassen plot it was also evident that no region in the pig brain was devoid of target binding; even the lowest binding region (olfactory bulbs) had ~5 times higher binding than the determined V_{ND} of 2.9 mL/cm³ (fig.9c). The lack of reference region was in line with the conserved nature of the HDAC proteins across evolution⁶⁰. However, the very low V_{ND} gives [¹¹C]Martinostat an excellent signal-to-background ratio, even in low binding regions.

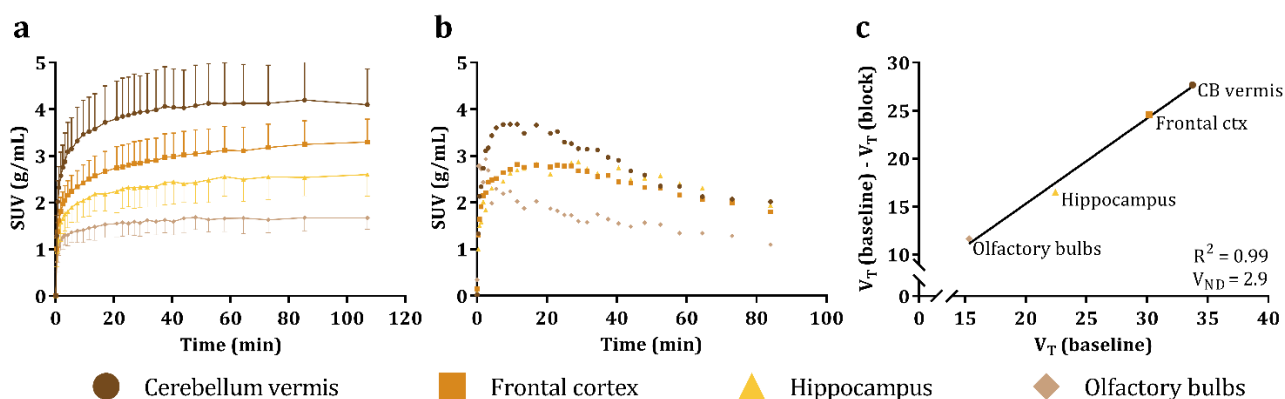


Figure 9 - [¹¹C]Martinostat in the pig brain. a) Time-activity curves following i.v. [¹¹C]Martinostat injection showing the radioligand uptake across various brain regions (mean \pm SD, n = 13). b) Time-activity curves of the [¹¹C]Martinostat signal when co-administered with 0.05 mg/kg unlabelled Martinostat (n = 1). c) Lassen plot of regional differences in [¹¹C]Martinostat V_T s at baseline and blocked condition (n = 1).

4.1.2 Kinetic modelling and simplified quantification of [¹¹C]Martinostat

After determining high brain uptake and wide distribution of [¹¹C]Martinostat in the pig brain, we used one of the great advantages the pig offers in PET imaging: full kinetic modelling with metabolite corrected arterial input function. Across the four investigated brain regions, we determined that 1-TC and 2-TC models resulted in the lowest and highest V_{TS} , respectively (table 1). The Logan and MA1 approaches provided very similar V_{TS} , but the AIC was much lower for the MA1 model and was therefore deemed most suitable. [¹¹C]Martinostat required long acquisition time to ensure stable V_T estimates which has also been established for non-human primate and human imaging^{76,77}. Our MA1 calculated V_{TS} from pig brain were comparable with 2-TC derived V_{TS} from non-human primate brain⁷⁷, whereas the V_{TS} from human brain were reported 3–4 times lower⁷⁶; however, V_{ND} in humans remains to be determined. Good correlations between the V_{TS} from 2-TC and Logan, as well as 2-TC and SUVR, have been shown in the primate brain^{75,77}. In pig brain we found good correlation between MA1 derived V_{TS} and SUVR as well as BP_{ND} and SUVR.

Of the tested quantification models we recommend using MA1 or SUVR, depending on the availability of arterial input function and the desired outcome measure, e.g. V_T for Lassen plots.

		V_T (mL/cm ³)				BP_{ND}	
		1-TC	2-TC	Logan	MA1	MA1	SUVR _{X-121}
Frontal cortex	mean ± SD	36.9 ± 9.6	44.6 ± 10.6	40.7 ± 9	41.7 ± 9.1	13.5 ± 3.2	2 ± 0.2
	<i>AIC</i>	4.4	-34.4	124	-16.1	-	-
Hippocampus	mean ± SD	26.6 ± 5.3	34.6 ± 9.1	28.9 ± 6.2	30.8 ± 6.8	9.7 ± 2.4	1.5 ± 0.1
	<i>AIC</i>	49.6	41.7	146	5.6	-	-
Olfactory bulbs	mean ± SD	16.5 ± 3.7	20.9 ± 5	17.9 ± 3.3	18.9 ± 3.7	5.6 ± 1.3	-
	<i>AIC</i>	61.3	46.2	142	2.4	-	-
Cerebellum vermis	mean ± SD	42.6 ± 10.2	49.6 ± 12.5	45.5 ± 10	47.4 ± 10.6	15.5 ± 3.7	2.5 ± 0.3
	<i>AIC</i>	17.4	-19.3	147	-11.5	-	-

Table 1 – Kinetic modelling of [¹¹C]Martinostat. Data is presented as mean ± SD with the mean Akaike information criteria (AIC) below in italic. BP_{ND} s were calculated with the formula $(V_T(ROI)-V_{ND})/V_{ND}$, using the MA1 determined V_T values. For SUVR calculations the olfactory bulbs were used as reference region.

We evaluated the test-retest variability of [¹¹C]Martinostat in four pigs by scanning them twice in one session. For MA1 derived V_{TS} of frontal cortex, 3 out of 4 animals had 7-12% differences between scans while one had 39% change in V_T . Meanwhile, test-retest frontal cortex SUVR

differed <9% in all four animals. This indicated that SUVR was perhaps a more stable measure of [^{11}C]Martinostat binding which we then sought to compare to *in vitro* measures of the HDAC1-3 protein levels. To establish relevant parameters for a power analysis of a [^{11}C]Martinostat PET study in pigs, we examined the effect size of psilocybin on HDAC1-2 in a subset of 12 pigs (as described in section 4.2.4.). Since the wb analysis showed no difference between saline and psilocybin treated pigs, we decided not to carry out the originally planned studies of the effect of psilocybin on [^{11}C]Martinostat binding in the pig brain.

4.1.3 *In vivo/in vitro* correlations of HDAC1-3 protein levels

Golden standard for protein detection is western blotting. We therefore tested the correlation between the *in vivo* HDAC1-3 levels measured by [^{11}C]Martinostat to that measured *in vitro* by western blotting. Employing standard curves of known amounts of recombinant protein, we quantified the levels of HDAC1-3 in cerebellum vermis, frontal cortex and hippocampus, as these represent high and medium binding regions of [^{11}C]Martinostat. We found a strong correlation between HDAC1 and HDAC2 levels, as well as medium correlation between HDAC2 and HDAC3 levels (fig.10a). These results were in line with the general consensus concerning an interplay and possible redundancy of various HDAC isoforms⁹⁹⁻¹⁰¹. However, distinct roles have also been shown¹⁰², proving the evolutionary point of conserving the protein isoforms. In our study we summed the *in vitro* quantified HDAC isoforms and found significant correlation to the *in vivo* SUVR measure (fig.10b), but no correlation with MA1 derived V_{T} s (fig.10c).

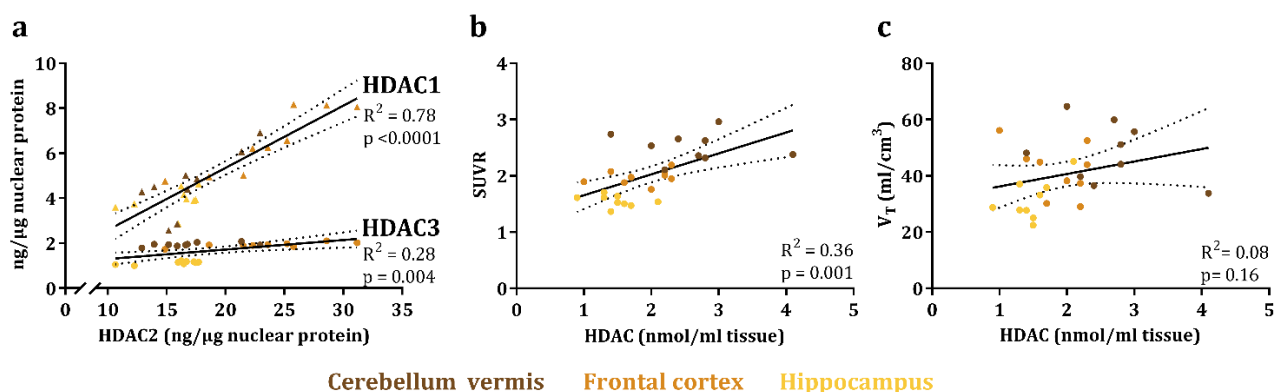


Figure 10 - Correlations of *in vivo* and *in vitro* measures of HDAC1-3. a) Correlation between levels of HDAC2 and either HDAC1 (▲) or HDAC3 (●) across three brain regions. Correlation between *in vitro* measured HDAC1-3 levels and *in vivo* measured SUVR (b) or V_{T} (c). ($n = 9$)

We speculated that despite long scan duration, the V_T measures could still be biased due to the slow kinetics of [^{11}C]Martinostat, which might play a role in the correlation to the *in vitro* measured protein levels.

Based on our direct *in vivo/in vitro* comparison we recommend using SUVR as proxy for cerebral HDAC1-3 levels in the pig brain.

4.1.4 VPA as competitor to [^{11}C]Martinostat binding

VPA is an inhibitor of class I and IIa HDACs which includes the [^{11}C]Martinostat targets HDAC1-3. We therefore investigated whether an acute dose could block the [^{11}C]Martinostat signal *in vivo* when co-administered. All regions were investigated, but for clarity only data from the frontal cortex is presented here. We found no change in SUVs following 40 mg/kg VPA i.v. (fig.11a), and an increased dose of 120 mg/kg VPA i.v. in three animals gave opposing results: increased radioligand uptake (fig.11b), decreased uptake (fig.11c) or somewhat unchanged uptake (fig.11d). Employing the previously established SUVR quantification method with the olfactory bulbs as reference region, we did not find any consistent effects of VPA administration on [^{11}C]Martinostat binding in pig brain (fig.11e).

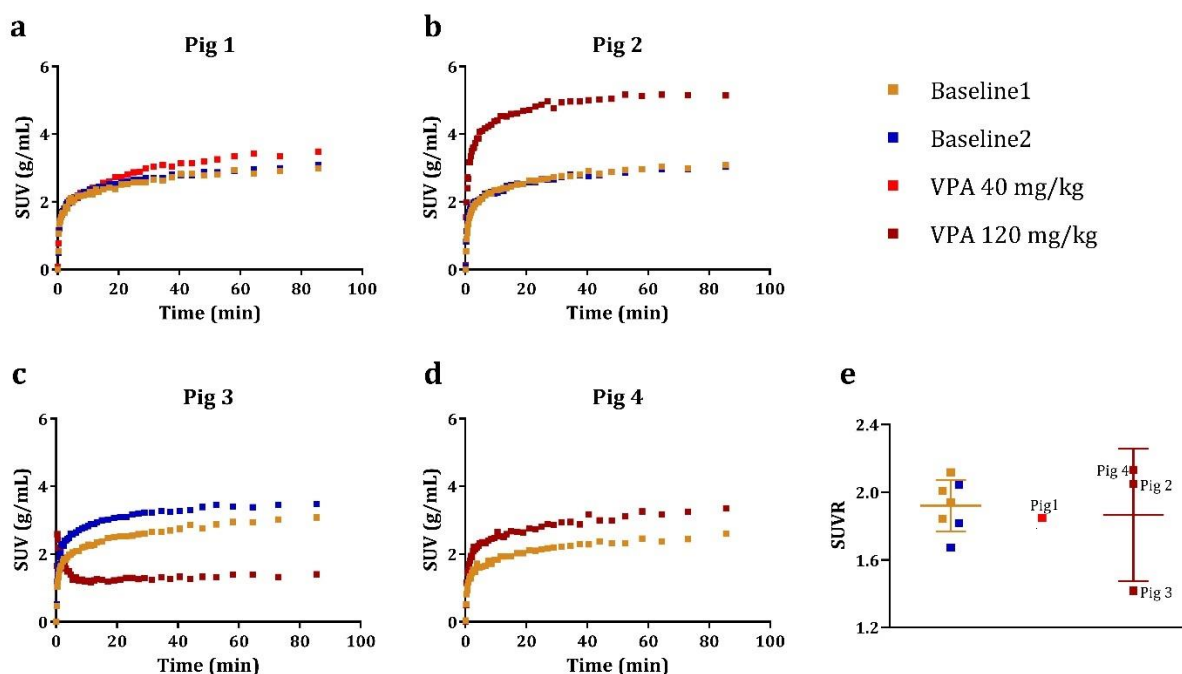


Figure 11 – Effects of valproic acid on [^{11}C]Martinostat uptake and binding in frontal cortex. a) No change in radioligand uptake in frontal cortex after administration of 40 mg/kg VPA. In three different pigs, 120 mg/kg VPA injection increased (b), decreased (c) or unaltered (d) the radioligand uptake in frontal cortex. e) Quantification of the [^{11}C]Martinostat signal in frontal cortex by SUVR with olfactory bulbs as reference region.

It has previously been shown that peripheral uptake of [^{11}C]Martinostat can be blocked by the hydroxamic acid HDAC inhibitor SAHA, a drug of very similar structure to Martinostat itself¹⁰³. However, we were not able to block the [^{11}C]Martinostat signal in the brain by VPA which is a short-chain fatty acid HDAC inhibitor. It appeared that VPA could change the radioligand uptake (fig.11b-c), despite minimal drug-radioligand interaction (fig.11e), suggesting that VPA and [^{11}C]Martinostat does not share the same binding site. VPA is used as an antiepileptic drug in clinical settings, however, the mode of action is still unknown¹⁰⁴. Although our study cannot determine the pharmacological mode of action, some cerebral changes are evident.

We next investigated the brains from the animals undergoing the PET experiments with VPA and quantified HDAC1-2 by western blotting. We found that the levels of HDAC1 and HDAC2 in VPA treated pigs were within the range of non-treated pigs (fig.12 left) and, interestingly, the protein levels of pig 2 and pig 3 were very similar. This provided further proof, that the altered radioligand uptake caused by VPA administration did not reflect an actual change in protein target, but rather some altered physiological parameter affecting the radioligand distribution. However, we did find that VPA was able to inhibit HDAC activity, as measured by a change in acetylation levels of H3 and H4 (fig.12 right) – in line with the established HDAC inhibitory effect of VPA¹⁰⁵

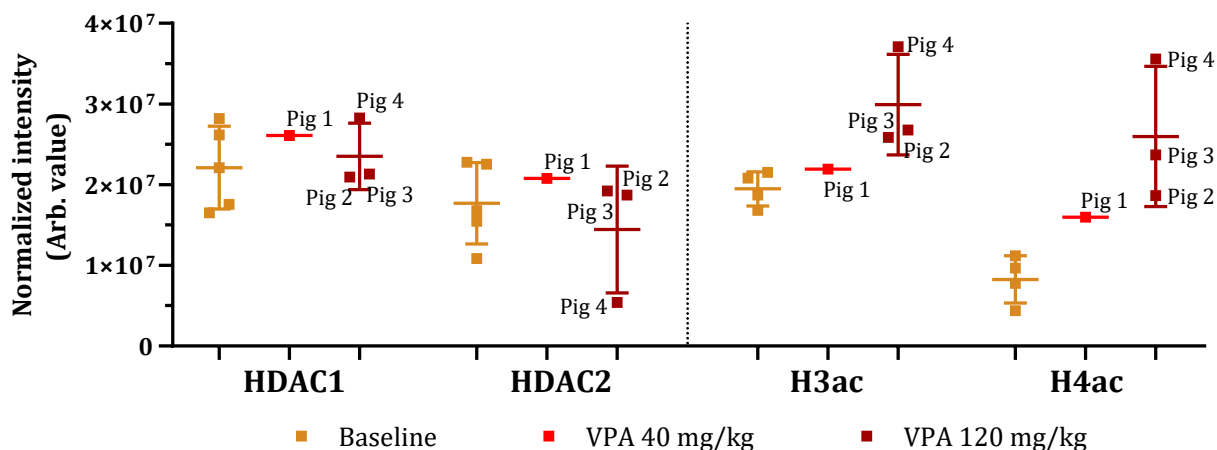


Figure 12 – Effects of VPA on HDAC1, HDAC2, H3ac and H4ac levels in frontal cortex. VPA did not affect levels of HDAC1 and HDAC2, but increased acetylation levels of H3 and H4 (mean \pm SD, n = 9). Note the similarity in HDAC1-2 levels of pigs 2-3 measured by western blotting opposed to the PET radioligand signal (fig.11b-c).

4.2 *In vivo* and *in vitro* effects of psilocybin in pigs

Psychedelics have been investigated extensively in rodents, however, for the past 30 years, no reports of the hallucinogenic compound psilocybin have used awake large animals. In a dose-escalating study we determined an effective dose of 0.08 mg/kg i.v. psilocybin in pigs. We found that plasma levels of the active metabolite, psilocin, rapidly decreased after i.v. administration (fig.13a), with a $T_{1/2}$ of 20 min as determined by exponential one phase decay. The 5-HT_{2A}R radioligand [¹¹C]Cimbi-36 had high uptake in neocortex whereas lower uptake was seen in the cerebellum (fig.13a) at baseline conditions. The neocortical signal completely collapsed onto the cerebellar signal following co-administration of 0.064 mg/kg psilocybin. V_T values were comparable to previously published results¹⁰⁶, with highest binding in the cortex, lower binding in subcortical regions and lowest binding in the cerebellum. Lassen plot of derived V_T s determined that 0.064 mg/kg psilocybin resulted in 67% occupancy of the 5-HT_{2A}R and a V_{ND} of 4.2 mL/cm³ (fig.13b). A human study from our group found that this level of occupancy is reached in humans by a 15-30 mg oral dose¹⁰⁷, which is considered a moderate to high dose. Furthermore, they found that plasma psilocin concentrations comparable to our pig study resulted in high intensity ratings of the psychedelic experience. Taken together, and assuming these findings are directly translatable, a dose of 0.08 mg/kg psilocybin i.v. should have strong effects in the pig brain.

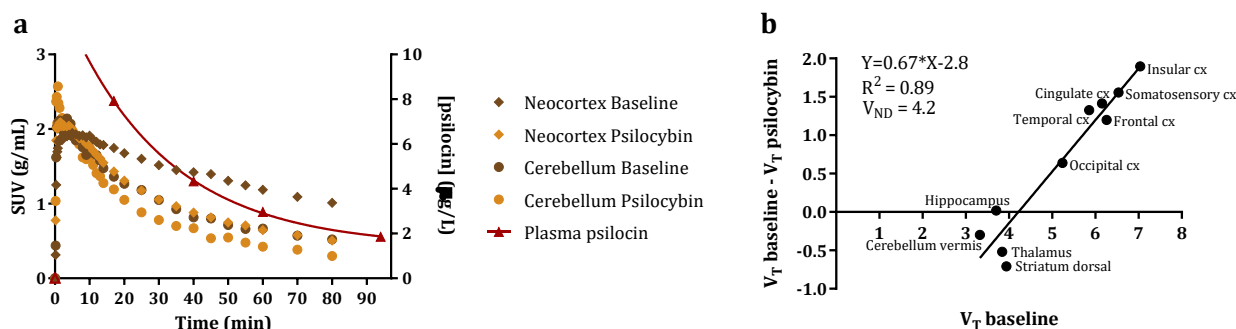


Figure 13 – 0.064 mg/kg psilocybin occupied 67% of 5-HT_{2A} receptors. a) Time-activity curves of [¹¹C]Cimbi-36 at baseline and after 0.064 mg/kg psilocybin in neocortex and cerebellum (left y-axis). Plasma psilocin concentrations after i.v. administration (right y-axis). **b)** Total distribution volumes (V_T) derived from 2 tissue compartment modelling analysed by Lassen plot to determine 5-HT_{2A} receptor occupancy. (n = 1)

4.2.1 Characterization of the porcine behavioural response to psilocybin

Confident in the determined dose, we administered 0.08 mg/kg psilocybin iv to 11 pigs and gave their corresponding controls a saline injection. Following 0.08 mg/kg psilocybin we observed a profound and consistent change in pig behaviour lasting approx. 20 min (fig.14b-d) after which the effects were subtle and varying between subjects. We determined three behavioural parameters that were significantly increased following psilocybin administration: headshakes; hind- or front-leg scratching; and rubbing against pen wall or trough, (fig.14). The pigs exhibited a highly significant and consistent increase in headshakes (fig.14a), which we suggest to be analogous to the well-characterized rodent head-twitch response (HTR) to 5-HT_{2A}R activation^{108,109}. The two other parameters, scratching and rubbing, were also significantly increased with scratching displaying the largest effect size of all parameters (fig.14a).

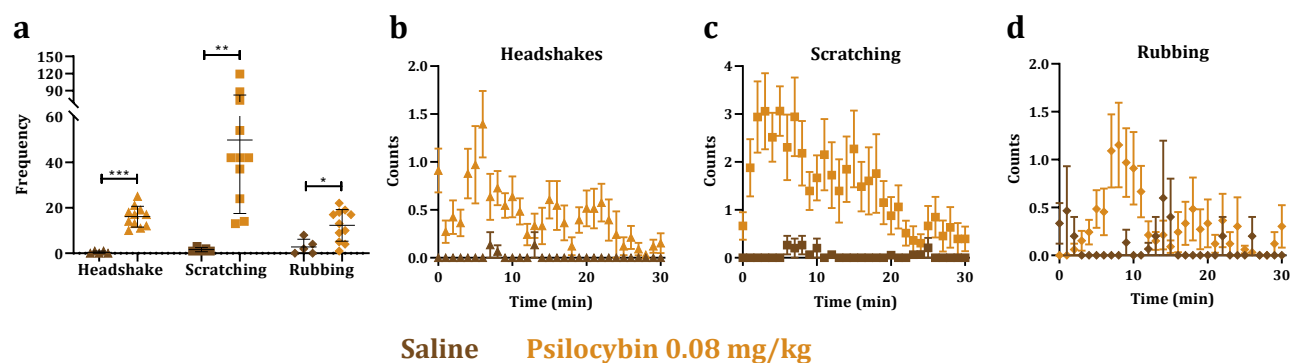


Figure 14 – Behavioural effects of psilocybin administration to pigs. a) cumulated frequency of headshake, scratching and rubbing for 30 min after administration of saline or psilocybin (mean \pm SD, n = 16). Temporal profile of the behavioural parameters headshake (b), scratching (c) and rubbing (d) during the 30 min after saline or psilocybin injection (mean \pm SEM, n = 16).

Previously, only Löscher and colleagues have injected awake pigs with 5-HT_{2A}R agonists, namely DOI, 5-MeO-DMT and LSD¹¹⁰. All compounds produced various ‘psychotomimetic’ effects, but only 5-MeO-DMT and LSD induced headshakes. Pre-treatment by the 5-HT_{2A}R antagonist ketanserin could block all the psychotomimetic effects but not headshakes. Furthermore, they showed that 5-HT_{1A}R agonists induced headshakes in pigs¹¹¹. We recognize these results, but also note their use of very high doses of 5-HT_{2A}R agonists with substantially higher potency than psilocybin. None of the pigs used in our study displayed any of the

psychotomimetic behaviours described by Löscher, suggesting a general difference in behavioural response. As previously described, the psilocybin dose used in our study occupied ~67% of 5-HT_{2A}R, and we found headshake behaviour to be consistently increased in all animals exposed to psilocybin. Furthermore, Löscher *et al* did not report any scratching or rubbing behaviour, further emphasizing substantial differences in behavioural measures following different dosing regimens of various 5-HT_{2A}R agonists.

Scratching and rubbing parameters might be considered two aspects of the same type of behaviour, however, the individual temporal profiles showed a delayed onset of rubbing behaviour compared to immediate onset of scratching behaviour (fig.14c+d). Several non-scientific reports of feeling itchy after ingestion of ‘magic mushrooms’ were found on the internet, however, no scientific reports of allergic reactions to psilocybin has been published. Neither were any of the classic psychedelics part of the otherwise comprehensive review of allergic reactions to illicit substances by Swerts *et al.*¹¹². However, we speculate whether the scratching and rubbing behaviour observed in pigs were signs of histaminergic reactions since psilocin has affinity towards various histaminergic receptors (fig.15b)¹¹³.

In summary, we characterized the porcine behavioural response to psilocybin, and found significantly increased headshakes, scratching and rubbing for a duration of ~20 min.

4.2.2 Ketanserin as inhibitor of psilocybin induced behaviour

To further validate the characteristic porcine behavioural response to psilocybin, we investigated the ability of the 5-HT_{2A}R antagonist ketanserin to abort the behaviour. In one pig, 1 mg/kg ketanserin was administered iv 6 min after 0.08 mg/kg psilocybin i.v. injection. The animal abruptly stopped the scratching behaviour (fig.15a), however, not a single headshake was observed – unlike its 11 counterparts – prohibiting determination of headshakes as a 5-HT_{2A}R specific response in pigs. Cross-affinities to

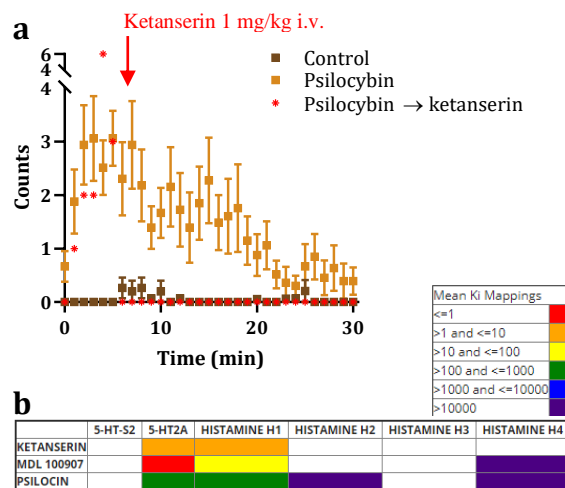


Figure 15 – Multi-receptor affinities might play a role in psilocin effects. a) administration of 1 mg/kg ketanserin i.v. inhibits scratching behaviour induced by 0.08 mg/kg psilocybin injection i.v. **b)** cross-affinities between 5-HT_{2A}R and histamine receptors by ketanserin, MDL 100907 and psilocin. (mean ± SEM, n = 17). Modified from¹¹³

the histamine 1 receptor of 5-HT_{2A}R antagonists¹¹⁴ adds an additional layer of complexity when deciphering receptor specific effects (fig.15b). Future studies are warranted to disentangle this phenomenon, however, if the scratching is in fact a porcine 5-HT_{2A}R specific behavioural parameter, our study is the first ever demonstration of ketanserin's potential to abort the psychedelic effects. If proven efficacious, such pharmacological action would have profound utility in clinical settings as an antidote against overdoses of various 5-HT_{2A}R agonists or severe 'bad trips' in psilocybin-assisted psychotherapy.

4.2.3 Cerebral transcriptomic changes following psilocybin exposure

We investigated the lasting transcriptional effects induced by a single psilocybin exposure, aiming to provide molecular evidence of the prolonged effects observed in humans. RNAseq of prefrontal cortex tissue of animals euthanized either 1 day or 1 week after a single psilocybin injection revealed only very subtle effects which were within inter-individual variation levels (fig.16a). Psilocybin has been shown to profoundly distort brain networks¹¹⁵, yet our data suggested negligible gene expression changes were sustained at 1 day and 1 week after psilocybin exposure (fig.16b+c). Electroconvulsive therapy (ECT) is another tremendously impactful therapeutic modality used to treat severe depression. However, a rodent study of cerebral gene expression changes following ECT found a surprisingly short-lasting effect of the treatment¹¹⁶ in line with our RNAseq data. Another possibility could be that psilocybin only affects a subset of cells and if the signal in this subset is subtle, it might simply be lost in the heterogeneity of a tissue sample.

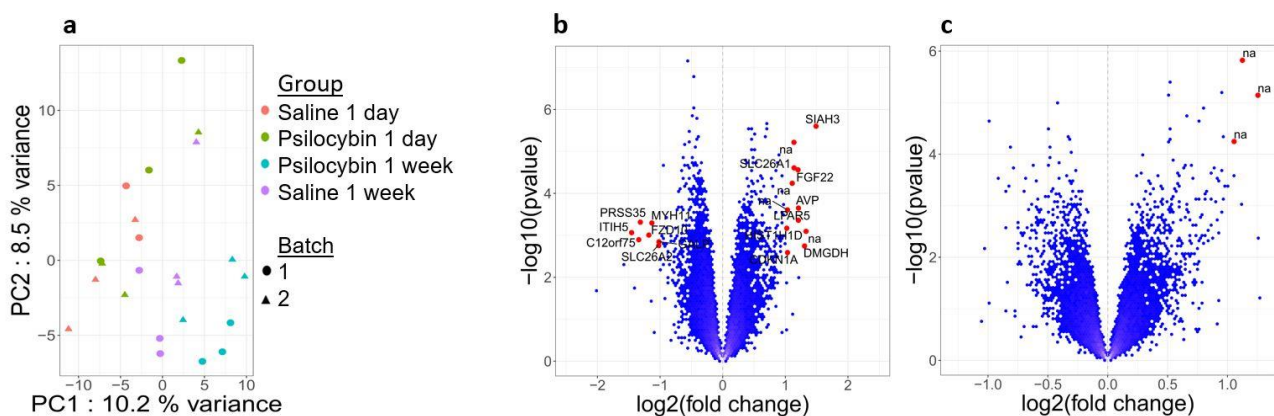


Figure 16 – Bioinformatic analysis of RNAseq data. a) Principal component analysis of the RNAseq data from prefrontal cortex of pigs exposed to psilocybin/saline. Volcano plots of differentially expressed (DE) genes 1 day (b) or 1 week (c) after psilocybin. Red dot signifies genes (labelled) that pass the threshold: $abs(\log_2 \text{ fold change}) > 1$ and $FDR < 5\%$.

We used Gene Set Enrichment Analysis to tease out expression changes within functional gene families. Although we did not find any genetic pathways regulated at both investigated time-points, we found a substantial immunological signal 1 week after psilocybin exposure. We chose to pursue the leading-edge genes within the Response to Type 1 Interferon pathway. However, RTqPCR did not find any changes of the 10 investigated genes in any group (fig.17).

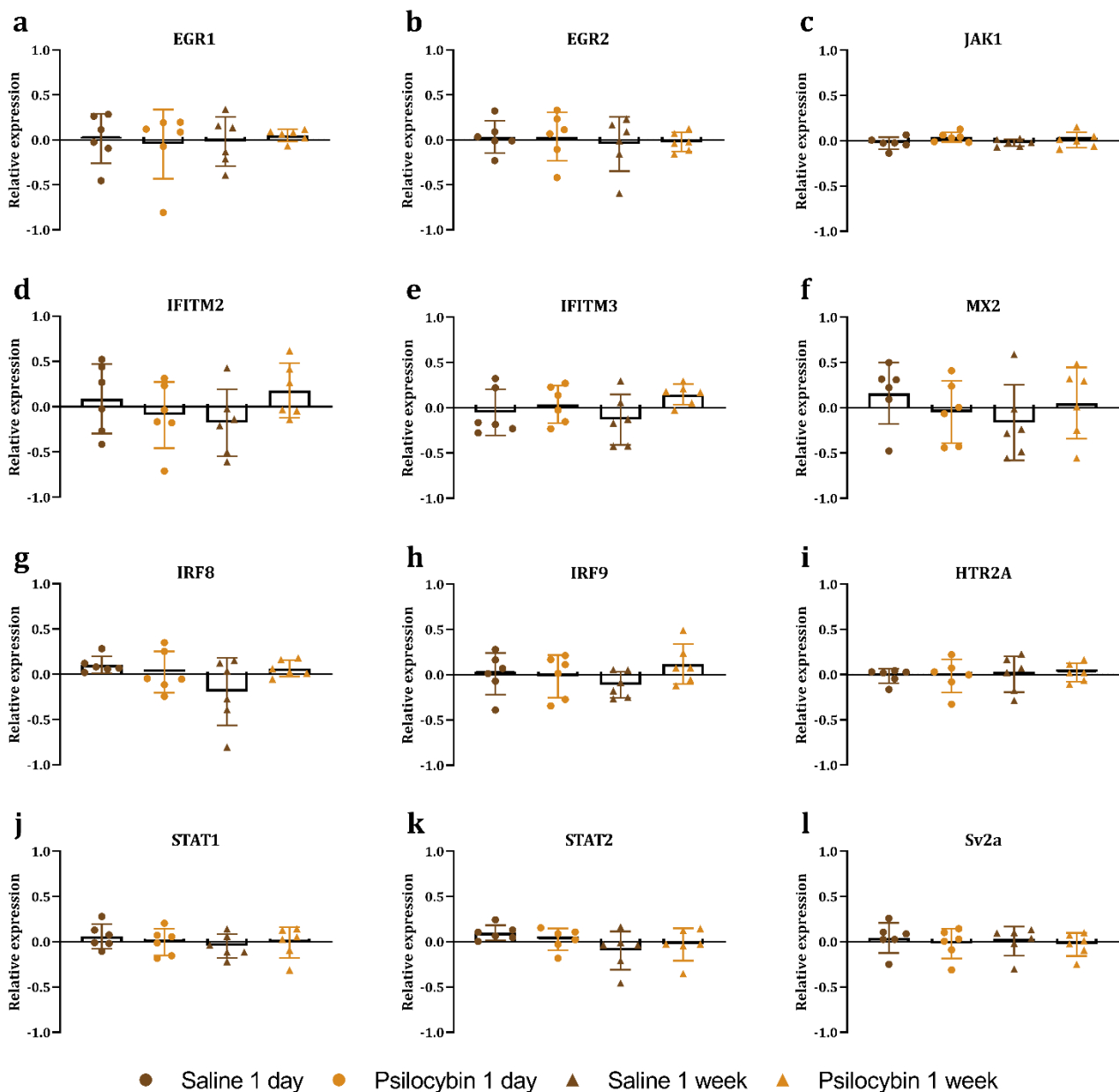


Figure 17 - Gene expression changes in prefrontal cortex following a single psilocybin exposure, as assessed by RTqPCR. (n = 6/group, technical triplicates)

Lately, neuroinflammation has gained increased attention in psychiatric diseases, such as depression, due to positive treatment outcomes of anti-inflammatory compounds¹¹⁷. Increased

levels of interferon alpha can cause neurotoxicity¹¹⁸ and when used as antiviral treatment in hepatitis C patients, clinical scores of anxiety and depression increased¹¹⁹. A recent review by Flanagan and Nichols described the role of 5-HT_{2A}R in inflammation and how psychedelics may be anti-inflammatory¹²⁰. Although we were unable to confirm altered immunologic gene expression following a single psilocybin exposure, our RNAseq results collectively point towards an interesting link between a single psilocybin administration and sustained neuroinflammation alterations. Could the lasting effects of psilocybin in humans be mediated by neuroinflammation changes? Preliminary support for the notion comes from preclinical work, where the 5-HT_{2A}R agonist DOI reduces cytokine and chemokine expression in response to TNF α or ovalbumin challenges in multiple tissue types¹²⁰.

Another possible mechanism of therapeutic action of psilocybin is neural plasticity. Psychedelics have been found to promote structural and functional plasticity of neurons by increased synaptic density¹²¹. We explored the effect of psilocybin on the gene expression of *HTR2A* and synaptic vesicle 2a (*SV2A*), suggested to be a marker of synaptic density¹²². Neither of these targets displayed altered expression after single psilocybin exposure (fig.17i+l).

In summary, a single psilocybin exposure did not induce profound gene expression changes after 1 day or 1 week, yet GSEA found multiple inflammatory pathways were altered 1 week post-psilocybin. However, RTqPCR did not find any alterations of inflammatory or synaptic gene expression at either investigated time point.

4.2.4 A single psilocybin exposure does not alter histone deacetylase 1-2

We initially hypothesized that epigenetic changes could be underlying the lasting effects experienced by humans after a single psilocybin exposure. However, from the 24 pigs used in the present study, no significant effects of psilocybin on HDAC1-2 protein levels were evident (fig.18). The very recently postulated Psilocybin-Telomere hypothesis implies that part of the therapeutic action of psilocybin is due to increased telomere length, which is correlated with improved mental health¹²³. HDAC2 recruitment has indeed been shown to be involved in telomerase activity¹²⁴, however, our data do not support the notion of altered epigenetic effector proteins at the HDAC1 and HDAC2 level after a single psilocybin exposure.

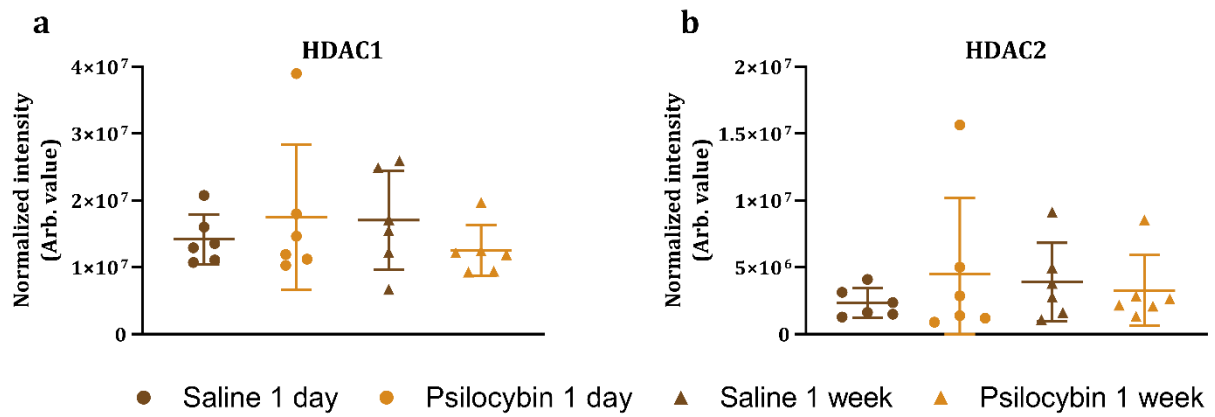


Figure 18 - HDAC1 and HDAC2 protein levels following psilocybin exposure. Immunoreactivity of HDAC1 (a) and HDAC2 (b) proteins in the pig prefrontal cortex following single psilocybin administration (n = 6/group, technical triplicates).

5. LIMITATIONS

Although the two studies presented in the thesis were designed and conducted according to best practice and our knowledge at the time, some limitations should be mentioned. In the following, some of these limitations are discussed.

In the present studies we used only female adolescent pigs and there is a potential concern that studying male pigs or pigs at a different age could have returned a different outcome. Generally, sex differences in cerebral 5-HT_{2A}R binding are not seen in healthy individuals¹²⁵. Although cerebral 5-HT_{2A}R binding declines with age¹²⁵, then the behavioral response to psychedelics is not age-dependent and for that reason, it does not seem plausible that inclusion of different ages of the pigs would have mattered. There were also practical reasons for the choice of sex and age. Male pigs have a very prominent odour and are generally more aggressive and difficult to handle than female pigs. The smell is a particular concern to those using the scanner room for clinical purposes. Moreover, before PET scanning a urine catheter is placed to minimize stress and discomfort, and females are easier to catheterize than males.

Although clinical studies have shown age- and sex differences in cerebral [¹¹C]Martinostat binding, our purpose was to validate *in vitro* vs. *in vivo* and for that reason it was deemed sufficient to use female pigs about 8-9 weeks of age.

For the psilocybin study, it could have been interesting to have investigated both sexes, but since the study design initially involved PET scans of the animals before and after psilocybin dosing, the abovementioned considerations made us use female pigs only. There is some evidence to suggest that 5-HT_{2A}R levels may change in response to hormonal treatment¹²⁶, but the pigs used in the current study could be considered adolescent, most likely not in cycles yet. Therefore, we deemed it sufficient to use young female pigs only.

Another potential limitation of our study is the confounding effects of anaesthesia, necessary for the [¹¹C]Martinostat PET scanning. All animals were treated similarly and were anaesthetized for approximately the same duration of time. To the best of our knowledge, no reports of propofol-HDAC interaction has been made, whereas isoflurane on the other hand is neurotoxic in the hippocampus through an HDAC effect¹²⁷. Importantly, the *in vivo-in vitro*

cross-validation was performed on the exact same animals, so a potential confounding effect of anaesthesia should have the same impact in both groups.

One of the biggest strong-holds of the psilocybin study, is that we administered the drug to awake animals. The pigs did, however, undergo short (about 30 min) anaesthesia in conjunction with insertion of the ear catheter several days before the experiment. We cannot exclude that this short-lasting anaesthesia with ~18 mg esketamine in the mix several days before the experiment could have affected the outcome, particularly since ketamine is a compound with potential anti-depressant effects¹²⁸. When used as an anti-depressant in people, esketamine 28-84 mg is administrated intra-nasally a few times a week and must be given in conjunction with an oral anti-depressant. However, due to the low dose and short half-life of esketamine¹²⁹ we do not believe the confounding effect of the short anaesthetic period is very pronounced in our study.

Pertaining to the [¹¹C]Martinostat study, other limitations to consider is 1) the use of only three brain regions to establish the *in vivo-in vitro* correlation, 2) V_{ND} estimation from a single blocking study, and 3) the loss of the olfactory bulbs during brain extraction, which prevented us from validating it *in vitro* as pseudo-reference region. Although more brain regions might have helped to establish an even firmer relationship, we are confident in our findings since we chose 3 anatomically well-defined and easily distinguishable regions which represented a decent range of expected HDAC protein concentrations. The examined brain regions were the same as defined in the PET anatomical atlas, however not the entire region was used for *in vitro* protein extraction, which means that we did assume a certain tissue homogeneity across a defined PET region. Furthermore, a better estimation of V_{ND} by several blocking studies might have improved the estimates of BP_{ND} , however, without blocking studies in every animal it still assumes somewhat similar non-displaceable bindings between animals.

Regarding the psilocybin study, other limitations include 1) the chosen time-points for euthanasia, 2) influencing factors of the RNAseq, and 3) the brain region which was investigated.

We did not have a-priori knowledge to choose 1 day and 1 week as fruitful euthanasia time-points, and we cannot exclude that other times might have been more appropriate. We wished to investigate the changes induced by psilocybin which might be sustained for a longer period

of time. It is debateable if one week is enough to call it lasting changes, but at least observed gene expression changes would be considered to have taken place at that time. We do find it reasonable to assume that the molecular changes established 1 week after a single administration of a drug with such a short half-life as psilocybin, are involved in the sustained effects. A human study of psilocybin in treatment resistant depressed patients describe positive effects within the first week of administration – an effect we wished to elucidate the molecular side of¹³⁰.

Countless factors can affect the RNAseq, since this methodology employs a multitude of processing steps which are all able to induce bias or noise. A few factors to consider in our study is a batch effect, RNA extraction yield, RNA degradation measures, and no a-priori positive control time-point of euthanasia. However, we believe our study is well-powered for a large animal study and do actually find it rather consoling that no major brain alterations take place following a single psilocybin administration.

In the present study we only investigated prefrontal cortex tissue by RNAseq. We cannot rule out that other brain regions would show other effects but we chose the prefrontal cortex because of its high density of 5-HT_{2A}R¹², its implications in the pathophysiology of depression³⁰, and its involvement in the psilocybin-induced psychedelic state¹¹⁵. We captured the full transcriptomic picture by using entire tissue sections, but it might be that certain cell types respond stronger to psilocybin treatment than others, and in that case other molecular strategies should be employed, e.g., cell sorting prior to RNAseq.



6. CONCLUSIONS AND FUTURE DIRECTIONS

The present thesis has focused on molecular investigations of the pig brain, by means of both *in vivo* and *in vitro* methodologies.

For [¹¹C]Martinostat we determined a wide distribution and slow kinetics of the HDAC1-3 radioligand in the pig brain. A low V_{ND} gave [¹¹C]Martinostat an excellent signal-to-background ratio, however we found no region devoid of target, but suggested the olfactory bulbs as a suitable reference region in pigs. For quantification of [¹¹C]Martinostat binding, we deemed the MA1 kinetic model best for V_T computation although it was the SUVR measure that correlated significantly with *in vitro* measured HDAC1-3 protein levels. We used VPA to show the HDAC inhibitory activity in the pig brain without specific interaction with [¹¹C]Martinostat. Therefore, in a steady-state like settings, SUVR of [¹¹C]Martinostat will be a useful proxy for cerebral HDAC levels *in vivo*.

The ability to measure epigenetic changes *in vivo* poses a tremendous potential for future disease aetiology as well as pharmacological investigations. Epigenetic components have already been established in a wide variety of disorders, however, most evidence is from post-mortem tissue or blood as biomarker. Epigenetic signatures might be established well before disease manifestation and if so, [¹¹C]Martinostat could be used to identify these, thereby directing early treatment efforts. Furthermore, investigations of epigenetic status of the diseased yet drug-naïve brain could direct future treatment modalities or reveal previously unknown disease mechanisms. Having established the validity of [¹¹C]Martinostat in pigs, novel as well as known animal disease models or pharmaceuticals can be evaluated with respect to their effects on *in vivo* levels of HDAC1-3 proteins.

We determined an effective porcine dose of psilocybin in terms of high plasma psilocin concentrations and occupancy of the 5-HT_{2A}R. If translatable to human standards, a dose of 0.08 mg/kg psilocybin i.v. had profound effects on the pig brain. We characterized the behavioural response of pigs to psilocybin and found significantly increase in headshakes, scratching and rubbing behaviour. We proposed the headshakes to be a porcine 5-HT_{2A}R-agonist specific analogue to the rodent HTR. Further investigations employing receptor specific antagonists is required to determine receptor involvement in the various behavioural parameters. Although profound and consistent effects of the psilocybin dose was observed *in vivo*, the transcriptomic

profile 1 day and 1 week post-psylocybin only found subtle changes masked by inter-individual variation. An interesting approach would be to use cell-sorting to tease out the differential molecular imprint left by psylocybin. However, multiple inflammatory pathways were altered 1 week after psylocybin exposure.

Although psychedelics have been shown to promote synaptic plasticity and epigenetic alterations, we did not observe any such changes in the pig brain following a single dose of psylocybin. However, multiple unexplored targets could still be investigated, e.g. regulation of the mGluR2 gene expression (*Grm2*) and other synaptic markers like synaptophysin. Alternately, DNA methylation rather than histone modifications may represent an underlying epigenetic mechanism induced by psylocybin exposure. In our study, animals were euthanized at two different time points. A clear pattern of gene expression changes might not be evident at these specific times, whereas lasting structural changes could already have been established.

7. REFERENCES

1. Vialli, M. & Erspamer, V. Ricerche sul secreto delle cellule enterocromaffini. Nota IX. Intorno alla natura chimica della sostanza specifica. *Boll soc med chir Pavia* **51**, 1111–1116 (1937).
2. Rapport, M. M., Green, A. A. & Page, I. H. Serum vasoconstrictor, serotonin; isolation and characterization. *J. Biol. Chem.* **176**, 1243–1251 (1948).
3. Mawe, G. M. & Hoffman, J. M. Serotonin signalling in the gut-functions, dysfunctions and therapeutic targets. *Nat. Rev. Gastroenterol. Hepatol.* **10**, 473–486 (2013).
4. Barnes, N. M. & Sharp, T. A review of central 5-HT receptors and their function. *Neuropharmacology* **38**, 1083–1152 (1999).
5. Schmitt, J., Wingen, M., Ramaekers, J., Evers, E. & Riedel, W. Serotonin and Human Cognitive Performance. *Curr. Pharm. Des.* **12**, 2473–2486 (2006).
6. Azmitia, E. C. Evolution of serotonin : sunlight to suicide. *Handb. Behav. Neurosci.* **31**, 3–22 (2020).
7. Jéquier, E., Lovenberg, W. & Sjoerdsma, A. Tryptophan hydroxylase inhibition: the mechanism by which p-chlorophenylalanine depletes rat brain serotonin. *Mol. Pharmacol.* **3**, 274–278 (1967).
8. Donner, N. & Handa, R. J. Estrogen receptor beta regulates the expression of tryptophan-hydroxylase 2 mRNA within serotonergic neurons of the rat dorsal raphe nuclei. *Neuroscience* **163**, 705–718 (2009).
9. Nelson, D. L. 5-HT-5 receptors. *Curr. Drug Targets CNS Neurol. Disord.* **3**, 53–58 (2004).
10. Shih, J. C. Monoamine oxidase isoenzymes: genes, functions and targets for behavior and cancer therapy. *J. Neural Transm.* **125**, 1553–1566 (2018).
11. Aznar, S. & Hervig, M. E. S. The 5-HT_{2A} serotonin receptor in executive function: Implications for neuropsychiatric and neurodegenerative diseases. *Neurosci. Biobehav. Rev.* **64**, 63–82 (2016).
12. Beliveau, V. *et al.* A high-resolution in vivo atlas of the human brain’s serotonin system. *J. Neurosci.* **37**, 120–128 (2017).
13. López-Giménez, J. F. & González-Maeso, J. Hallucinogens and serotonin 5-HT_{2A} receptor-mediated signaling pathways. *Curr. Top. Behav. Neurosci.* **36**, 45–73 (2018).
14. Varnäs, K., Halldin, C. & Hall, H. Autoradiographic distribution of serotonin transporters and receptor subtypes in human brain. *Hum. Brain Mapp.* **22**, 246–260 (2004).
15. Jakab, R. L. & Goldman-Rakic, P. S. 5-Hydroxytryptamine_{2A} serotonin receptors in the primate cerebral cortex: Possible site of action of hallucinogenic and antipsychotic drugs in pyramidal cell apical dendrites. *Proc. Natl. Acad. Sci. U. S. A.* **95**, 735–740 (1998).
16. López-Giménez, J. F., Vilaró, M. T., Palacios, J. M. & Mengod, G. Mapping of 5-HT_{2A} receptors and their mRNA in monkey brain: [3H]MDL100,907 autoradiography and in situ hybridization studies. *J. Comp. Neurol.* **429**, 571–589 (2001).
17. Weber, E. T. & Andrade, R. Htr_{2a} gene and 5-HT_{2A} receptor expression in the cerebral cortex studied using genetically modified mice. *Front. Neurosci.* **4**, 1–12 (2010).
18. Marin, P. *et al.* Classification and signaling characteristics of 5-HT receptors: toward

- the concept of 5-HT receptosomes. *Handb. Behav. Neurosci.* **31**, 91–120 (2020).
19. Kurrasch-Orbaugh, D. M., Watts, V. a L. J., Barker, E. L. & Nichols, D. E. Phospholipase C and Phospholipase A2 Signaling Pathways Have Different Receptor Reserves. *J Pharmacol Exp Ther.* **304**, 229–237 (2003).
 20. Raymond, J. R. *et al.* Multiplicity of mechanisms of serotonin receptor signal transduction. *Pharmacol. Ther.* **92**, 179–212 (2001).
 21. Bockaert, J., Claeysen, S., Bécamel, C., Dumuis, A. & Marin, P. Neuronal 5-HT metabotropic receptors: Fine-tuning of their structure, signaling, and roles in synaptic modulation. *Cell Tissue Res.* **326**, 553–572 (2006).
 22. Bhatnagar, A. *et al.* The Dynamin-dependent, Arrestin-independent Internalization of 5-Hydroxytryptamine 2A (5-HT_{2A}) Serotonin Receptors Reveals Differential Sorting of Arrestins and 5-HT_{2A} Receptors during Endocytosis. *J. Biol. Chem.* **276**, 8269–8277 (2001).
 23. Carlsson, A. Does dopamine play a role in schizophrenia? *Psychol. Med.* **7**, 583–597 (1977).
 24. Geyer, M. A. & Vollenweider, F. X. Serotonin research: Contributions to understanding psychoses. *Trends Pharmacol. Sci.* **29**, 445–453 (2008).
 25. Ebdrup, B. H., Rasmussen, H., Arnt, J. & Glenthøj, B. Serotonin 2A receptor antagonists for treatment of schizophrenia. *Expert Opin. Investig. Drugs* **20**, 1211–1223 (2011).
 26. Rasmussen, H. *et al.* Decreased Frontal Serotonin_{2A} Receptor Binding in Antipsychotic-Naive Patients With First-Episode Schizophrenia. *Arch Gen Psychiatry* **67**, 9–16 (2010).
 27. Hurlemann, R. *et al.* 5-HT_{2A} receptor density is decreased in the at-risk mental state. *Psychopharmacology (Berl)*. **195**, 579–590 (2008).
 28. Schildkraut, J. J. The catecholamine hypothesis of affective disorders: a review of supporting evidence. *Am. J. Psychiatry* **122**, 509–522 (1965).
 29. Lapin, I. P. & Oxenkrug, G. F. Intensification of the central serotonergic processes as a possible determinant of the thymoleptic effect. *Lancet* **293**, 132–136 (1969).
 30. Savitz, J. B. & Drevets, W. C. Neuroreceptor imaging in depression. *Neurobiol. Dis.* **52**, 49–65 (2013).
 31. Frokjaer, V. G. *et al.* Frontolimbic Serotonin 2A Receptor Binding in Healthy Subjects Is Associated with Personality Risk Factors for Affective Disorder. *Biol. Psychiatry* **63**, 569–576 (2008).
 32. Guiard, B. P. & Di Giovanni, G. Central serotonin-2A (5-HT_{2A}) receptor dysfunction in depression and epilepsy: The missing link? *Front. Pharmacol.* **6**, 1–17 (2015).
 33. Spies, M. *et al.* Common HTR_{2A} variants and 5-HTTLPR are not associated with human in vivo serotonin 2A receptor levels. *Hum. Brain Mapp.* 1–11 (2020). doi:10.1002/hbm.25138
 34. Osmond, H. A Review of the Clinical Effects of Psychotomimetic Agents. *Ann. N. Y. Acad. Sci.* **66**, 418–434 (1957).
 35. Nichols, D. E. Psychedelics. *Pharmacol Rev* **68**, 264–355 (2016).
 36. Hofmann, A. How LSD originated†. *J. Psychedelic Drugs* **11**, 53–60 (1979).
 37. Whitaker-Azmitia, P. M. The discovery of serotonin and its role in neuroscience. *Neuropsychopharmacology* **21**, 2S-8S (1999).
 38. González-Maeso, J. *et al.* Hallucinogens Recruit Specific Cortical 5-HT_{2A} Receptor-Mediated Signaling Pathways to Affect Behavior. *Neuron* **53**, 439–452 (2007).
 39. Tyls, F., Páleníček, T. & Horáček, J. Psilocybin - Summary of knowledge and new

- perspectives. *Eur. Neuropsychopharmacol.* **24**, 342–356 (2014).
40. Moreno, J. L., Holloway, T., Albizu, L., Sealfon, S. C. & González-Maeso, J. Metabotropic glutamate mGlu2 receptor is necessary for the pharmacological and behavioral effects induced by hallucinogenic 5-HT_{2A} receptor agonists. *Neurosci. Lett.* **493**, 76–79 (2011).
 41. Hasler, F., Bourquin, D., Brenneisen, R., Bär, T. & Vollenweider, F. X. Determination of psilocin and 4-hydroxyindole-3-acetic acid in plasma by HPLC-ECD and pharmacokinetic profiles of oral and intravenous psilocybin in man. *Pharm. Acta Helv.* **72**, 175–184 (1997).
 42. Hasler, F., Grimberg, U., Benz, M. A., Huber, T. & Vollenweider, F. X. Acute psychological and physiological affects of psilocybin in healthy humans: A double-blind, placebo-controlled dose-effect study. *Psychopharmacology (Berl)*. **172**, 145–156 (2004).
 43. Carhart-Harris, R. L. *et al.* The administration of psilocybin to healthy, hallucinogen-experienced volunteers in a mock-functional magnetic resonance imaging environment: A preliminary investigation of tolerability. *J. Psychopharmacol.* **25**, 1562–1567 (2011).
 44. MacLean, K. A., Johnson, M. W. & Griffiths, R. R. Mystical Experiences Occasioned by the Hallucinogen Psilocybin Lead to Increases in the Personality Domain of Openness. *J. Psychopharmacol.* **25**, 1453–1461 (2011).
 45. Griffiths, R. R. *et al.* Psilocybin occasioned mystical-type experiences: Immediate and persisting dose-related effects. *Psychopharmacology (Berl)*. **218**, 649–665 (2011).
 46. Griffiths, R. R., Richards, W. A., McCann, U. & Jesse, R. Psilocybin can occasion mystical-type experiences having substantial and sustained personal meaning and spiritual significance. *Psychopharmacology (Berl)*. **187**, 268–283 (2006).
 47. Griffiths, R. R. *et al.* Mystical-type experiences occasioned by psilocybin mediate the attribution of personal meaning and spiritual significance 14 months later. *J. Psychopharmacol.* **22**, 621–32 (2008).
 48. Johnson, M. W., Garcia-Romeu, A., Cosimano, M. P. & Griffiths, R. R. Pilot Study of the 5-HT_{2A} R Agonist Psilocybin in the Treatment of Tobacco Addiction. *J. Psychopharmacol.* **28**, 983–992 (2014).
 49. Bogenschutz, M. P. *et al.* Psilocybin-assisted treatment for alcohol dependence: A proof-of-concept study. *J. Psychopharmacol.* **29**, 289–299 (2015).
 50. Carhart-Harris, R. L. *et al.* Psilocybin with psychological support for treatment-resistant depression: An open-label feasibility study. *The Lancet Psychiatry* **3**, 619–627 (2016).
 51. Grob, C. S. *et al.* Pilot study of psilocybin treatment for anxiety in patients with advanced-stage cancer. *Arch. Gen. Psychiatry* **68**, 71–78 (2011).
 52. Waddington, C. H. The epigenotype. *Int. J. Epidemiol.* **41**, 10–13 (2012).
 53. Inbar-Feigenberg, M., Choufani, S., Butcher, D. T., Roifman, M. & Weksberg, R. Basic concepts of epigenetics. *Fertil. Steril.* **99**, 607–15 (2013).
 54. Kouzarides, T. Chromatin modifications and their function. *Cell* **128**, 693–705 (2007).
 55. Moore, L. D., Le, T. & Fan, G. DNA methylation and its basic function. *Neuropsychopharmacology* **38**, 23–38 (2013).
 56. Allis, C. D. & Jenuwein, T. The molecular hallmarks of epigenetic control. *Nat. Rev. Genet.* **17**, 487–500 (2016).

57. Yan, M. S.-C., Matouk, C. C. & Marsden, P. A. Epigenetics of the vascular endothelium. *J. Appl. Physiol.* **109**, 916–926 (2010).
58. Bernstein, B. E., Meissner, A. & Lander, E. S. The mammalian epigenome. *Cell* **128**, 669–81 (2007).
59. Sterner, D. E. & Berger, S. L. Acetylation of Histones and Transcription-Related Factors. *Microbiol. Mol. Biol. Rev.* **64**, 435–459 (2000).
60. Seto, E. & Yoshida, M. Erasers of Histone Acetylation: The Histone Deacetylase Enzymes. *Cold Spring Harb. Perspect. Biol.* **6**, (2014).
61. Lv, J., Xin, Y., Zhou, W. & Qiu, Z. The epigenetic switches for neural development and psychiatric disorders. *J. Genet. Genomics* **40**, 339–346 (2013).
62. Wang, C. *et al.* In vivo imaging of histone deacetylases (HDACs) in the central nervous system and major peripheral organs. *J. Med. Chem.* **57**, 7999–8009 (2014).
63. Duenas-Gonzalez, A. *et al.* Valproic acid as epigenetic cancer drug: Preclinical, clinical and transcriptional effects on solid tumors. *Cancer Treat. Rev.* **34**, 206–222 (2008).
64. Phiel, C. J. *et al.* Histone Deacetylase Is a Direct Target of Valproic Acid, a Potent Anticonvulsant, Mood Stabilizer, and Teratogen. *J. Biol. Chem.* **276**, 36734–36741 (2001).
65. Citrome, L. *et al.* Adjunctive Divalproex and Hostility among Patients with Schizophrenia Receiving Olanzapine or Risperidone. *Psychiatr. Serv.* **55**, 290–294 (2004).
66. Chuang, D. M., Leng, Y., Marinova, Z., Kim, H. J. & Chiu, C. T. Multiple roles of HDAC inhibition in neurodegenerative conditions. *Trends Neurosci.* **32**, 591–601 (2009).
67. Nestler, MD, P. Epigenetic Mechanism of Depression. *Journal* **71**, 454–456 (2014).
68. Kelly, D. L. *et al.* Adjunct divalproex or lithium to clozapine in treatment-resistant schizophrenia. *Psychiatr. Q.* **77**, 81–95 (2006).
69. Kurita, M. *et al.* HDAC2 regulates atypical antipsychotic responses through the modulation of mGlu2 promoter activity. *Nat. Neurosci.* **15**, 1245–1254 (2012).
70. Hendricks, J. A. *et al.* In vivo PET imaging of histone deacetylases by 18F-suberoylanilide hydroxamic acid (18F-SAHA). *J. Med. Chem.* **54**, 5576–5582 (2011).
71. Hooker, J. M. *et al.* Histone deacetylase inhibitor MS-275 exhibits poor brain penetration: Pharmacokinetic studies of [11C]MS-275 using positron emission tomography. *ACS Chem. Neurosci.* **1**, 65–73 (2010).
72. Reid, A. E. *et al.* Evaluation of 6-[[18F]fluoroacetamido)-1-hexanoicanilide for PET imaging of histone deacetylase in the baboon brain. *Nucl. Med. Biol.* **36**, 247–258 (2009).
73. Schroeder, F. A. *et al.* PET imaging demonstrates histone deacetylase target engagement and clarifies brain penetrance of known and novel small molecule inhibitors in rat. *ACS Chem. Neurosci.* **5**, 1055–1062 (2014).
74. Donovan, L. *et al.* Imaging HDACs in vivo: cross-validation of the [11C]Martinostat radioligand in the pig brain. *Mol. Imaging Biol.* 1–18 (2019). doi:10.1007/s11307-019-01403-9
75. Gilbert, T. M. *et al.* Neuroepigenetic signatures of age and sex in the living human brain. *Nat. Commun.* **10**, 1–9 (2019).
76. Wey, H.-Y. *et al.* Insights into neuroepigenetics through human histone deacetylase PET imaging. *Sci. Transl. Med.* **8**, 1–10 (2016).
77. Wey, H.-Y. *et al.* Kinetic Analysis and Quantification of [11C]Martinostat for in Vivo HDAC Imaging of the Brain. *ACS Chem. Neurosci.* **6**, 708–715 (2015).

78. Gilbert, T. M. *et al.* PET neuroimaging reveals histone deacetylase dysregulation in schizophrenia. *J. Clin. Invest.* **129**, (2018).
79. Lind, N. M. *et al.* The use of pigs in neuroscience: Modeling brain disorders. *Neurosci. Biobehav. Rev.* **31**, 728–751 (2007).
80. Niblock, M. M. *et al.* Comparative anatomical assessment of the piglet as a model for the developing human medullary serotonergic system. *Brain Res. Rev.* **50**, 169–183 (2005).
81. Cumming, P. *et al.* A PET study of effects of chronic 3,4-methylenedioxymethamphetamine (MDMA, ‘ecstasy’) on serotonin markers in Göttingen minipig brain. *Synapse* **61**, 478–487 (2007).
82. Hansen, H. D. *et al.* Direct comparison of [18F]MH.MZ and [18F]altanserin for 5-HT_{2A} receptor imaging with PET. *Synapse* **67**, 328–337 (2013).
83. Kornum, B. R. *et al.* Evaluation of the novel 5-HT₄ receptor PET ligand [11C]SB207145 in the Göttingen minipig. *J. Cereb. Blood Flow Metab.* **29**, 186–196 (2009).
84. Heurling, K. *et al.* Quantitative positron emission tomography in brain research. *Brain Res.* **1670**, 220–234 (2017).
85. Suzuki, M. *Molecular imaging leads a revolution in diagnosis and drug discovery.* *Frontline* **4**, (2009).
86. Leth-Petersen, S. *et al.* Metabolic Fate of Hallucinogenic NBOMes. *Chem. Res. Toxicol.* **29**, 96–100 (2016).
87. Gillings, N. A restricted access material for rapid analysis of [11C]-labeled radiopharmaceuticals and their metabolites in plasma. *Nucl. Med. Biol.* **36**, 961–965 (2009).
88. Villadsen, J. *et al.* Automatic delineation of brain regions on MRI and PET images from the pig. *J. Neurosci. Methods* **294**, 51–58 (2017).
89. Mintun, M. A., Raichle, M. E., Kilbourn, M. R., Wooten, G. F. & Welch, M. J. A quantitative model for the in vivo assessment of drug binding sites with positron emission tomography. *Ann. Neurol.* **15**, 217–227 (1984).
90. Gunn, R. N., Gunn, S. R. & Cunningham, V. J. Positron emission tomography compartmental models. *J. Cereb. Blood Flow Metab.* **21**, 635–652 (2001).
91. Innis, R. B. *et al.* Consensus Nomenclature for in vivo Imaging of Reversibly Binding Radioligands. *J. Cereb. Blood Flow Metab.* **27**, 1533–1539 (2007).
92. Cunningham, V. J., Rabiner, E. a, Slifstein, M., Laruelle, M. & Gunn, R. N. Measuring drug occupancy in the absence of a reference region: the Lassen plot re-visited. *J. Cereb. blood flow Metab.* **30**, 46–50 (2010).
93. Lassen, N. A. *et al.* Benzodiazepine receptor quantification in vivo in humans using [11C]flumazenil and PET: Application of the steady-state principle. *J. Cereb. Blood Flow Metab.* **15**, 152–165 (1995).
94. Logan, J. Graphical analysis of PET data applied to reversible and irreversible tracers. *Nucl. Med. Biol.* **27**, 661–670 (2000).
95. Ichise, M., Toyama, H., Innis, R. B. & Carson, R. E. Strategies to improve neuroreceptor parameter estimation by linear regression analysis. *J. Cereb. Blood Flow Metab.* **22**, 1271–1281 (2002).
96. Akaike, H. A New Look at the Statistical Model Identification. *IEEE Trans. Automat. Contr.* **ac-19**, 716–723 (1974).
97. Posch, A., Kohn, J., Oh, K., Hammond, M. & Liu, N. V3 Stain-free Workflow for a

- Practical, Convenient, and Reliable Total Protein Loading Control in Western Blotting. *J. Vis. Exp.* 1–9 (2013). doi:10.3791/50948
98. Inc., A. Next Generation Sequencing Service. Available at: <https://www.abmgood.com/Next-Generation-Sequencing-Service.html>. (Accessed: 22nd February 2020)
99. Gu, Y. *et al.* Investigation of the expression patterns and correlation of DNA methyltransferases and class I histone deacetylases in ovarian cancer tissues. *Oncol. Lett.* **5**, 452–458 (2013).
100. Jurkin, J. *et al.* Distinct and redundant functions of histone deacetylases HDAC1 and HDAC2 in proliferation and tumorigenesis. *Cell Cycle* **10**, 406–412 (2011).
101. Wilting, R. H. *et al.* Overlapping functions of Hdac1 and Hdac2 in cell cycle regulation and haematopoiesis. *EMBO J.* **29**, 2586–2597 (2010).
102. Somanath, P., Herndon Klein, R. & Knoepfler, P. S. CRISPR-mediated HDAC2 disruption identifies two distinct classes of target genes in human cells. *PLoS One* **12**, 1–21 (2017).
103. Wang, C. *et al.* In vivo imaging of histone deacetylases (HDACs) in the central nervous system and major peripheral organs. *J. Med. Chem.* **57**, 7999–8009 (2014).
104. Zhu, M. M. *et al.* The pharmacogenomics of valproic acid. *J. Hum. Genet.* **62**, 1009–1014 (2017).
105. Göttlicher, M. *et al.* Valproic acid defines a novel class of HDAC inhibitors inducing differentiation of transformed cells. *EMBO J.* **20**, 6969–6978 (2001).
106. Jørgensen, L. M. *et al.* Cerebral 5-HT release correlates with [11C]Cimbi36 PET measures of 5-HT_{2A} receptor occupancy in the pig brain. *J. Cereb. Blood Flow Metab.* 1–10 (2016). doi:10.1177/0271678X16629483
107. Madsen, M. K. *et al.* Psychedelic effects of psilocybin correlate with serotonin 2A receptor occupancy and plasma psilocin levels. *Neuropsychopharmacology* **44**, 1328–1334 (2019).
108. Halberstadt, A. L. & Geyer, M. A. Characterization of the head-twitch response induced by hallucinogens in mice: Detection of the behavior based on the dynamics of head movement. *Psychopharmacology (Berl)*. **227**, 727–739 (2013).
109. Halberstadt, A. L. & Geyer, M. A. Effect of hallucinogens on unconditioned behavior. *Curr. Top. Behav. Neurosci.* **36**, 159–199 (2018).
110. Löscher, W., Witte, U., Fredow, G., Ganter, M. & Bickhardt, K. Pharmacodynamic effects of serotonin (5-HT) receptor ligands in pigs: stimulation of 5-HT₂ receptors induces malignant hyperthermia. *Naunyn. Schmiedebergs. Arch. Pharmacol.* **341**, 483–493 (1990).
111. Löscher, W., Witte, U., Fredow, G., Traber, J. & Glaser, T. The behavioural responses to 8-OH-DPAT, ipsapirone and the novel 5-HT_{1A} receptor agonist Bay Vq 7813 in the pig. *Naunyn. Schmiedebergs. Arch. Pharmacol.* **342**, 271–277 (1990).
112. Swerts, S. *et al.* Allergy to illicit drugs and narcotics. *Clin. Exp. Allergy* **44**, 307–318 (2014).
113. PDSP Database - UNC. Available at: <https://pdsp.unc.edu/databases/dataMining/viewKiGraph.php>. (Accessed: 16th February 2020)
114. O’Dowd, A. & Miller, D. J. Analysis of an H₁ receptor-mediated, zinc-potentiated vasoconstrictor action of the histidyl dipeptide carnosine in rabbit saphenous vein. *Br. J. Pharmacol.* **125**, 1272–1280 (1998).

115. Carhart-Harris, R. L. *et al.* Neural correlates of the psychedelic state as determined by fMRI studies with psilocybin. *Proc. Natl. Acad. Sci. U. S. A.* **109**, 2138–43 (2012).
116. Dyrvig, M., Christiansen, S. H., Woldbye, D. P. D. & Lichota, J. Temporal gene expression profile after acute electroconvulsive stimulation in the rat. *Gene* **539**, 8–14 (2014).
117. Köhler, O., Krogh, J., Mors, O. & Benros, M. E. Inflammation in Depression and the Potential for Anti-Inflammatory Treatment. *Curr. Neuropharmacol.* **14**, 732–742 (2016).
118. Rho, M. *et al.* A potential role for interferon- α in the pathogenesis of HIV-associated dementia. *Brain. Behav. Immun.* **9**, 366–377 (1995).
119. Bonaccorso, S. *et al.* Immunotherapy with interferon-alpha in patients affected by chronic hepatitis C induces an intercorrelated stimulation of the cytokine network and an increase in depressive and anxiety symptoms. *Psychiatry Res.* **105**, 45–55 (2001).
120. Flanagan, T. W. & Nichols, C. D. Psychedelics as anti-inflammatory agents. *Int. Rev. Psychiatry* **0**, 1–13 (2018).
121. Ly, C. *et al.* Psychedelics Promote Structural and Functional Neural Plasticity. *Cell Rep.* **23**, 3170–3182 (2018).
122. Bajjalieh, S. M., Frantz, G. D., Weimann, J. M., McConnell, S. K. & Scheller, R. H. Differential expression of synaptic vesicle protein 2 (SV2) isoforms. *J. Neurosci.* **14**, 5223–5235 (1994).
123. Germann, C. B. The Psilocybin-Telomere Hypothesis: An empirically falsifiable prediction concerning the beneficial neuropsychopharmacological effects of psilocybin on genetic aging. *Med. Hypotheses* **134**, 109406 (2020).
124. Li, A. Y.-J. *et al.* High-Mobility Group A2 Protein Modulates hTERT Transcription To Promote Tumorigenesis. *Mol. Cell. Biol.* **31**, 2605–2617 (2011).
125. Adams, K. H. *et al.* A database of [18F]-altanserin binding to 5-HT_{2A} receptors in normal volunteers: Normative data and relationship to physiological and demographic variables. *Neuroimage* **21**, 1105–1113 (2004).
126. Moses, E. L. *et al.* Effects of estradiol and progesterone administration on human serotonin 2A receptor binding: A PET study. *Biol. Psychiatry* **48**, 854–860 (2000).
127. Joksimovic, S. M. *et al.* Histone deacetylase inhibitor entinostat (MS-275) restores anesthesia-induced alteration of inhibitory synaptic transmission in the developing rat hippocampus. *Mol. Neurobiol.* **55**, 22–228 (2018).
128. Matveychuk, D. *et al.* Ketamine as an antidepressant: overview of its mechanisms of action and potential predictive biomarkers. *Ther. Adv. Psychopharmacol.* **10**, 204512532091665 (2020).
129. Bahr, R., Lopez, A. & Rey, J. A. Intranasal esketamine (Spravato™) for use in treatment-resistant depression in conjunction with an oral antidepressant. *P T* **44**, 340–375 (2019).
130. Carhart-Harris, R. L. *et al.* Psilocybin with psychological support for treatment-resistant depression: An open-label feasibility study. *The Lancet Psychiatry* **3**, 619–627 (2016).
131. serotonergic receptors pdf editor » rocitumbpred.gq. Available at: <http://rocitumbpred.gq/serotonergic-receptors-pdf-editor>. (Accessed: 28th February 2020)

Paper I

LL Donovan, JH Magnussen, A Dyssegaard,
S Lehel, JM Hooker, GM Knudsen, HD Hansen

Imaging HDACs *In Vivo*: Cross-Validation of the
[¹¹C]Martinostat Radioligand in the Pig Brain

Molecular Imaging and Biology 2019
10.1007/s11307-019-01403-9



Mol Imaging Biol (2019)
DOI: 10.1007/s11307-019-01403-9
© World Molecular Imaging Society, 2019



RESEARCH ARTICLE

Imaging HDACs *In Vivo*: Cross-Validation of the [¹¹C]Martinostat Radioligand in the Pig Brain

L. L. Donovan,^{1,2} J. H. Magnussen,¹ A. Dyssegaard,¹ S. Lehel,³ J. M. Hooker,⁴
G. M. Knudsen,^{1,2} H. D. Hansen¹

¹Neurobiology Research Unit and Center for NeuroPharm, Copenhagen University Hospital Rigshospitalet, 9 Blegdamsvej, 2100, Copenhagen O, Denmark

²Faculty of Health and Medical Sciences, University of Copenhagen, 2200, Copenhagen N, Denmark

³PET and Cyclotron Unit, Copenhagen University Hospital Rigshospitalet, 2100, Copenhagen O, Denmark

⁴MGH/HST A. A. Martinos Center for Biomedical Imaging, Massachusetts General Hospital, Charlestown, MA, 02129, USA

Abstract

Purpose: With the emerging knowledge about the impact of epigenetic alterations on behavior and brain disorders, the ability to measure epigenetic alterations in brain tissue *in vivo* has become critically important. We present the first *in vivo/in vitro* cross-validation of the novel positron emission tomography (PET) radioligand [¹¹C]Martinostat in the pig brain with regard to its ability to measure histone deacetylase 1–3 (HDAC1–3) levels *in vivo*.

Procedures: Nine female Danish landrace pigs underwent 121-min dynamic PET scans with [¹¹C]Martinostat. We quantified [¹¹C]Martinostat uptake using both a simple ratio method and kinetic models with arterial input function. By the end of the scan, the animals were euthanized and the brains were extracted. We measured HDAC1–3 protein levels in frontal cortex, cerebellum vermis, and hippocampus and compared the protein levels and regional outcome values to the [¹¹C]Martinostat PET quantification.

Results: [¹¹C]Martinostat distributed widely across brain regions, with the highest uptake in the cerebellum vermis and the lowest in the olfactory bulbs. Based on the Akaike information criterion, the quantification was most reliably performed by Ichise MA1 kinetic modeling, but since the radioligand displayed very slow kinetics, we also calculated standard uptake value (SUV) ratios which correlated well with V_T . The western blots revealed higher brain tissue protein levels of HDAC1/2 compared to HDAC3, and HDAC1 and HDAC2 levels were highly correlated in all three investigated brain regions. The *in vivo* SUV ratio measure correlated well with the *in vitro* HDAC1–3 levels, whereas no correlation was found between V_T values and HDAC levels.

Conclusions: We found good correlation between *in vivo* measured SUV ratios and *in vitro* measures of HDAC 1–3 proteins, supporting that [¹¹C]Martinostat provides a good *in vivo* measure of the cerebral HDAC1–3 protein levels.

Key words: Positron emission tomography, Martinostat, Epigenetics, Histone deacetylase, Pig, Western blot, HDAC1, HDAC2, HDAC3, Brain

Electronic supplementary material The online version of this article (<https://doi.org/10.1007/s11307-019-01403-9>) contains supplementary material, which is available to authorized users.

Correspondence to: H. Hansen; e-mail: hanne.d.hansen@nru.dk

Published online: 09 July 2019

Introduction

Epigenetic modifying enzymes, such as histone deacetylase (HDAC), have received increasing attention over the last decades, since they have been recognized as part of the pathophysiology of multiple neurological and psychiatric pathologies, such as Parkinson's disease, Alzheimer's disease, and depression (for review, see [1, 2]), and are therefore potential diagnostic and therapeutic targets [3]. HDAC proteins are epigenetic modifiers which deacetylate histone tails, resulting in decreased gene transcription. Until the development of the positron emission tomography (PET) radioligand [¹¹C]Martinostat in 2014 [4], however, molecular investigations of cerebral epigenetic alterations had been confined to animal studies or postmortem human brain examinations.

[¹¹C]Martinostat is an adamantane-based hydroxamic acid, which is able to image HDAC paralogs 1, 2, and 3, and has very minimal off-target binding [4]. *In vitro* assays determined a partition coefficient (log D) of 2.03 for [¹¹C]Martinostat, and IC₅₀ values in the nanomolar range for all three targets: HDAC1 = 0.3 nM, HDAC2 = 2.0 nM, and HDAC3 = 0.6 nM [4]. The radioligand has good brain penetrance, with a peak brain concentration after 20 min in non-human primates [5]. [¹¹C]Martinostat has been tested in rodents, non-human primates, and humans [3–7]; however, we report the first direct comparison of *in vitro* and *in vivo* measures of HDAC1–3. We chose to perform this cross-validation of [¹¹C]Martinostat in pigs, because the pig offers several advantages as an animal model compared to rodents: The brain is gyrencephalic like the human brain, and the size is substantially larger than that of mice and rats, which provides a better match to the spatial resolution of PET scans and a tremendous amount of postmortem tissue for further molecular investigations. Being a large animal, the pig also allows for acquiring an arterial input function during the PET scan, and this is a requirement to calculate the total distribution volume (V_T). Therefore, the increased housing cost and handling difficulties, compared to rodents, are made up for in data quality. Finally, studies in pigs are cheaper and the use of pigs is not considered as ethically challenging as in non-human primates. The use of pigs thus does not necessitate that they are reused for many different experiments, and this rules out concerns about carry-over effects from previous experiments. However, the Danish Landrace pigs used in this study is bred to grow fast, so longitudinal studies require a different breed of pigs, e.g., Göttingen minipigs.

Materials and Methods

Radiochemistry

[¹¹C]Martinostat was prepared at the Copenhagen University Hospital Rigshospitalet using carbon-11 methyl iodide in a modified procedure, as described earlier by Wang et al. [4].

[¹¹C]Martinostat yields ranged from 235 to 730 MBq and molar radioactivity ranged from 30 to 709 GBq/μmol at end-of-synthesis.

Animals

Nine female pigs (crossbreed of Landrace × Yorkshire × Duroc) weighing 20–22 kg (approx. 9 weeks old) were used in the present study. Animals were sourced from a local farm and acclimatized for 7–9 days in an enriched environment prior to experiments. For PET scanning, anesthesia was induced approx. 3 h prior to scanning by i.m. injection of 0.13 ml/kg zoletil veterinary mixture (11.36 mg/mL xylazine, 11.36 mg/ml ketamine, 1.82 mg/ml butorphanol, 1.82 mg/ml methadone) and maintained by 15 mg/kg/h propofol infusion i.v. Femoral arteries and mammary veins were used for i.v. access. Endotracheal intubation allowed for ventilation with 20 % oxygen in air at 10 ml/kg. Urine catheter was placed to avoid discomfort and stress. The animals were closely monitored throughout the experiment, with peripheral O₂ and end-tidal CO₂ saturation, heart rate, blood pressure, and temperature. The animals were terminated by 15 ml pentobarbital/lidocaine i.v. injection. After euthanasia, the brains were swiftly removed, snap frozen on dry-ice, and stored at –80 °C until use. All animal procedures were performed in accordance with the European Commission's Directive 2010/63/EU, approved by the Danish Council of Animal Ethics (Journal no. 2012-15-2934-00156), and were in compliance with the ARRIVE guidelines.

PET Scanning Protocol

The pigs were PET-scanned with a high-resolution research tomograph (HRRT) scanner (CPS Innovations/Siemens, USA). Data acquisition lasted 121 min after a bolus injection of [¹¹C]Martinostat. Injected dose was 334.3 ± 99.1 MBq (mean ± SD) while injected mass was 0.87 ± 0.94 μg (mean ± SD). In one pig, we performed a self-blocking study with a bolus injection of 0.5 mg/kg cold Martinostat, administered immediately prior to injection of [¹¹C]Martinostat. The unlabeled Martinostat was dissolved in DMSO and diluted in sterile water to reach a 10 % DMSO solution.

Blood Sampling and Analyses

Manual arterial blood samples were drawn at 2.5, 5, 10, 20, 30, 45, 60, 90, and 121 min after injection, while an ABSS autosampler (Allogg Technology, Sweden) continuously measured arterial whole blood radioactivity during the first 30 min. Manual blood samples were collected for measurements of total radioactivity in whole blood and plasma using a gamma well counter (Cobra 5003; Packard Instruments, Meriden, USA). Radiolabeled parent and metabolite

Donovan L.L. et al.: HDAC1–3 in the Pig Brain

fractions were determined in plasma using an automatic column-switching radio-HPLC (high-performance liquid chromatography) as previously described [8], but with some modifications. Up to 4 ml of filtered but otherwise unadulterated plasma was loaded onto a Shimadzu Shimpack MAYI-ODS column (30 × 4.6 mm, 50 μm, Holm&Halby, Denmark) to trap lipophilic component of the plasma sample using a mixture of 20 mM disodium hydrogen phosphate, 2 mM sodium 1-decane sulfonate, and 2 % 2-propanol. The mobile phase was adjusted to pH 7.2 with phosphoric acid. After a 4-min extraction phase, the trapping column was eluted, by reversed direction of flow, with analysis eluent consisting of 24 % acetonitrile in 100 mM sodium dihydrogen phosphate (pH 2.6) containing 5 mM sodium 1-decane sulfonate. The analysis eluent was then passed through an analytical column (Onyx Monolithic C-18, 50 × 4.6 mm, Phenomenex Aps, Denmark) to separate the retained components. Flow rate was adjusted to 5 ml/min and the total analysis time was 8.5 min. To increase sensitivity in samples with low levels of radioactivity, eluents (10 ml) from the HPLC were collected with a fraction collector (Foxy Jr FC144; Teledyne, Lincoln, NE, USA), and fractions were counted offline in a gamma well counter (2480 Wizard2 Automatic Gamma Counter, Wallac Oy, Turku, Finland).

PET Quantification

The PET emission data was reconstructed into time frames of increasing lengths: 6 × 10, 6 × 20, 4 × 30, 9 × 60, 8 × 120, 4 × 180, 2 × 240, 1 × 300, 1 × 360, 1 × 420, 1 × 600, 1 × 900, 1 × 1680 s. The reconstruction used an ordinary Poisson three-dimensional ordered-subset expectation maximization with point spread function modeling (OP-3D-OSEM-PSF), 16 subsets and 10 iterations [9, 10] with all standard corrections. Attenuation correction was done using the HRRT maximum *a posteriori* transmission reconstruction method (MAP-TR) μ-map [11]. Images consist of 207 planes of 256 × 256 voxels of 1.22 × 1.22 × 1.22 mm in size.

Brain parcellation was performed according to the newly developed PET-MRI (magnetic resonance imaging) pig brain atlas method [12]. The input for the methodology was frame-length weighted, summed PET images of the total scan time (0–121 min). The extracted regional radioactive concentration (kBq/ml) was normalized to injected dose (MBq) and corrected for animal weight (kg) to give standardized uptake values (SUV, g/ml). The atlas contains 178 regions [13], but for the present study, only the cerebellum vermis, frontal cortex, hippocampus, and olfactory bulbs were compared to *in vitro* data. All graphical presentations were created using GraphPad Prism 7 (GraphPad, USA).

PMOD 3.7 (PMOD Technologies, Switzerland) was used for kinetic modeling. V_T values were calculated using the 1 tissue compartment (1TC), 2 tissue compartment (2TC),

Ichise Multilinear Analysis 1 (MA1), and Logan invasive models. For the MA1 and Logan models, all model fits were visually inspected with regard to the residuals to determine an optimal threshold time (t^*) for each region of interest (ROI), so to avoid frame-inclusion bias between scans. For each ROI and across all scans, we chose the earliest frame in which the residuals of the fit appeared normally distributed and in homoscedastic manner. For Logan modeling, t^* was 28 in frontal cortex, hippocampus, and olfactory bulbs and 24 for cerebellum vermis. In MA1 modeling cerebellum vermis and frontal cortex, t^* was 33, hippocampus 26, and olfactory bulbs 28.

For the self-block study, we calculated the occupancy and non-displaceable volume of distribution (V_{ND}) using the V_T values from the MA1 model in a Lassen plot [14]. Non-displaceable binding potentials (BP_{ND}) were determined by reverse calculations from MA1 $V_{T,S}$ using the formula:

$$BP_{ND} = (V_T - V_{ND}) / V_{ND}.$$

It has previously been suggested to use the SUV ratio (SUV_R) as a simplified quantification method [5]; here, we used linear regression to find the time (x) where a plateau of the time-activity curve was reached (slope of line = 0). For each scan and each ROI, an average SUV_{X-121} was calculated from timepoint x to the end of the scan (121 min). For the olfactory bulbs, which is here used as pseudo-reference region, the plateau was reached at 33 min. SUV_Rs are consequently calculated by dividing the ROI-SUV_{X-121} by the corresponding olfactory bulbs SUV₃₃₋₁₂₁, providing a SUV_{R,X-121}.

Nuclear Protein Extraction

Tissue samples from frontal cortex (605 mg ± 82), cerebellum vermis (424 mg ± 120), and hippocampus (537 mg ± 120) ($n = 9$ /region) were used for nuclear protein extraction. Tissue was homogenized in 10 ml ice-cold lysis buffer containing 0.4 M sucrose, 10 mM HEPES (pH 8), 5 mM β-mercaptoethanol, protease inhibitor cocktail (P8340, Sigma-Aldrich) using a Polytron PT1200 (Kinematica, Switzerland). Volume was adjusted to 30 ml with ice-cold lysis buffer, followed by centrifugation (20 min 3000 g 4 °C). The pellet was resuspended in 1 ml ice-cold buffer 2 containing 0.25 M sucrose, 10 mM HEPES (pH 8), 1 % Triton X-100, 10 mM MgCl₂, 5 mM β-mercaptoethanol, protease inhibitor cocktail (P8340, Sigma-Aldrich), transferred to low-bind protein microtubes (Sarstedt, Germany), and centrifuged (10 min 12,000 g 4 °C). The pelleted nuclei were lysed by 30 min ice-incubation in RIPA buffer (150 mM NaCl, 1 % Triton X-100, 0.5 % sodiumdeoxycholate, 1 % sodium dodecyl sulfate, 50 mM Tris-HCl, protease inhibitor cocktail (P8340, Sigma-

Aldrich)), followed by centrifugation (20 min 20,800 g 4 °C). Protein concentrations of the supernatants were determined using the *DC*TM Protein Assay (BioRad, USA) according to the manufacturer's protocol, including a serial dilution of known BSA concentration, and absorbance was measured by iMark Microplate Absorbance Reader (BioRad, USA).

Western Blotting

All reagents and equipment were from BioRad (USA), unless otherwise stated.

Nine micrograms nuclear protein was denatured in the presence of 4× Laemmli buffer supplemented with 10 % β-mercaptoethanol at 95 °C for 5 min. The samples were subjected to sodium dodecyl sulfate–polyacrylamide gel electrophoresis (SDS–PAGE) in CriterionTM TGX Stain-FreeTM Precast Gels at 200 V, and followingly blotted onto Immun-Blot® low fluorescence polyvinylidene difluoride (PVDF) membranes using the Trans-Blot® TurboTM 7 min standard program. After membrane washing 4× 5 min in TBS-T (10 % TBS pH 7.5, 0.1 % Tween-20), the membranes were blocked by 5 % Blotting-Grade Blocker in TBS for 1 h at RT. The membranes were incubated overnight at 4 °C in primary antibody solution with the following dilutions: HDAC1 1:10,000 (PA1–860, Thermo Scientific, USA), HDAC2 1:20,000 (PA1–861, Thermo Scientific, USA), HDAC3 1:1000 (PA1–862, Thermo Scientific, USA). Following 4× 5 min washing in TBS-T, the membranes were incubated in 1:2000 polyclonal goat anti-rabbit horseradish peroxidase (HRP)-conjugated secondary antibody (P0448, Dako, Denmark) for 1 h at RT. After washing the membrane 1× 15 min and 4× 5 min in TBS-T, Western Lightning ECL Pro (NEL121001EA, Perkin Elmer, USA) was used for visualization by 1 min incubation immediately before imaging by ChemiDoc XRS+.

Recombinant HDAC1–3 protein was kindly provided by Prof. Christian Olsen (Center for Biopharmaceuticals, University of Copenhagen). Calibration rows of known HDAC protein amounts were included in the workflow described above: HDAC1 5–250 ng (50,051, bpsbioscience, USA), HDAC2 5–250 ng (50,002, bpsbioscience, USA), and HDAC3 2.5–60 ng for frontal cortex and cerebellum vermis samples, and 1.25–40 ng for hippocampal samples (50,003, bpsbioscience, USA).

Image Lab 6.1 (BioRad, USA) was used for image analysis, with rolling disc (70 mm) background subtraction and total loaded protein normalization. Statistical tests were performed in GraphPad Prism 7 (GraphPad, USA). Quantified HDAC isoforms (X ng/μg nuclear protein) were directly correlated to one another. In order to compare the *in vitro* measured HDAC1–3 to the *in vivo* PET measure, the tissue volume and yield from protein extraction was corrected. Total HDAC per ml fresh brain tissue were determined as

$$\left(\frac{X \text{ nmol HDAC1-3}}{9 \mu\text{g protein}}\right) * \left(\frac{\text{total mg protein extracted}}{\text{total mL tissue used for extraction}}\right).$$

Results

Regional Distribution of HDAC Proteins

After injection of [¹¹C]Martinostat, we observed high brain uptake of the radioligand with a peak SUV of 4 in the cerebellum vermis. The kinetics of the radioligand was very slow, with no observable wash-out from any brain region during the 121 min acquisition time (Fig. 1a). [¹¹C]Martinostat showed a widespread regional distribution (Fig. 1d), with the highest uptake in cerebellum vermis and cortical areas and lowest uptake in olfactory bulbs and subcortical areas.

Self-Block Experiment

To investigate the specificity of [¹¹C]Martinostat, we co-administrated the radioligand with 0.5 mg/kg unlabeled Martinostat in a single pig. Co-administration reduced the radioactive signal substantially (Fig. 1c) and induced markedly faster radioligand kinetics (Fig. 1b), and all three regional time activity curves (TACs) approached that of the olfactory bulbs. As expected, blocking was associated with lower regional V_T values. The quantitative effect of co-administration of unlabeled Martinostat (0.5 mg/kg) was determined from the Lassen plot (Fig. 1c). We found 89 % occupancy of the administered Martinostat, and a V_{ND} of 2.87 ml/cm³.

Parent Compound Data

[¹¹C]Martinostat administration caused a rapid peak in plasma radioactivity (Fig. 2c), which plateaued around 20 min after injection and with a slight increase occurring at around 60 min. A representative [¹¹C]Martinostat radiochromatogram at 30 min after radiotracer injection is shown in Fig. 2a. The plasma parent fraction of [¹¹C]Martinostat decreased during the acquisition time, with approx. 60 % intact radioligand left after 30 min and 20 % at 121 min (Fig. 2b). The parent fraction was fitted to a 1-exponential curve, for quantification.

Quantification

Quantification of [¹¹C]Martinostat was performed with the 1-tissue compartment (TC), 2TC, Logan invasive, and MA1 kinetic models. Visual inspection of the fits revealed a general poor fit of the 1TC model whereas the 2TC model

Donovan L.L. et al.: HDAC1–3 in the Pig Brain

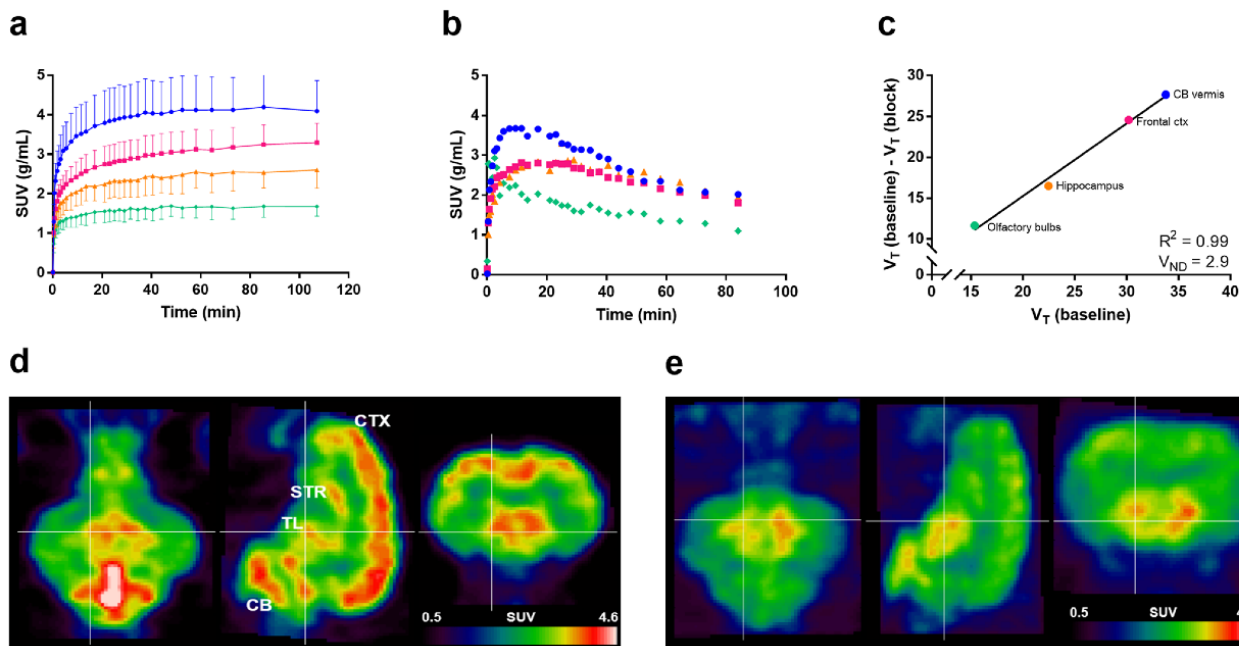


Fig. 1. Regional distribution and pharmacokinetics of [^{11}C]Martinostat in the pig brain. **a** Regional time-activity curves for [^{11}C]Martinostat at baseline (mean \pm SD, $n = 13$). **b** Regional time-activity curves for [^{11}C]Martinostat after administration of 0.5 mg/kg unlabeled Martinostat. **c** Lassen plot showing regional differences in total distribution volumes (V_T) of [^{11}C]Martinostat before and after administration of 0.5 mg/kg Martinostat ($R^2 = 0.99$, $n = 1$). **d** A representative summed frame-length weighted PET image (0–121 min) of radioactivity in the pig brain following [^{11}C]Martinostat injection. **e** Summed frame-length weighted PET image (0–121 min) with 3 mm filter of radioactivity in the pig brain following 0.5 mg/kg unlabeled Martinostat injection circle cerebellum vermis, square frontal cortex, triangle Hippocampus, diamond olfactory bulbs. SUV standardized uptake values, V_T total distribution volume. CB cerebellum, TL thalamus, STR striatum, CTX cortex.

fitted the data well (Suppl. Fig. 1, see Electronic Supplementary Material (ESM)). The MA1 model also fitted the data well using individual t^* for each ROI (see method section for t^* determination). Similar to MA1 quantification, a ROI-specific t^* was used for the Logan invasive model and the resulting V_T s were similar to those from MA1 modeling (Table 1). Of all four models (Table 1), the MA1 model had the lowest Akaike information criterion (AIC) scores and therefore MA1 is considered the best model choice.

To evaluate test-retest variability within animals, four pigs were scanned twice. In three animals, the difference in V_T was in the order of 7–12 % in frontal cortex, but the fourth animal had a 39 % difference in V_T . However, in regard to the SUVRs, all four pigs had <9 % difference between scans in frontal cortex.

Simplified Quantification

In the absence of an ideal reference region in the pig brain, we could not apply any reference tissue models to the data but Wey et al. [7] described the use of SUVR as an alternative and simplified quantification method. We found a relatively low V_{ND} in the pig brain, so we proceeded by

investigating the use of SUVR as a BP_{ND} surrogate (Table 1). Whereas in the human brain, a white matter region was used a pseudo-reference region, we here chose to use the olfactory bulb, as this region had the lowest binding in the pig brain. For the SUVR method to be valid, the TACs need to remain relatively constant over time, and this was achieved at timepoints that differed between brain regions: olfactory bulbs = 33 min, cerebellum vermis = 39 min, hippocampus = 50 min, and frontal cortex = 68 min. Note, the radioligand kinetics in the frontal cortex was so slow, we only had three frames for calculating the SUVR in this region.

The BP_{ND} s calculated on the basis of MA1 generated V_T s and self-blocking derived V_{ND} ($BP_{ND} = (V_T - V_{ND})/V_{ND}$), correlated well with the SUVRs (Suppl. Fig. 2a, see ESM).

Brain Tissue HDAC Determination

In vitro western blotting revealed substantial differences in protein amounts between the three HDAC subtypes: HDAC1 5 ± 1.5 ng/ μg , HDAC2 18.7 ± 4.9 ng/ μg , and HDAC3 1.7 ± 0.4 ng/ μg nuclear protein (Fig. 3b). To examine if the large amount of HDAC2 was the major determinant of the *in vivo*–*in vitro* correlations, we also investigated the relationship between the HDACs themselves. We found strong positive correlation

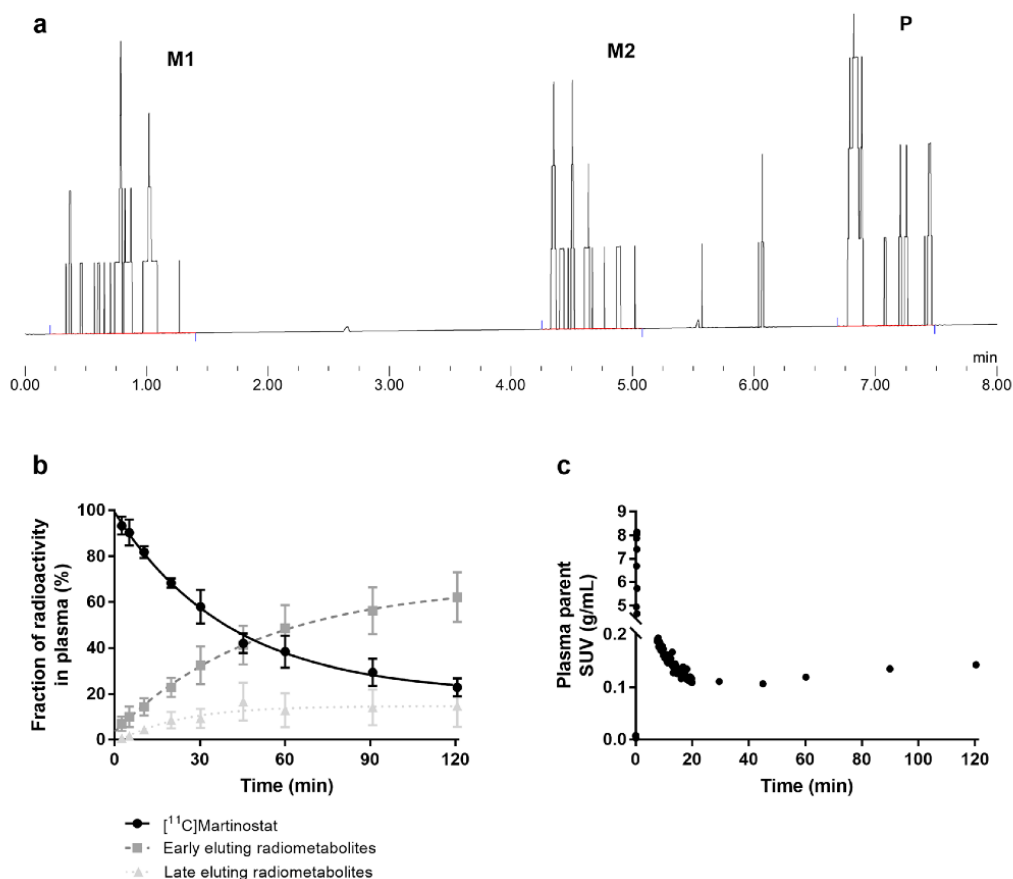


Fig. 2. [^{11}C]Martinostat parent compound. **a** Representative radiochromatogram 30 min after injection indicating the elution times of early (M1) and late (M2) eluting radiometabolites, and the parent compound [^{11}C]Martinostat (P) ($n = 1$). **b** Time course of the percentage of [^{11}C]Martinostat and metabolites measured in pig arterial plasma ($n = 10$). **c** Representative metabolite-corrected arterial input as a function of time after [^{11}C]Martinostat administration ($n = 1$).

between HDAC1 and HDAC2 in all three investigated brain regions ($R^2 = 0.78$ $p < 0.0001$, Fig. 3b). HDAC2 and HDAC3 levels were also correlated ($R^2 = 0.28$ $p = 0.004$, Fig. 3b), although the HDAC3 protein levels only differed slightly between regions.

We found a good correlation between *in vitro* HDAC levels, corrected for tissue volume and protein extraction yield, and the *in vivo* SUVR measure ($R^2 = 0.36$, $p = 0.001$, Fig. 3c), whereas the HDAC1–3 protein

Table 1. Regional total volumes of distribution (V_T) data resulting from four different arterial input models, non-displaceable binding potentials (BP_{ND}), and standardized uptake value ratio (SUVR)

		V_T (ml/cm 3)			BP_{ND}		
		1TC	2TC	Logan	MA1	MA1	SUVR $_{\text{X-121}}$
Frontal cortex	mean \pm SD	36.9 \pm 9.6	44.6 \pm 10.6	40.7 \pm 9	41.7 \pm 9.1	13.5 \pm 3.2	2 \pm 0.2
	<i>AIC</i>	<i>4.4</i>	<i>-34.4</i>	<i>124</i>	<i>-16.1</i>	–	–
Hippocampus	mean \pm SD	26.6 \pm 5.3	34.6 \pm 9.1	28.9 \pm 6.2	30.8 \pm 6.8	9.7 \pm 2.4	1.5 \pm 0.1
	<i>AIC</i>	<i>49.6</i>	<i>41.7</i>	<i>146</i>	<i>5.6</i>	–	–
Olfactory bulbs	mean \pm SD	16.5 \pm 3.7	20.9 \pm 5	17.9 \pm 3.3	18.9 \pm 3.7	5.6 \pm 1.3	–
	<i>AIC</i>	<i>61.3</i>	<i>46.2</i>	<i>142</i>	<i>2.4</i>	–	–
Cerebellum vermis	mean \pm SD	42.6 \pm 10.2	49.6 \pm 12.5	45.5 \pm 10	47.4 \pm 10.6	15.5 \pm 3.7	2.5 \pm 0.3
	<i>AIC</i>	<i>17.4</i>	<i>-19.3</i>	<i>147</i>	<i>-11.5</i>	–	–

Data is presented as mean \pm SD with the mean Akaike information criteria (AIC) below in italic. BP_{ND} was calculated by the formula $(V_T(\text{ROI}) - V_{\text{ND}})/V_{\text{ND}}$, using the MA1 determined V_T values. For SUVR calculations, an average SUV of time intervals described in the method section was used and the olfactory bulbs were used as pseudo-reference region

1TC 1 tissue compartment model, 2TC 2 tissue compartment model, MA1 Ichise multilinear analysis 1

Donovan L.L. et al.: HDAC1–3 in the Pig Brain

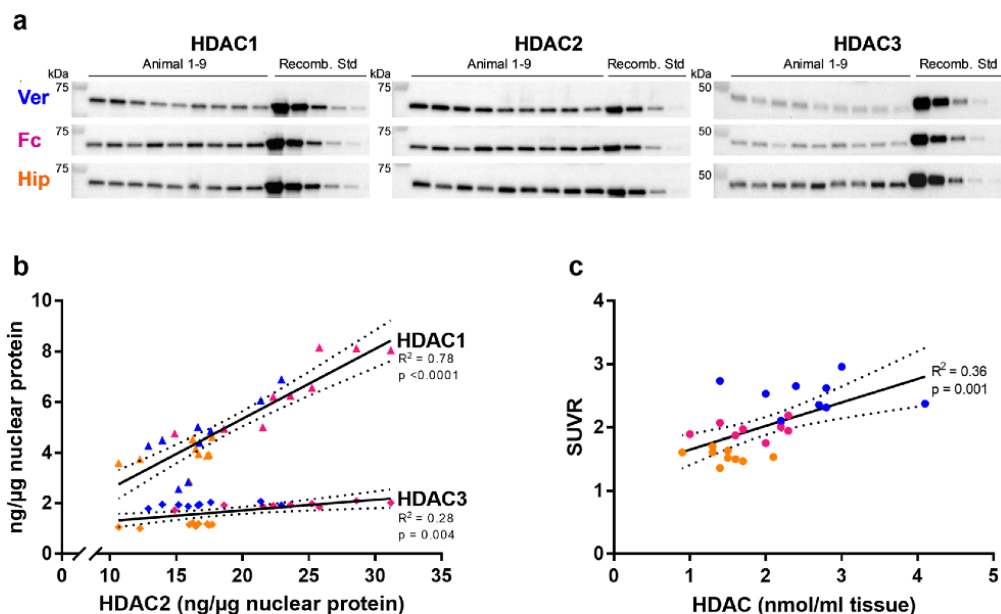


Fig. 3. Correlation between *in vivo* and *in vitro* measures of HDACs. **a** Equal amounts of nuclear protein from $[^{11}\text{C}]$ Martinostat scanned pigs were quantified by human recombinant standards of HDAC1–3 through western blotting ($n = 9$, 3 brain regions). **b** Linear correlation between HDAC2 and either HDAC1 (triangle $R^2 = 0.78$ $p < 0.0001$) or HDAC3 (diamond $R^2 = 0.28$ $p = 0.0042$) in the three investigated brain regions ($n = 9$). **c** Linear correlation between the summed amounts of HDAC1–3, measured by western blotting and corrected for tissue volume and protein extraction yield, and the individual pig's corresponding SUVR, measured by $[^{11}\text{C}]$ Martinostat PET imaging ($R^2 = 0.36$ $p = 0.001$ $n = 9$ pigs, three brain regions). ver cerebellum vermis (blue), fc frontal cortex (magenta), hip hippocampus (orange).

concentrations did not correlate with the V_T values ($p = 0.16$, Suppl. Fig. 3, see ESM).

Discussion

Here, we present for the first time an *in vivo*–*in vitro* cross-validation of the $[^{11}\text{C}]$ Martinostat PET radioligand in pigs. We found a good correlation between HDAC1–3 proteins and the $[^{11}\text{C}]$ Martinostat binding quantified with SUVR, supporting the use of $[^{11}\text{C}]$ Martinostat PET for *in vivo* neuroimaging of HDAC1–3.

The $[^{11}\text{C}]$ Martinostat PET experiments in pigs revealed high brain uptake and slow radioligand kinetics, similar to what has been described in non-human primates [4, 5] and in humans [7]. We found uptake in both white and gray matter regions, which underscores the conserved nature of the proteins [15]. The highest brain uptake was found in the cerebellum vermis and the lowest in the olfactory bulbs.

Quantification of PET data was performed with four different arterial input kinetic models: 1TC, 2TC, Logan invasive, and MA1. All models produced similar V_T values, although the 1TC underestimated the binding slightly, which is evident by the model fit (Suppl. Fig. 3, see ESM). Given that the MA1 generated the lowest AIC values, we suggest this model to be the most appropriate kinetic model for quantification of $[^{11}\text{C}]$ Martinostat in the pig brain. Previous studies in non-human primates and humans used the 2TC

model to compute V_T values based on model fits assessed by AIC values and model selection criterion [4, 5, 7]. Furthermore, V_T s from the Logan invasive model have shown good correlation with those from the 2TC model in non-human primates [5]. Our MA1 calculated V_T s from the pig brain are in line with 2TC calculated V_T s from the non-human primate brain, whereas the V_T s from the human brain are in the order of 3–4 times lower, but V_{ND} in humans remains to be measured.

The self-block experiment revealed that 0.5 mg Martinostat/kg resulted in 89 % occupancy and that V_{ND} constitutes only about 6 % of V_T in high-binding regions and less than 16 % of V_T in low-binding regions, which means that $[^{11}\text{C}]$ Martinostat has an excellent signal-to-noise ratio. The ROI with the lowest baseline binding, the olfactory bulbs, had a V_T value ~ 5 times higher than the V_{ND} , meaning that the pig brain has no ideal reference region that can be used for non-invasive reference tissue modeling. We also evaluated if the SUVR measure provides a good alternative to full kinetic modeling, as has been described in humans [7]. Indeed, SUVRs correlated well with the V_T values for the three pig brain regions investigated here (Suppl. Fig. 1b, see ESM), but for brain regions with particularly high $[^{11}\text{C}]$ Martinostat binding, such as the frontal cortex, SUVR may be biased. This also indicates that long acquisition time is necessary, if SUVR is to be used as surrogate for BP_{ND} . Importantly, however,

SUVR may not be a suitable quantification method if the experimental setting involves interventions that alter radioligand kinetics. For a quantification model that would be compatible with altered kinetics of the radioligand, full arterial input modeling is necessary.

Using specific antibodies for HDAC1–3 and dilution rows of recombinant protein, we quantified the protein levels in three different brain regions: cerebellum vermis, frontal cortex, and hippocampus. We found 3–4 times higher levels of HDAC2 than HDAC1 and 2–3 times higher levels of HDAC1 than HDAC3 (HDAC2 > HDAC1 > HDAC3). The literature on brain tissue HDAC subtype quantification is sparse and results are inconsistent. In line with our results, Anderson et al. found HDAC1,2 >> HDAC3 in whole mouse brain lysate [16], whereas Wang et al. found protein levels to be HDAC3 > HDAC2 > HDAC1 in various mouse brain regions [17], and Chen et al. found HDAC2 > HDAC3 > HDAC1 in mouse cortex [18]. Generally, it seems that HDAC3 levels vary quite a lot between species and brain regions [7, 17].

We found a strong correlation between HDAC1 and HDAC2 protein levels, which is in line with previous reports [19, 20]. The reports found stronger correlation between HDAC1/2 and HDAC3, than what we found, but our samples had limited variability of HDAC3 levels, with similar levels in two out of three regions. Needless to say, had we included more than three regions, we would be able to make better conclusions regarding the inter-relationships, but that was not the scope of our validation study. Regardless of the described differences, there is a general agreement of the interplay and possible redundancy between the HDAC isoforms: Several reports show that knock-out of HDAC1 increases the levels of HDAC2, and *vice versa* [21, 22]. However, distinct roles have also been described, such as the necessity of HDAC2 for HDAC1 recruitment [23].

In our study, we conducted the correlation analysis between the PET measures and the summed concentration of the three HDAC subtypes. Since [¹¹C]Martinostat binds to the HDAC 1–3 with different affinities [4], we also tested if weighing the HDAC 1–3 protein concentration with their individual affinities would improve the association between [¹¹C]Martinostat PET and *in vitro* measures but that did not result in substantial improvements of the fit.

The *in vitro* measures of HDAC1–3 levels correlated well with the *in vivo* SUVR; however, we did not see a similar correlation with the V_T . Although the SUVR and V_{TS} showed good correlation, the variation in the V_T values was much larger than in the SUVR. The SUVRs had test–retest variations <9 % in the frontal cortex in all four scans, consistent with the previous report from Wey et al. on SUVRs of [¹¹C]Martinostat in the human brain [7].

In order to ensure that we examined the exact same brain regions in our *in vivo* and *in vitro* comparisons, we chose three anatomically well-defined and easily distinguishable regions that represented a good range of expected HDAC protein concentrations. Inclusion of more regions might have

helped to establish an even firmer relationship, but three were deemed sufficient for our purpose. Also, we do recognize that our comparison assumes that the section used for *in vitro* western blotting are representative for the regions used for the PET quantification, *i.e.*, that HDAC protein concentrations only show small variations within the defined PET volume.

Anesthesia may potentially have confounding effect on experimental outcomes, but to the best of our knowledge, no one has reported an effect of propofol on the HDAC proteins. Isoflurane, on the other hand, has been shown to induce neurotoxicity in the developing hippocampus of rats, with HDACs playing an important role [24]. Further studies are needed to ensure that propofol does not affect the epigenetic machinery. In this study, however, all animals have received the same anesthetic regime and have been under anesthesia for the same duration of time. Therefore, we have no reason to believe that the anesthesia is affecting the comparison of data across animals. Also, the *in vitro* cross-validation was performed on the PET-scanned pigs, so a potential effect of anesthesia would not influence the correlations.

It may be seen as a limitation that we only investigated the blocking effect on the PET data of one dose (0.5 mg/kg) of Martinostat limiting us to just one estimate of V_{ND} . A better estimation of V_{ND} might have improved our estimate of BP_{NDs} , and this is also based on the assumption that the non-displaceable binding is similar across the animals.

The sample size in this study is relatively small; however, we are confident in the results given that the correlations are made across multiple brain regions, and we have performed technical replicates of the *in vitro* work. The olfactory bulbs are difficult to extract from the pig skull and are often lost during whole-brain extraction and accordingly, we were unfortunately unable to validate the olfactory bulbs *in vitro* as pseudo-reference region. In the absence of available porcine recombinant HDAC1–3 proteins, we used human recombinant protein to generate the calibration curves for the western blot. Because the proteins are well conserved across eukaryotes [25], we found it safe to assume similar affinity of the antibodies between species. Finally, for practical reasons, only adolescent females were used in this study but we find it reasonable to assume that our findings can be generalized to the fully developed adult brain as well as in both sexes.

The NCBI HomoloGene database reveals that the HDAC1–3 proteins are conserved across evolution, from fungi to plants and animals (HomoloGene ref no. 68426, 68187, and 48250 for HDAC 1, 2, and 3 respectively). More specifically, the NCBI protein BLAST function reveals the sequence similarity between pig and human is 99 %, 100 %, and 100 % for HDAC1, 2, and 3 respectively. Therefore, we believe that the function of the proteins is preserved through evolution, and our results is translatable and validates [¹¹C]Martinostat as a PET radioligand in pigs as well as humans.

Conclusions

We performed the first direct *in vivo/in vitro* cross-validation of the PET-radioligand [¹¹C]Martinostat. We found good correlation between *in vitro* quantified HDAC1–3 levels and *in vivo* measured SUVRs. We recommend to use SUVR as a good proxy for HDAC1–3 levels. We find that the changed kinetics after blocking of HDACs calls for a different quantification method, of which the MA1 model provides the best solution.

Acknowledgments. The authors would like to give thanks to C.A. Olsen for kindly providing recombinant HDAC proteins and the staff of Department of Experimental Medicine at University of Copenhagen for excellent assistance.

Funding information. This study was funded by The Lundbeck Foundation (grant no. R180-2014-3171 and R233-2016-3416).

Compliance with Ethical Standards

Conflict of Interest

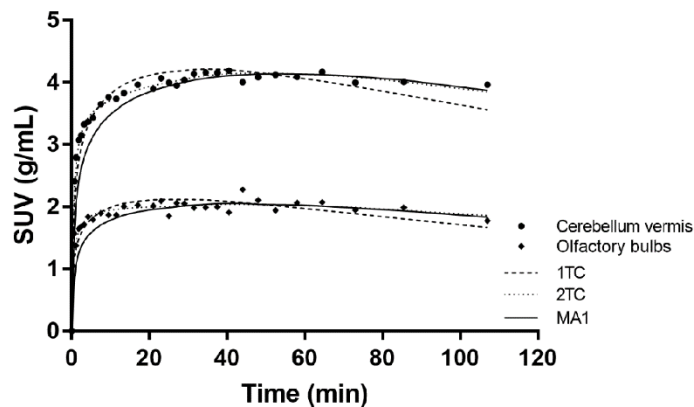
LLD, GMK, and HDH report grants from The Lundbeck Foundation. JHM, AD, SL declare no conflict of interest. JMH reports grants from NIH, Brain and Behavior Foundation, CureAlz Foundation; non-financial support and other from MGH; personal fees from Rodin Therapeutics, Psy Therapeutics, Merck, NIMH, Evelop Biosciences, Treventis, American Chemical Society, SV Life Sciences, Sunovion, Vertex, Therapeutics; grants and personal fees from Alzheimer's Drug Discovery Foundation; and other from Eikonizo. In addition, Dr. Hooker has a patent PCT/US2014/061179 with royalties paid to NucMedCor and Rodin Therapeutics (Previously).

References

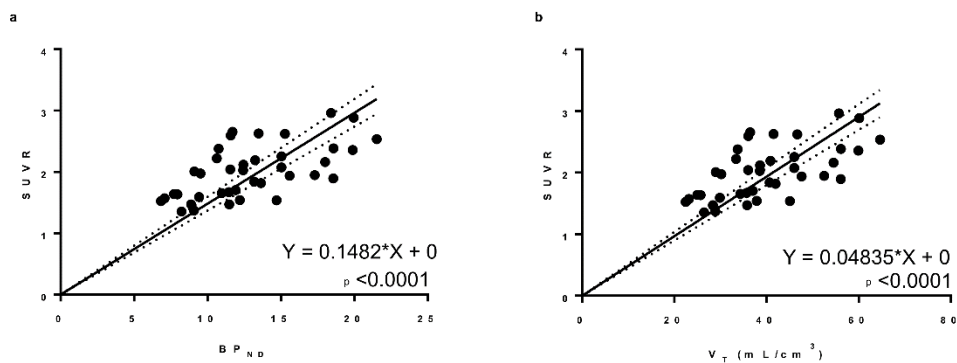
- Abel T, Zukin S (2008) Epigenetic targets of HDAC inhibition in neurodegenerative and psychiatric disorders. *Curr Opin Pharmacol* 8:57–64
- Penney J, Tsai L-H (2014) Histone deacetylases in memory and cognition. *Neuroscience* 7:3–10
- Gilbert TM, Zürcher NR, Wu CJ, Bhanot A, Hightower BG, Kim M, Albrecht DS, Wey HY, Schroeder FA, Rodriguez-Thompson A, Morin TM, Hart KL, Pellegrini AM, Riley MM, Wang C, Stufflebeam SM, Haggarty SJ, Holt DJ, Loggia ML, Perlis RH, Brown HE, Roffman JL, Hooker JM (2018) PET neuroimaging reveals histone deacetylase dysregulation in schizophrenia. *J Clin Invest* 129:364–372. <https://doi.org/10.1172/JCI123743>
- Wang C, Schroeder FA, Wey HY, Borra R, Wagner FF, Reis S, Kim SW, Holson EB, Haggarty SJ, Hooker JM (2014) In vivo imaging of histone deacetylases (HDACs) in the central nervous system and major peripheral organs. *J Med Chem* 57:7999–8009
- Wey H-Y, Wang C, Schroeder FA, Schroeder FA, Logan J, Price JC, Hooker JM (2015) Kinetic analysis and quantification of [¹¹C]Martinostat for in vivo HDAC imaging of the brain. *ACS Chem Neurosci* 6:708–715
- Schroeder FA, Wang C, Van De Bittner GC et al (2014) PET imaging demonstrates histone deacetylase target engagement and clarifies brain penetrance of known and novel small molecule inhibitors in rat. *ACS Chem Neurosci* 5:1055–1062
- Wey H-Y, Gilbert TM, Zürcher NR et al (2016) Insights into neuroepigenetics through human histone deacetylase PET imaging. *Sci Transl Med* 8:351ra106. <https://doi.org/10.1126/scitranslmed.aaf7551>
- Gillings N (2009) A restricted access material for rapid analysis of [¹¹C]-labeled radiopharmaceuticals and their metabolites in plasma. *Nucl Med Biol* 36:961–965
- Hong IK, Chung ST, Kim HK et al (2007) Ultra fast symmetry and SIMD-based projection-backprojection (SSP) algorithm for 3-D PET image reconstruction. *IEEE Trans Med Imaging* 6:789–803
- Sureau FC, Reader AJ, Comtat C, Leroy C, Ribeiro MJ, Buvat I, Trebassen R (2008) Impact of image-space resolution modeling for studies with the high-resolution research tomograph. *J Nucl Med* 49:1000–1008
- Keller SH, Svarer C, Sibomana M (2013) Attenuation correction for the HRRT PET-scanner using transmission scatter correction and total variation regularization. *IEEE Trans Med Imaging* 32:1611–1621
- Villadsen J, Hansen HD, Jørgensen LM et al (2017) Automatic delineation of brain regions on MRI and PET images from the pig. *J Neurosci Methods* 294:51–58
- Saikali S, Meurice P, Sauleau P, Eliat PA, Bellaud P, Randuineau G, Vêrin M, Malbert CH (2010) A three-dimensional digital segmented and deformable brain atlas of the domestic pig. *J Neurosci Methods* 192:102–109
- Cunningham VJ, E a R, Slifstein M et al (2010) Measuring drug occupancy in the absence of a reference region: the Lassen plot revisited. *J Cereb Blood Flow Metab* 30:46–50
- Seto E, Yoshida M (2014) Erasers of histone acetylation: the histone deacetylase enzymes. *Cold Spring Harb Perspect Biol* 6. <https://doi.org/10.1101/cshperspect.a018713>
- Anderson KW, Chen J, Wang M, Mast N, Pikuleva IA, Turko IV (2015) Quantification of histone deacetylase isoforms in human frontal cortex, human retina, and mouse brain. *PLoS One* 10:e0126592. <https://doi.org/10.1371/journal.pone.0126592>
- Wang Y, Zhang YL, Hennig K, Gale JP, Hong Y, Cha A, Riley M, Wagner F, Haggarty SJ, Holson E, Hooker J (2013) Class I HDAC imaging using [³H]CI-994 autoradiography. *Epigenetics* 8:756–764
- Chen YT, Zang XF, Pan J, Zhu XL, Chen F, Chen ZB, Xu Y (2012) Expression patterns of histone deacetylases in experimental stroke and potential targets for neuroprotection. *Clin Exp Pharmacol Physiol* 39:751–758
- Gu Y, Yang P, Shao Q et al (2013) Investigation of the expression patterns and correlation of DNA methyltransferases and class I histone deacetylases in ovarian cancer tissues. *Oncol Lett* 5:452–458
- Quint K, Agaimy A, Di Fazio P et al (2011) Clinical significance of histone deacetylases 1, 2, 3, and 7: HDAC2 is an independent predictor of survival in HCC. *Virchows Arch* 459:129–139
- Jurkin J, Zupkovitz G, Lagger S, Grausenburger R, Hagelkruys A, Kenner L, Seiser C (2011) Distinct and redundant functions of histone deacetylases HDAC1 and HDAC2 in proliferation and tumorigenesis. *Cell Cycle* 10:406–412
- Wiltling RH, Yanover E, Heideman MR, Jacobs H, Horner J, van der Torre J, DePinho RA, Dannenberg JH (2010) Overlapping functions of Hdac1 and Hdac2 in cell cycle regulation and haematopoiesis. *EMBO J* 29:2586–2597
- Somanath P, Herndon Klein R, Knoepfler PS (2017) CRISPR-mediated HDAC2 disruption identifies two distinct classes of target genes in human cells. *PLoS One* 12:1–21
- Joksimovic SM, Osuru HP, Oklopčić A et al (2018) Histone deacetylase inhibitor entinostat (MS-275) restores anesthesia-induced alteration of inhibitory synaptic transmission in the developing rat hippocampus. *Mol Neurobiol* 55:22–228
- Gregoret IV, Lee YM, Goodson HV (2004) Molecular evolution of the histone deacetylase family: functional implications of phylogenetic analysis. *J Mol Biol* 338:17–31

Publisher's Note. Springer Nature remains neutral with regard to jurisdictional claims in published maps and institutional affiliations.

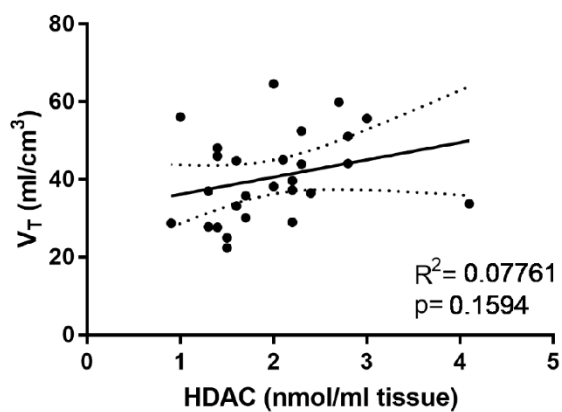
Supplementary Material



Supplementary Figure 1: Kinetic modelling fits. Representative time activity curves of high binding (cerebellum vermis) and low binding (olfactory bulbs) regions, with kinetic model curve fittings of 1 tissue compartment (1TC), 2 tissue compartment (2TC), and Ichise MA1 (MA1) ($n = 1$).



Supplementary Figure 2: Correlation between *in vivo* measures of HDAC levels. A) Linear correlation between [^{11}C]Martinostat SUV R and BP_{ND} as determined by $(V_{\text{T}} - V_{\text{ND}})/V_{\text{ND}}$. B) Linear correlation between SUV R and Ichise MA1 quantified distribution volumes of [^{11}C]Martinostat with full arterial input function. SUV R = standardized uptake value ratios, BP_{ND} = non-displaceable binding potential, V_{T} = distribution volume.



Supplementary Figure 3: *In vivo* versus *in vitro* measures of HDAC1-3. Linear regression of summed HDAC1-3 protein, quantified *in vitro* by western blotting, and [¹¹C]Martinostat binding, measured *in vivo* and quantified by Ichise MA1 kinetic modelling (n = 9 pigs, 3 brain regions). V_T = distribution volume.

Paper II

LL Donovan, JV Johansen, NF Ros, E Jaberi,
K Linnet, S Johansen, B Ozenne, S Issazadeh-
Navikas, HD Hansen, GM Knudsen

Effects of a single dose of psilocybin on
behaviour, brain 5-HT_{2A} receptor occupancy
and gene expression in the pig.

Manuscript in revision.

Effects of a single dose of psilocybin on behaviour, brain 5-HT_{2A} receptor occupancy and gene expression in the pig.

Lene Lundgaard Donovan^{a,b}, Jens Vilstrup Johansen^c, Nídia Fernandez Ros^a, Elham Jaber^c, Kristian Linnet^d, Sys Stybe Johansen^d, Brice Ozenne^{a,e}, Shohreh Issazadeh-Navikas^c, Hanne Demant Hansen^a, Gitte Moos Knudsen^{a,b}

^aNeurobiology Research Unit and Center for NeuroPharm, Copenhagen University Hospital Rigshospitalet, 2100 Copenhagen O, Denmark.

^bFaculty of Health and Medical Sciences, University of Copenhagen, 2200 Copenhagen N, Denmark.

^cBiotech Research and Innovation Centre (BRIC), Faculty of Health and Medical Sciences, University of Copenhagen, 2200 Copenhagen N, Denmark

^dDepartment of Forensic Medicine, Section of Forensic Chemistry, Faculty of Health and Medical Sciences, University of Copenhagen, 2200 Copenhagen N, Denmark

^eDepartment of Public Health, Section of Biostatistics, Faculty of Health and Medical Sciences, University of Copenhagen, 2200 Copenhagen N, Denmark

Corresponding author:

Gitte Moos Knudsen

Neurobiology Research Unit 6931; Rigshospitalet

Blegdamsvej 9

2100 Copenhagen O

DK – Denmark

Email: gmk@nru.dk

Running title: Effects of a single dose of psilocybin in the pig

Number of words: 5200

Abstract

Psilocybin has in some studies shown promise as treatment of major depressive disorder and psilocybin therapy was in 2019 twice designated as breakthrough therapy by the U.S. Food and Drug Administration (FDA). A very particular feature is that ingestion of just a single dose of psilocybin is associated with lasting changes in personality and mood. The underlying molecular mechanism behind its effect is, however, unknown. In a translational pig model, we here present the effects of a single dose of psilocybin on pig behaviour, receptor occupancy and gene expression in the brain. An acute i.v. injection of 0.08 mg/kg psilocybin to awake female pigs induced characteristic behavioural changes in terms of headshakes, scratching and rubbing, lasting around 20 min. A similar dose was associated with a cerebral 5-HT_{2A} receptor occupancy of 67%, as determined by positron emission tomography, and plasma psilocin levels were comparable to what in humans is associated with an intense psychedelic experience. We found that 19 genes were differentially expressed in prefrontal cortex one day after psilocybin injection, and 3 genes after 1 week. Gene Set Enrichment Analysis demonstrated that multiple immunological pathways were regulated 1 week after psilocybin exposure. This provides a framework for future investigations of the lasting molecular mechanisms induced by a single dose of psilocybin. In the light of an ongoing debate as to whether psilocybin is a safe treatment for depression and other mental illnesses, it is reassuring that our data suggest that any effects on gene expression are very modest.

Keywords: Psychedelic, Brain, Behaviour, 5-HT_{2A} receptor, Gene expression, Immune response

Introduction

Psychedelics are mind-altering compounds that have been used recreationally and religiously for thousands of years (Nichols, 2016). One of these psychedelic compounds is psilocybin which can be found in ‘magic mushrooms’. Psilocybin is a prodrug and upon ingestion, it is quickly dephosphorylated into the active compound psilocin (Hasler et al., 1997). Psilocin is a non-selective drug, but it induces its psychoactive effects by activating the serotonin 2A receptor (5-HT_{2A}R) (Vollenweider et al., 1998). In humans this leads to, e.g., elementary imagery, disembodiment, and audio-visual synaesthesia (Carbonaro et al., 2018; Madsen et al., 2019), and when administered to rodents it induces a characteristic head-twitch response (HTR) (Halberstadt and Geyer, 2018). The psychoactive and molecular effects can be blocked by 5-HT_{2A}R antagonists (Ly et al., 2018; Quednow et al., 2012; Tylš et al., 2015; Vollenweider et al., 1998), and 5-HT_{2A}R gene-deficient animals do not display HTR upon 5-HT_{2A}R activation by agonists (González-Maeso et al., 2007). Recently, scientists have gained renewed interest in psychoactive drugs and clinical trials are currently testing the therapeutic potential of psilocybin. Phase I studies have shown promise for treatment of anxiety and major depressive disorder (Carhart-Harris et al., 2018, 2016; Griffiths et al., 2016; Grob et al., 2011; Ross et al., 2016), leading to the FDA categorization of psilocybin as ‘Breakthrough Therapy’ towards major depressive disorder. A compelling feature of psilocybin therapy is the lasting effects of a single high dose for 3-6 months (Carhart-Harris et al., 2018, 2016). It is a surprising and very interesting finding that psilocybin has long-lasting effects beyond the acute psychedelic experience and in spite of the short *in vivo* half-life of the drug (Tylš et al., 2014). Psilocybin is also known to induce lasting changes in personality, higher openness and lower neuroticism, after just a single peroral hallucinogenic dose (Erritzoe et al., 2018; Griffiths et al., 2011, 2008; MacLean et al., 2011). This is remarkable, given that personality traits are generally considered stable throughout adulthood (Costa and McCrae, 2005).

Such long-lasting effects of psilocybin are likely to be driven by changes in gene expression that result in lasting plastic changes in the brain. In turn, the gene expression changes could be driven by epigenetic mechanisms, such as histone modifications or DNA methylation.

In the current study, we investigate the cerebral molecular mechanisms underlying the lasting effects produced by psilocybin. Since this requires access to brain tissue from a higher species, we first developed a large animal model in the pig. In order to make the model comparable to humans, we based the dose of psilocybin to be used in an awake pig on both behavioural effects and on brain 5-HT_{2A}R occupancy (Madsen et al., 2019). Once the dose was established, we gave awake pigs either saline or one dose of psilocybin intravenously (i.v.) and took out the brains either 24 hours or one week later. We then performed RNA sequencing of prefrontal cortex tissue to determine the gene expression pattern in an exploratory fashion. We hypothesized that genetic pathways regulated in the brain 24 hours and one week after psilocybin administration are key to the lasting effects seen in humans.

Experimental procedures

Animals, drugs and treatment

Twenty-five female Danish slaughter pigs (Yorkshire x Duroc x Landrace) weighing 20 kg (approx. 9 weeks old) were included. The animals were sourced from a local farm and allowed to acclimatize for at least one week. The animals were housed in individual pens with enriched environment on a 12-hour light/dark cycle, free access to water and weight-adjusted food twice daily. All animal experiments conformed to the European Commission's Directive 2010/63/EU and the ARRIVE guidelines. The Danish Council of Animal Ethics had approved all procedures (Journal no. 2016-15-0201-01149).

Experimental design

A dose-response study first determined an appropriate porcine dose of i.v. psilocybin, which we subsequently confirmed to be in the same 5-HT_{2A}R occupancy-range as described for humans. Subsequently we used a non-blinded placebo controlled study design. To provide insights into the molecular mechanisms underlying lasting effects of a single dose of psilocybin we euthanized animals either 1 day or 1 week post-intervention. Our outcome measures were behavioural scores and gene expression from RNAseq and RTqPCR of prefrontal cortex tissue.

Psilocybin administration

Five to seven days prior to administration of psilocybin/placebo, the pigs were accustomed to human handling by daily interaction and a permanent long-line catheter was inserted into an ear vein of the pig.

Psilocybin was kindly provided by Dr. Páleníček (National Institute of Mental Health, Czech Republic), and dissolved in distilled water to a 1 mg/mL solution on the day of experiment.

One pig was used to establish the dose-response relationship: 0.01, 0.04, 0.08, 0.16 mg/kg i.v. and the pig was observed for changes in behaviour, e.g. headshakes, and various parameters such as temperature and skin colour were noted. The duration of any observed behavioural changes was also noted. The lowest dose (0.01 mg/kg) did not alter behaviour, doses of 0.04 and 0.08 mg/kg had noticeable effects on behaviour, and 0.16 mg/kg had strong sedative effects. We chose to proceed with 0.08 mg/kg of psilocybin.

While the pig was awake and freely moving around, either 0.08 mg/kg psilocybin in 5 mL saline (N=12) or 5 mL saline as placebo (N=12) was administered i.v. in the ear catheter. The pigs were video recorded, and 3 independent observers blinded to the intervention scored the videos according to number of headshakes, scratching and rubbing. Twelve of the pigs were euthanized 24 hours after the intervention, the remaining twelve pigs 1 week after the intervention. The pigs were euthanized by 15 mL pentobarbital i.v. and the brain including cerebellum and brain stem

was swiftly removed, separated into hemispheres and snap-frozen by powdered dry-ice. Brain tissue was stored at -80°C until further use.

Statistical Analysis

Descriptive statistics was computed for each treatment group (mean \pm SD), whereas statistical significance of the difference in mean behavioural score across groups was assessed using a permutation test of 50,000 permutations. Two pigs were video recorded both during normal and psilocybin-influenced behaviour, hence the difference in group mean was modelled using a linear mixed effect model.

5-HT_{2A} receptor occupancy of psilocybin

We confirmed 5-HT_{2A}R occupancy of psilocybin (0.08 mg/kg) by PET scan with the 5-HT_{2A}R agonist radioligand [¹¹C]Cimbi-36 (Ettrup et al., 2013, 2011). Anaesthesia was induced by i.m. injection of 0.13 ml/kg Zoletil veterinary mixture (11.36 mg/mL xylazine, 11.36 mg/ml ketamine, 1.82 mg/ml butorphanol, 1.82 mg/ml methadone) ~3 h prior to scanning and maintained by inhalation isoflurane. I.v. access was established in the femoral arteries and mammary veins. Endotracheal intubation allowed for ventilation with 20 % oxygen in air at 10 ml/kg. Urine catheter was placed to avoid discomfort and stress. Peripheral O₂ and end-tidal CO₂ saturation, heart rate, blood pressure, and temperature were closely monitored throughout the experiment.

[¹¹C]Cimbi-36 was prepared at the Copenhagen University Hospital Rigshospitalet using carbon-11 methyl triflate, as described earlier (Leth-Petersen et al., 2016).

The pig was PET-scanned with a high-resolution research tomography (HRRT) scanner (CPS Innovations/Siemens, USA). PET data were acquired 90 min after bolus injection of [¹¹C]Cimbi-36 (574 and 399 MBq, injected mass 0.73 and 0.45 μ g). Immediately prior to the second scan, 0.064 mg/kg psilocybin was injected i.v.

Manual arterial blood samples were drawn at 2.5, 5, 10, 20, 30, 40, 50, 70, 90 min after injection, while an ABSS autosampler (Allogg Technology, Sweden) continuously measured arterial whole blood radioactivity during the first 30 min. Manual blood samples were collected for measurements of total radioactivity in whole blood and plasma using a gamma well counter (Cobra 5003; Packard Instruments, Meriden, USA). Radiolabelled parent and metabolite fractions were determined in plasma using an automatic column-switching radio-HPLC (high-performance liquid chromatography) as previously described (Gillings, 2009).

The PET emission data was reconstructed into 38 dynamic frames of increasing length: 6×10 , 6×20 , 4×30 , 9×60 , 2×180 , 8×300 , 3×600 s. The reconstruction used an ordinary Poisson three-dimensional ordered-subset expectation maximization with point spread function modelling (OP-3D-OSEM-PSF), 16 subsets and 10 iterations (Hong et al., 2007; Sureau et al., 2008) with all standard corrections. Attenuation correction was done using the HRRT maximum a posteriori transmission reconstruction method μ -map (Keller et al., 2013). Images consist of 207 planes of 256×256 voxels of $1.22 \times 1.22 \times 1.22$ mm in size. An automated method for co-registration and brain parcellation was used (Villadsen et al., 2017). The input for the methodology was frame-length weighted, summed PET images of the total scan time (0–90 min). The extracted regional radioactive concentration (kBq/ml) was normalized to injected dose (MBq) and corrected for animal weight (kg) to give standardized uptake values (SUV, g/ml). All graphical presentations were created using GraphPad Prism 8.2 (GraphPad, USA). PMOD 3.0 (PMOD Technologies, Switzerland) was used for kinetic modelling. Total distribution volumes (V_T) were calculated by the 2-tissue compartment model, and the regional V_T values in the blocked versus non-blocked condition determined occupancy (Cunningham et al., 2010).

Plasma psilocin levels were measured by ultra-high performance liquid chromatography coupled to tandem mass spectrometry as previously described (Madsen et al., 2019). Psilocin half-life in the pig was calculated by exponential one phase decay using GraphPad Prism 8.2.

Ex vivo analyses

RNA sequencing

Prefrontal cortex tissue weighing 143 ± 35 mg (N=24) was sent to Admera Health, New Jersey, USA for RNA sequencing. RNA was extracted using RNeasy Lipid Tissue Mini Kit (Qiagen, Germany) and quality controlled via BioAnalyzer (Agilent, California, USA). NEBNext Ultra II RNA with Poly-A selection (New England Biolabs, Massachusetts, USA) was used to create libraries, while Qubit HS DNA assay (Thermo Fisher Scientific, California, USA) and TapeStation 2200 (Agilent, California, USA) checked the quantity and size distribution. Sequencing was performed on Illumina HiSeq 2x150 X platform (Illumina, California, USA) across two 2x150 lanes to reach ~20-22M paired-end reads per sample.

Bioinformatics analyses

The raw paired-end (PE) 150 bp reads were quality assessed with FastQC (Andrews, 2010) and Fastq Screen (Andrews, 2011) and afterwards trimmed mainly to remove low quality bases, adapter sequences and poly-A-only reads using 'fastp' v0.20.0 (Chen et al., 2018) (default settings except: `--detect_adapter_for_pe --correction --trim_poly_x --cut_tail --trim_front1 12 --trim_front2 12 --trim_tail1 1 --trim_tail2 1`).

The trimmed mRNA-seq reads were aligned to the susScr11 genome assembly using STAR (Dobin et al., 2013) (v2.6c) in two-pass mode allowing for overlapping read mates and guided by an ENSEMBL (UCSC, Feb.10 2019) gene annotation (settings: `--sjdbOverhang 100 --twopassMode Basic --outSAMtype BAM SortedByCoordinate --outSAMattributes All --`

outSAMunmapped Within --outFilterMismatchNoverLmax 0.1 --outFilterMatchNmin 25 --outFilterMismatchNmax 10 --peOverlapNbasesMin 20).

After mapping, the reads were assigned to genes with featureCounts (Liao et al., 2014) (v1.5.1, settings: --primary -p -B -O --fraction -s 0 -J) generating a count table.

The samples were again checked for quality post-alignment e.g. generating genebody coverage plots and data-derived TIN scores (Wang et al., 2016) (transcript integrity Number, analogous to the RIN score) using the RSeQC package (Wang et al., 2012). MultiQC (Ewels et al., 2016) was used to generate a summarized QC report of all the data preprocessing steps up to and including the generation of the count table.

All four groups (saline 1 day, psilocybin 1 day, saline 1 week, psilocybin 1 week) each contained samples from 6 pigs of 3 replicates in 2 batches, except for one sample in the ‘saline 1 day’, which had to be excluded due to a corrupted raw data sample.

The gene counts were imported into the statistical software R (v3.5.1) (R Core Team, n.d.), where all the remaining analyses were performed.

As the RNA degradation levels varied between samples, we also tried using an alternative gene annotation modified to contain the 3'-end of the original full-length gene annotation, henceforward called ‘full length’ and ‘3'-tag’ data. The rationale being that as the RNA fragments are mainly degraded from the 5'-end, a 3'-end annotation would result in gene read counts less influenced by varying degradation levels. We tested two modified gene annotations with a maximum total exon length of 500 nt and 1500 nt from the transcription end site and looked in more detail at the results of the most conservative 500 nt version. Furthermore, ribosomal and mitochondrial gene counts were removed.

The edgeR package (McCarthy et al., 2012) (3.24.0) was used for low-count filtering of the raw count data, and the limma package (Ritchie et al., 2015) (v3.38.2) was used for the count transformation ('voomWithQualityWeights') and statistical analysis.

To take into consideration potential batch effects and different degrees of overall mRNA degradation between samples, we applied batch correction ('removeBatchEffect' with median TIN scores and total ng as covariates) to the data. The batch corrected data was fitted to a linear model ('lmFit'), the desired contrasts extracted and an empirical Bayes method run on these contrasts to calculate the final gene statistics.

Using the clusterProfiler package (Yu et al., 2012) (v3.10.1) we ran a gene set enrichment analysis (GSEA) and a hyper enrichment test on the MSIGDB database (for the hyper test using genes with $FDR \leq 10\%$ in differential expression test). Genes were selected for RTqPCR validation from the leading edge gene lists (the highest ranked genes in a gene set based on the data) reported by GSEA for each tested gene set.

As the pig genome still has relatively little annotation, we used the biomaRt package (v2.38.0) to find the closest human gene homologs in the Ensembl database, and the human homologs were used for all the clusterProfiler analyses.

RTqPCR

RNA was extracted from 34 ± 13 mg prefrontal cortex tissue by RNeasy mini kit (Qiagen, Hilden, Germany) according to manufacturer's protocol, with the following modifications: 20 sec rotor-stator homogenization (IKA, Staufen, Germany), 30 sec centrifugation at 10,000 g, on-column DNase treatment, 2x 25 μ L elution. RNA concentration and purity were determined by NanoDrop2000 (Thermo Scientific, California, USA). 100 ng RNA of each sample was used for cDNA synthesis in quintuplicate by ImProm II Reverse Transcription System with 6mM $MgCl_2$ (Promega, Wisconsin, USA) according to manufacturer's protocol, with the following

modifications: 5 min at 60°C before enzyme addition and for reverse transcription the thermal programme was 5 min at 25°C, 60 min at 42°C and 15 min at 72°C for enzyme inactivation. No enzyme control was made for each sample and checked for genomic DNA presence by the *B2M* primer pair.

Primers were designed using Primer BLAST (Ye et al., 2012), with the following criteria: primer length 18-25, product size 120-150bp, melting temperature (T_m) 62-65°C, exon-intron junction spanning, at least 4 mismatches to unintended targets, GC content: 20-70%, Max poly-X: 4, and Max GC in primer 3' end: 3. Specificity was assessed by in silico ePCR (Arányi et al., 2006). Primers were purchased from Tag Copenhagen (Copenhagen, Denmark); details can be found in Supplementary Table 1. Primers were accepted if no primer-dimers were present in template wells and efficiency was between 1.8-2.2.

RTqPCR was performed by LightCycler 480 II in a 20 μ L reaction mixture consisting of 5 μ L template and 15 μ L master mix with iQ SYBR® Green Supermix (BioRad, California, USA) and 16 pmol of each primer. The amplification temperature programme consisted of 95°C for 30 sec, 45 cycles of 95°C for 5 sec and 60°C for 30 sec, followed by a melting curve programme. All samples, no template control (NTC) and a standard curve for the given primer pair were run in triplicate on the same qPCR plate. Inter-run calibrator was used to enable comparison across qPCR plates.

Data normalization was performed in qbase+ (Biogazelle, Belgium) to the geometric mean of 3 reference genes checked for stability by geNorm (Vandesompele et al., 2002), namely *GAPDH*, *TBP*, *ACTB*. Data was analysed on the log-scale and estimates are reported after back-transformation. Statistical significance was tested by multiple linear regressions for the 13 genes, including time of death, treatment, and their interaction as covariates. P-values were adjusted for multiple comparisons using a single step Dunnett procedure (Dmitrienko and D'Agostino, 2013).

Results

Psilocybin-effects on pig behaviour

The pig behaviour was scored from video recordings of the first 30 min after psilocybin administration. The number of scratches (50 ± 32) and rubs (12 ± 7) showed slightly higher inter-individual variability than headshakes did (16 ± 5) (Figure 1a). Headshakes, as classically induced by 5-HT_{2A}R stimulation, was significantly increased after psilocybin administration ($p = 0.0003$, Figure 1a). We identified two other characteristic psilocybin-induced behaviours: Hindleg scratching ($p = 0.006$, Figure 1a) and rubbing against the pen wall ($p = 0.03$, Figure 1a). Scratching was distinctly different between psilocybin and saline groups for ~20 min, whereas headshakes and rubbing were most pronounced within the first 10-15 min, but also more intermittent (Figure 1b and Supplementary Figure 1). After 30 min, all three behaviours had disappeared and were indistinguishable from control pig behaviour.

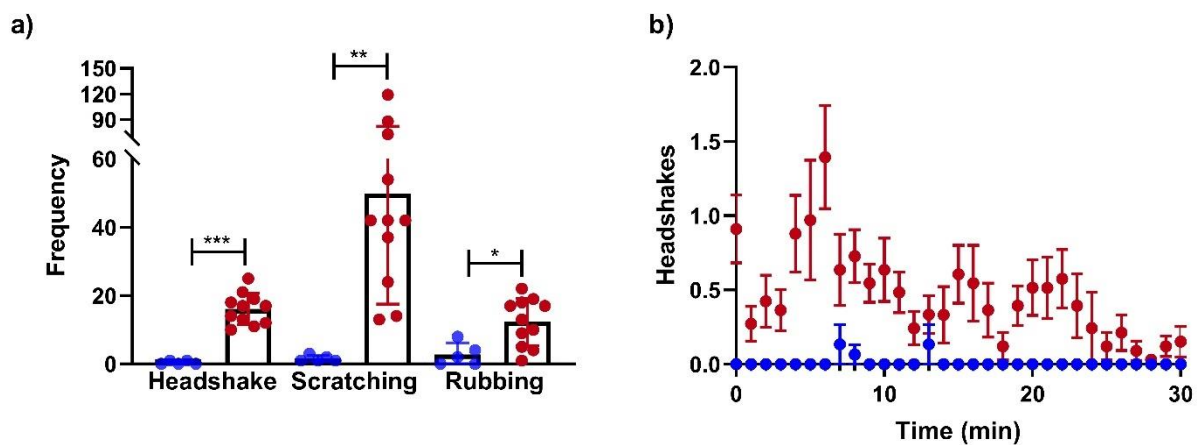


Figure 1: Pig behavioural effects after i.v. psilocybin. a) Cumulated scores of headshakes, scratching and rubbing during 30 min post-psilocybin compared to controls (mean \pm SD). b) Time-response curve of headshakes during the first 30 min after psilocybin injection (mean \pm SEM). Blue = control (N=5), red = 0.08 mg/kg psilocybin (N=11). *** $p < 0.001$, ** $p < 0.01$, * $p < 0.05$

5-HT_{2A} receptor occupancy of psilocybin

Plasma psilocin levels rapidly decreased after i.v. administration of psilocybin (Figure 2a), with a $T_{1/2}$ of 20 min determined by exponential one phase decay. [¹¹C]Cimbi-36 PET-scanning showed a high radioligand uptake in neocortex and lower uptake in cerebellum (Figure 2a). Co-administration of [¹¹C]Cimbi-36 and psilocybin lead to a profound reduction in the neocortical time-activity curve. V_T values were comparable to previously published results (Jørgensen et al., 2016), with highest binding in the cortex, lower binding in subcortical regions and lowest binding in the cerebellum. A Lassen plot analysis showed that 0.064 mg/kg psilocybin resulted in 67% occupancy of the 5-HT_{2A} receptor and a non-displaceable distribution volume (V_{ND}) of 4.2 ml/cm³ (Figure 2b).

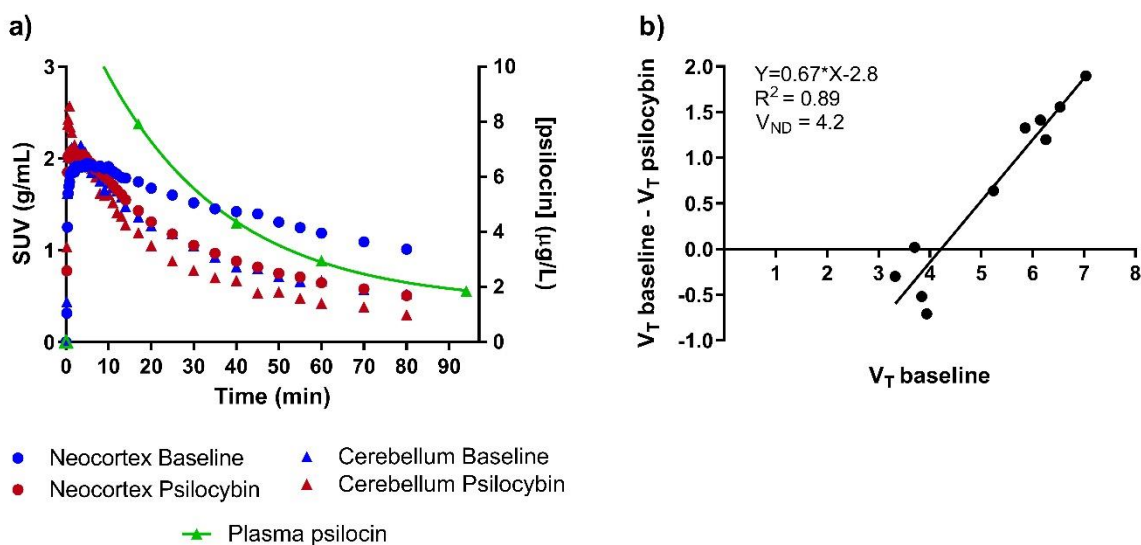


Figure 2: Psilocybin occupancy at the pig cerebral 5-HT_{2A} receptor. a) Time-activity curves of [¹¹C]Cimbi-36 at baseline (blue) and after 0.064 mg/kg psilocybin (red) in neocortex (circles) and cerebellum (triangles). Plasma psilocin concentrations after i.v. administration (green, right y-axis). **b)** Lassen plot of total distribution volumes (V_T) before and after i.v. psilocybin in a pig. (N = 1)

RNA sequencing

Principal component analysis of the full length data revealed a large inter-individual variation (Figure 3a), and we observed small effect sizes, i.e., foldchange of gene expression, both one day and one week after psilocybin (Figure 3b-e). When using threshold $\text{abs}(\log_2 \text{ fold change}) > 1$ and $\text{FDR} < 5\%$, only 5 genes were differentially expressed (DE) in the brain tissue taken out 1 day after psilocybin (Figure 3b), and no genes were DE in the tissue from 1 week after psilocybin (Supplementary Table 2). Next, we used GSEA to check for functional gene-family alterations. Within the C5 GO-database we found that 1 week after psilocybin exposure, the vast majority of regulated pathways were immune-related pathways such as Immune Response, Immune Effector Process and Response to Type 1 Interferon (see Supplementary Table 3 for the full list of regulated pathways).

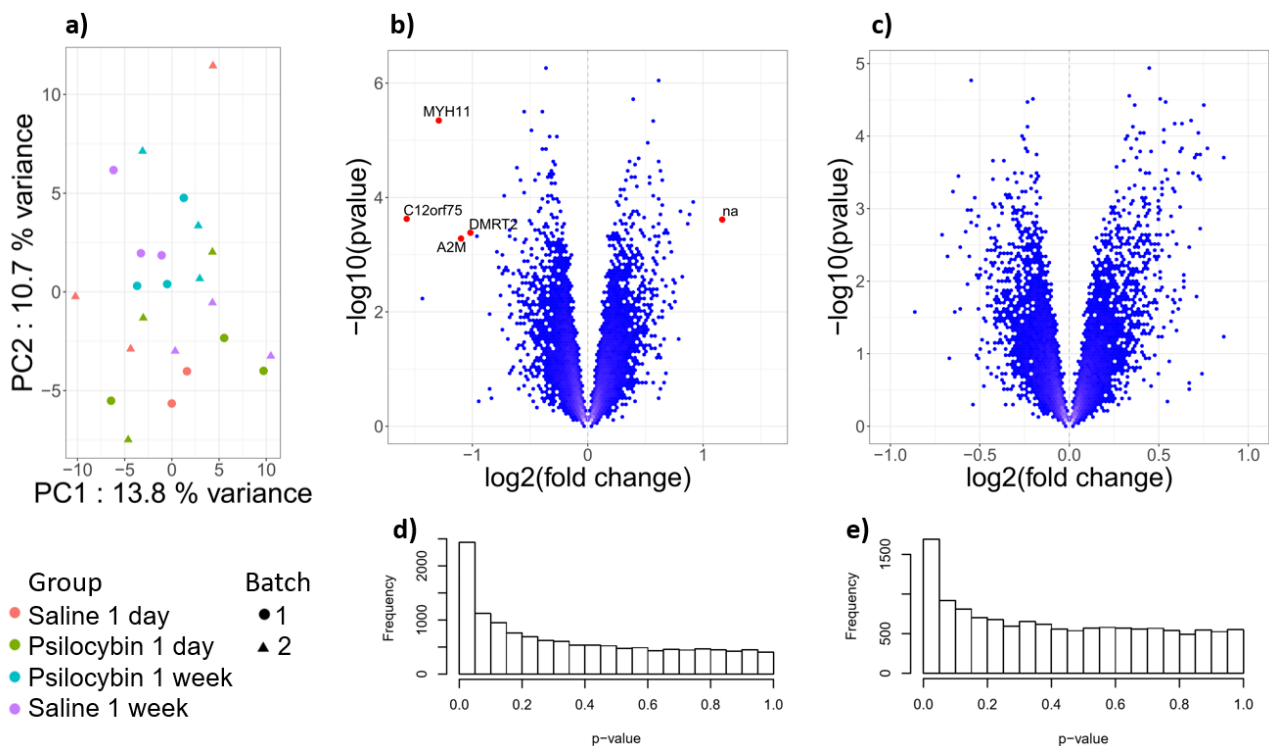


Figure 3: Bioinformatic analysis of full length RNA sequencing data. a) Principal component analysis visualizing the group and batch clusterings. Volcano plot and p-value histogram of 1 day (b+d) and 1 week (c+e), respectively.

In an attempt to increase specificity and minimize false-positives due to RNA degradation, we employed the 3'-tag modality (Sigurgeirsson et al., 2014) to the raw sequencing data. This improved the PCA plot slightly, with increased grouping of the psilocybin treated group euthanized 1 week post-psilocybin exposure (Figure 4a). However, effect sizes were still small but more DE genes were recovered (Figure 4b+c). Specifically, 19 genes after 1 day and 3 genes after 1 week (Figure 4b+c) (threshold: $\text{abs}(\log_2 \text{fold change}) > 1$ and $\text{FDR} < 5\%$) (Supplementary Table 2). Of these, 2 unknown genes were regulated at both time points, and 2 genes (*MYH11* and *C12orf75*) were common between the 3'-tag and full-length approach. GSEA computations of the 3'-tag genes replicated the finding of multiple immune-related pathways regulated after 1 week of psilocybin administration (Supplementary Table 3).

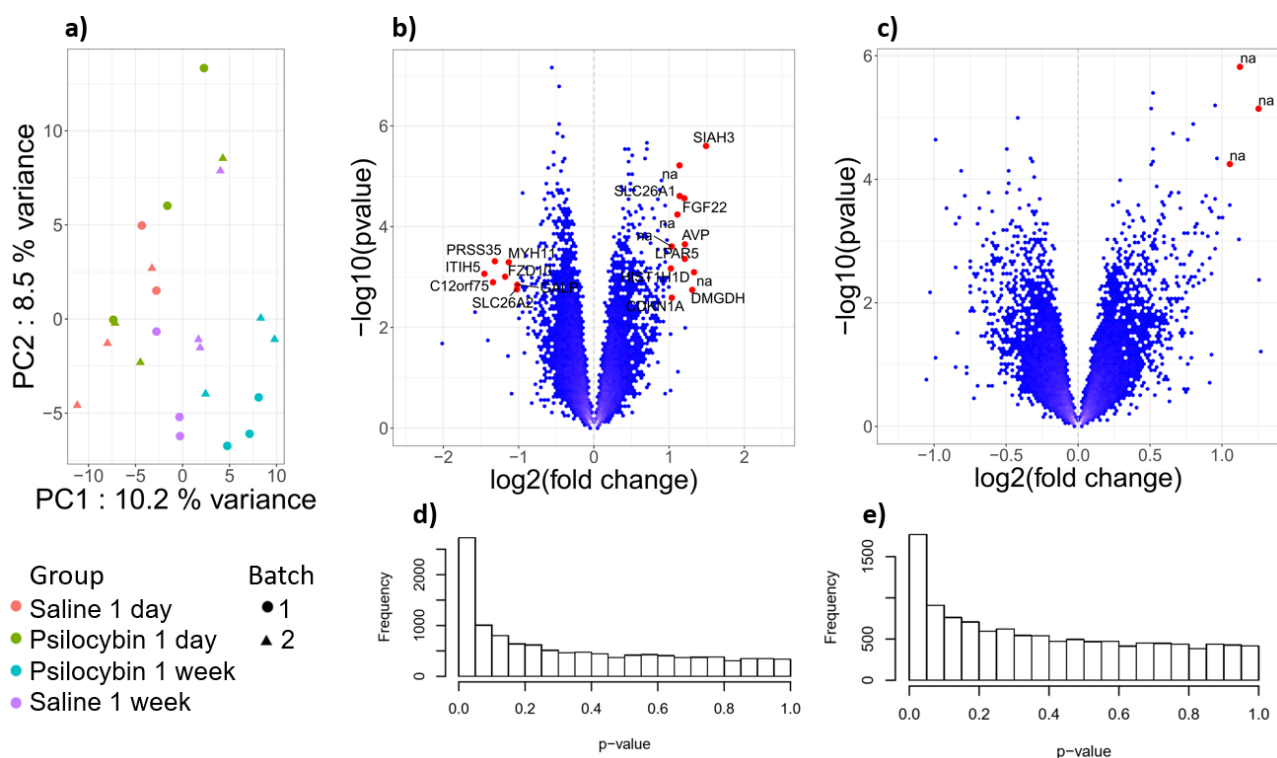


Figure 4: 3'-tag bioinformatic analysis of RNA sequencing data. a) Principal component analysis visualizing the group and batch clusterings. Volcano plot and p-value histogram of 1 day (b+d) and 1 week (c+e), respectively.

Group differences in gene expression

Based on the distributed immunological gene signal observed 1 week after psilocybin exposure, we chose to investigate genes involved in the Response to type 1 interferon pathway. We chose 9 genes from the leading edge analysis (*IFITM2*, *IFITM3*, *IRF8*, *IRF9*, *IFIT3*, *EGR1*, *PSMB8*, *STAT1*, *MX2*) and added another 3 genes of a-priori interest (*STAT2*, *JAK1*, *EGR2*) which we sought to validate by RTqPCR. None of the 12 investigated immunology genes were significantly altered on a group basis (Figure 5). However, *IFITM3* stood out as the only gene with borderline significance at the 1 week time point (32% increased relative gene expression; adjusted p = 0.0984). Of all genes at either time point, *IFITM2* at 1 week had the largest difference in relative gene expression by 43% (adjusted p = 0.21), and was also the gene with the largest change over time (increased relative gene expression of 70% at 1 week compared to 1 day; adjusted p = 0.185). We also investigated the expression level of the main effector receptor of psilocin, the 5-HT_{2A}R, but did not find any expression changes of the *HTR2A* gene following a single psilocybin administration (Figure 5; 2% increased relative gene expression; adjusted p >0.99).

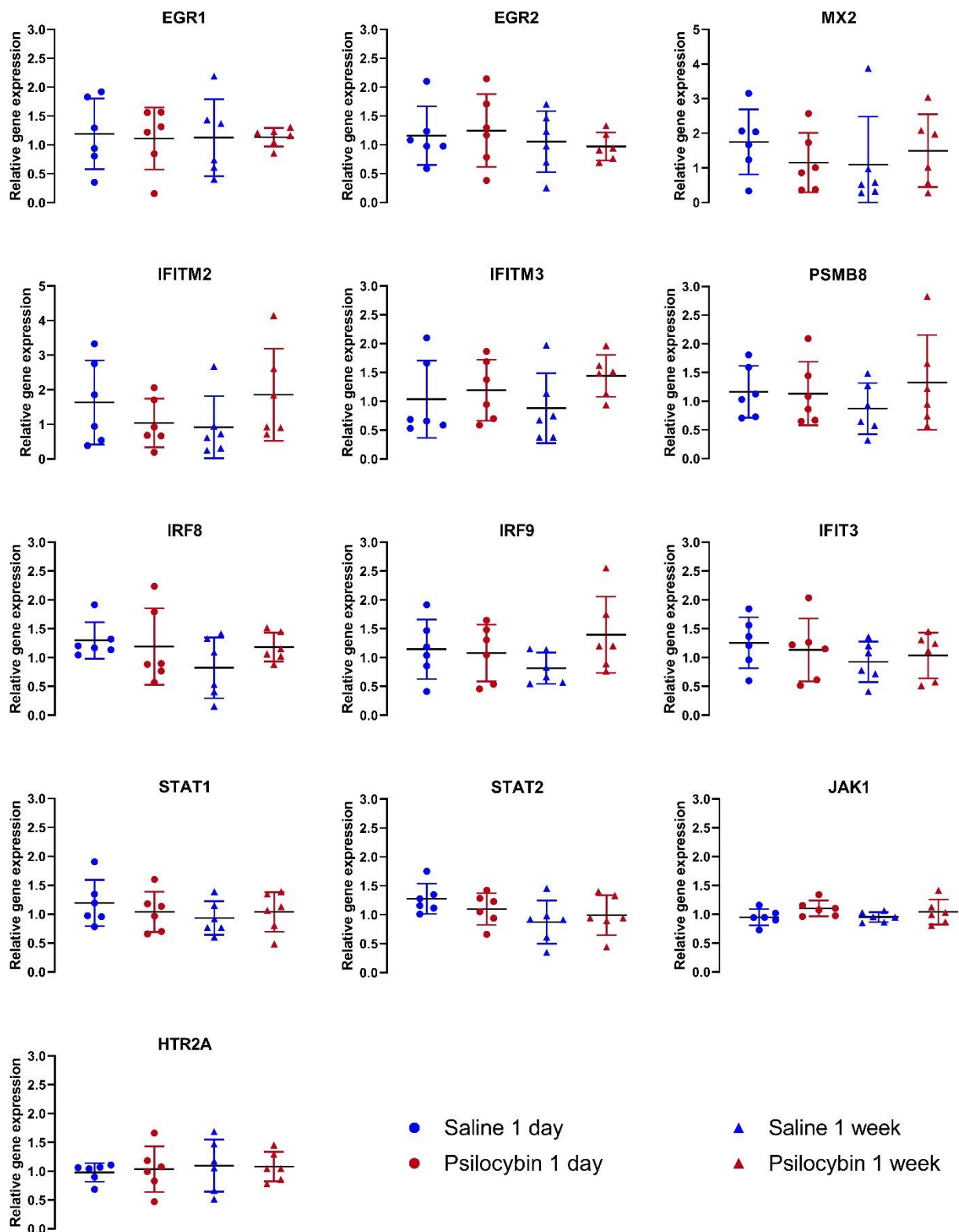


Figure 5: Relative gene expression of target genes determined by RNAseq. Graphical presentation of individual normalized gene expression values from PFC of psilocybin or saline treated pigs (N=6/group). Note the different scale of *MX2* and *IFITM2*.

Discussion

In the present study we first determined the dose of psilocybin that in pigs induces a) a characteristic pattern of behaviours, b) cerebral 5-HT_{2A}R occupancy and c) plasma psilocin levels in a range that is associated with an intense psychedelic experience in humans. Next, in an exploratory manner, we examined the gene expression effects in the prefrontal cortex one day or one week after a such dose of psilocybin that had been given to awake freely moving pigs.

Pilot data in a pig given four different doses of psilocybin suggested that an i.v. dose of 0.08 mg/kg produced a characteristic porcine behaviour: an up to 30 min lasting specific behaviour consisting of headshakes, scratching and rubbing., with a peak 5-10 min after i.v. psilocybin. The temporal course of a psychedelic experience in humans given i.v. psilocybin is similar to the behavioural changes in our study in pigs: An i.v. administration of 1.5-2 mg psilocybin to humans is associated with an almost immediate onset of perceptual changes, reaching peak intensity after only 4 min and subsiding after about 20 min (Carhart-Harris et al., 2011). In rodent models, the HTR is regarded specific for central 5-HT_{2A}R stimulation, and for serotonergic hallucinogens a strong positive correlation between HTR potencies in mice and reported hallucinogenic potencies in humans has been found (Halberstadt et al., 2020). Although the pig possess several advantages for use in medical research (Kornum and Knudsen, 2011; Tang and Mayersohn, 2018), only one previous study has investigated porcine behavioural response to the psychedelics LSD, DOI and 5-MeO-DMT (Löscher et al., 1990), but they did not investigate effects of psilocybin. They report that when giving high doses of LSD and 5-MeO-DMT, but not DOI, the pigs displayed headshakes along with other psychotomimetic parameters such as grimacing and backward locomotion (Löscher et al., 1990).

Based on the human equivalent dose-formula (U.S. Department of Health and Human Services, Food and Drug Administration, 2005), the 0.08 mg/kg (or total 1.9 ± 0.2 mg) dose used in our

study, is equivalent to a human dose of 0.064 mg/kg i.v. Further, with this dose, the peak psilocin plasma concentration in the pig is close to that reported in humans after peroral intake, being in the order of 12-19 µg/L (Madsen et al., 2019). Finally, the 0.064 mg/kg psilocybin dose resulted in a porcine brain 5-HT_{2A}R occupancy, in the order of 70%, which also is in the same order of magnitude as seen in humans while they are having an intense psychedelic experience on a peroral psilocybin dose of 0.15-0.3 mg/kg (Madsen et al., 2019).

We chose to use a weight-adjusted dose of psilocybin, which in two human studies have been found to produce more uniform plasma psilocin concentrations (Hasler et al., 1997; Madsen et al., 2019), as well as more similar psychedelic effects (Madsen et al., 2019). Obviously, we are unable to verify the extent to which the pigs experienced psychedelic effects the same way that humans do, but in any other aspect, the given dose of psilocybin elicited the same pharmacokinetics and associated effects of 5-HT_{2A}R stimulation as in humans. In order to translate eventual gene expression effects in the pig brain to the human situation, we found it instrumental to use doses that were comparable to those used in humans.

We next explored genetic pathways that presumably would be involved in the sustained effects seen in humans. RNA sequencing of porcine prefrontal cortex tissue at 1 day or 1 week following psilocybin exposure revealed only few DE genes, with small effect sizes. This observation was unexpected, given the profound and lasting effects that have been observed after a single dose of psilocybin. One explanation for this could be that in contrast to most rodent studies, the animals used in the present study were sourced locally from a healthy non-inbred stock, which may better represent the variation in the general human population than inbred strains of laboratory rodents do.

Interestingly, however, GSEA showed that immune-related genes constituted the largest group of genes significantly altered 1 week after psilocybin administration. Neuroinflammation is now recognized as key player in psychiatric diseases, such as depression, with positive outcomes of treatment with anti-inflammatory compounds (Köhler et al., 2016). Increased levels of interferon alpha (IFN α) can cause neurotoxicity (Rho et al., 1995), and when used as antiviral treatment in hepatitis C patients, clinical scores of anxiety and depression increase (Bonaccorso et al., 2001). Also, acute effects of IFN α administration on functional connectivity of hepatitis C patients' brain networks, display decreased connectivity in hub regions (Dipasquale et al., 2016), similar to what has been shown for acute effects of psilocybin intoxication (Carhart-Harris et al., 2012). A recent review by Flanagan and Nichols describes the role of 5-HT $_2A$ R in inflammation and how psychedelics may be anti-inflammatory (Flanagan and Nichols, 2018) and this lends support to the hypothesis that the long-lasting beneficial effects of psychedelics in psychiatric disorders are due to a reduction of neuroinflammation. Further support for the hypothesis comes from a preclinical study where the psychedelic compound (*R*)-DOI reduced cytokine and chemokine expression in response to TNF α or ovalbumin challenges in multiple tissue types (Flanagan and Nichols, 2018). Although we were unable to validate the results of altered immunologic gene expression following a single psilocybin exposure by RTqPCR, our RNA sequencing results points toward an interesting link between single psilocybin administration and sustained neuroinflammation alterations. Furthermore, whereas we studied healthy pigs, the anti-inflammatory effects of psilocybin may be more easily identified in pig or rodent models with neuroinflammation.

We cannot exclude that the chosen time-points (1 day and 1 week) were less optimal for capturing a response, but an investigation of gene expression effects of electroconvulsive therapy (ECT), a highly effective non-pharmacological treatment of depression, shows large variation in the temporal profiles of various gene families (Dyrvig et al., 2014). Immediate early genes had all

returned to baseline within the first 16 hours after ECT, and *EGR1* had returned to baseline only 4 hours after ECT so we did not expect to find *EGR1* to be DE in our study. They also reported that effector genes had a wide variation in their temporal profile, even within gene families the pattern varied greatly, and only the extensive investigation of 6 time points revealed the dynamic pattern, e.g. initial down-regulation followed by upregulation (Dyrvig et al., 2014).

Additional factors that could have impacted the RNA sequencing outcomes include: batch effect, RNA extraction yield, RNA degradation, no RNase inhibitor was added to the tissue samples, no a-priori positive control time-point. The 3'-tag counting is a simple but also rather crude method of reducing the effect of RNA degradation on the data. It should be kept in mind, however, that studies of post-mortem human brain tissue often are sampled under much more challenging and heterogeneous conditions.

In the current study, we investigated prefrontal cortex tissue for RNA sequencing, thereby capturing the full transcriptomic picture induced by psilocybin. We cannot rule out that other brain regions could have shown more larger effects. It is also possible that only specific subset of neuronal cells are activated by psilocybin, and in that case, one would need to resort to e.g. cell sorting (Martin and Nichols, 2016) to identify such gene regulations. However, from a general therapeutic point of view it is reassuring if such profound brain distortion only leaves small imprints on gene expression.

Conclusion

In this first study of psilocybin-induced effects in pigs we show that an intravenous dose of 0.08 mg/kg psilocybin is associated with psilocin pharmacokinetics and cerebral 5-HT_{2A}R occupancy in the same range as humans exposed to intense psychedelic experience. The awake pigs also displayed a behaviour consistent with known effects of central 5-HT_{2A}R stimulation, and with the expected duration. The gene expression pattern in frontal cortex induced by a single psilocybin exposure in awake pigs after 1 day and 1 week showed that a large number of immune-related genes were regulated 1 week post-psilocybin exposure. Although we were unable to confirm these findings by RTqPCR, we provide exploratory data from a large animal much more closely resembling the situation in humans that psilocybin administration in psychedelic doses does not severely impact overall brain gene expression. Future work must reveal if our data can be replicated and uncover the sustained molecular effector pathways of psilocybin.

References

- Andrews S (2010) Babraham Bioinformatics - FastQC A Quality Control tool for High Throughput Sequence Data. Available at: <http://www.bioinformatics.babraham.ac.uk/projects/fastqc/> [Accessed January 16, 2020].
- Andrews S (2011) Babraham Bioinformatics - FastQ Screen. Available at: http://www.bioinformatics.babraham.ac.uk/projects/fastq_screen/ [Accessed January 16, 2020].
- Arányi T, Váradi A, Simon I, Tusnády GE (2006) The BiSearch web server. *BMC Bioinformatics* 7:1–7.
- Bonaccorso S, Puzella A, Marino V, Pasquini M, Biondi M, Artini M, Almerighi C, Levrero M, Egyed B, Bosmans E, Meltzer HY, Maes M (2001) Immunotherapy with interferon-alpha in patients affected by chronic hepatitis C induces an intercorrelated stimulation of the cytokine network and an increase in depressive and anxiety symptoms. *Psychiatry Res* 105:45–55.
- Carbonaro TM, Johnson M, Hurwitz E, Griffiths RR (2018) Double-blind comparison of the two hallucinogens psilocybin and dextromethorphan: similarities and differences in subjective experiences. *Psychopharmacology (Berl)* 235:521–534.
- Carhart-Harris RL, Bolstridge M, Day CMJ, Rucker J, Watts R, Erritzoe DE, Kaelen M, Giribaldi B, Bloomfield M, Pilling S, Rickard JA, Forbes B, Feilding A, Taylor D, Curran H V., Nutt DJ (2018) Psilocybin with psychological support for treatment-resistant depression: six-month follow-up. *Psychopharmacology (Berl)* 235:399–408.
- Carhart-Harris RL, Bolstridge M, Rucker J, Day CMJ, Erritzoe D, Kaelen M, Bloomfield M, Rickard JA, Forbes B, Feilding A, Taylor D, Pilling S, Curran VH, Nutt DJ (2016) Psilocybin with psychological support for treatment-resistant depression: An open-label feasibility study. *The Lancet Psychiatry* 3:619–627.
- Carhart-Harris RL, Erritzoe D, Williams T, Stone JM, Reed LJ, Colasanti A, Tyacke RJ, Leech R, Malizia AL, Murphy K, Hobden P, Evans J, Feilding A, Wise RG, Nutt DJ (2012) Neural correlates of the psychedelic state as determined by fMRI studies with psilocybin. *Proc Natl Acad Sci U S A* 109:2138–2143.
- Carhart-Harris RL, Williams TM, Sessa B, Tyacke RJ, Rich AS, Feilding A, Nutt DJ (2011) The administration of psilocybin to healthy, hallucinogen-experienced volunteers in a mock-functional magnetic resonance imaging environment: A preliminary investigation of tolerability. *J Psychopharmacol* 25:1562–1567.
- Chen S, Zhou Y, Chen Y, Gu J (2018) Fastp: An ultra-fast all-in-one FASTQ preprocessor. *Bioinformatics* 34:i884–i890.
- Costa JPT, McCrae RR (2005) Personality in Adulthood, A Five-Factor Theory Perspective.
- Cunningham VJ, Rabiner E a, Slifstein M, Laruelle M, Gunn RN (2010) Measuring drug occupancy in the absence of a reference region: the Lassen plot re-visited. *J Cereb blood flow Metab*

30:46–50.

- Dipasquale O, Cooper EA, Tibble J, Voon V, Baglio F, Baselli G, Cercignani M, Harrison NA (2016) Interferon- α acutely impairs whole-brain functional connectivity network architecture – A preliminary study. *Brain Behav Immun* 58:31–39.
- Dmitrienko A, D’Agostino R (2013) Traditional multiplicity adjustment methods in clinical trials. *Stat Med* 32:5172–5218.
- Dobin A, Davis CA, Schlesinger F, Drenkow J, Zaleski C, Jha S, Batut P, Chaisson M, Gingeras TR (2013) STAR: Ultrafast universal RNA-seq aligner. *Bioinformatics* 29:15–21.
- Dyrvig M, Christiansen SH, Woldbye DPD, Lichota J (2014) Temporal gene expression profile after acute electroconvulsive stimulation in the rat. *Gene* 539:8–14.
- Erritzoe D, Roseman L, Nour MM, MacLean K, Kaelen M, Nutt DJ, Carhart-Harris RL (2018) Effects of psilocybin therapy on personality structure. *Acta Psychiatr Scand* 138:368–378.
- Ettrup A, Hansen M, Santini MA, Paine J, Gillings N, Palner M, Lehel S, Herth MM, Madsen J, Kristensen J, Begtrup M, Knudsen GM (2011) Radiosynthesis and in vivo evaluation of a series of substituted ^{11}C -phenethylamines as 5-HT $_2\text{A}$ agonist PET tracers. *Eur J Nucl Med Mol Imaging* 38:681–693.
- Ettrup A, Holm S, Hansen M, Wasim M, Santini MA, Palner M, Madsen J, Svarer C, Kristensen JL, Knudsen GM (2013) Preclinical safety assessment of the 5-HT $_2\text{A}$ receptor agonist PET radioligand [^{11}C]cimbi-36. *Mol Imaging Biol* 15:376–383.
- Ewels P, Magnusson M, Lundin S, Källner M (2016) MultiQC: Summarize analysis results for multiple tools and samples in a single report. *Bioinformatics* 32:3047–3048.
- Flanagan TW, Nichols CD (2018) Psychedelics as anti-inflammatory agents. *Int Rev Psychiatry* 0:1–13.
- Gillings N (2009) A restricted access material for rapid analysis of [^{11}C]-labeled radiopharmaceuticals and their metabolites in plasma. *Nucl Med Biol* 36:961–965.
- González-Maeso J, Weisstaub N V., Zhou M, Chan P, Ivic L, Ang R, Lira A, Bradley-Moore M, Ge Y, Zhou Q, Sealfon SC, Gingrich JA (2007) Hallucinogens Recruit Specific Cortical 5-HT $_2\text{A}$ Receptor-Mediated Signaling Pathways to Affect Behavior. *Neuron* 53:439–452.
- Griffiths RR, Johnson MW, Carducci MA, Umbricht A, Richards WA, Richards BD, Cosimano MP, Klinedinst MA (2016) Psilocybin produces substantial and sustained decreases in depression and anxiety in patients with life-threatening cancer: A randomized double-blind trial. *J Psychopharmacol* 30:1181–1197.
- Griffiths RR, Johnson MW, Richards WA, Richards BD, McCann U, Jesse R (2011) Psilocybin occasioned mystical-type experiences: Immediate and persisting dose-related effects. *Psychopharmacology (Berl)* 218:649–665.
- Griffiths RR, Richards WA, Johnson MW, McCann UD, Jesse R, Griffiths RR, Richards WA, Johnson MW, McCann UD (2008) Mystical-type experiences occasioned by psilocybin mediate the attribution of personal meaning and spiritual significance 14 months later. *J Psychopharmacol* 22:621–632.
- Griffiths RR, Richards WA, McCann U, Jesse R (2006) Psilocybin can occasion mystical-type

- experiences having substantial and sustained personal meaning and spiritual significance. *Psychopharmacology (Berl)* 187:268–283.
- Grob CS, Danforth AL, Chopra GS, Hagerty M, McKay CR, Halberstad AL, Greer GR (2011) Pilot study of psilocybin treatment for anxiety in patients with advanced-stage cancer. *Arch Gen Psychiatry* 68:71–78.
- Halberstadt AL, Chatha M, Klein AK, Wallach J, Brandt SD (2020) Correlation between the potency of hallucinogens in the mouse head-twitch response assay and their behavioral and subjective effects in other species. *Neuropharmacology* 167:107933.
- Halberstadt AL, Geyer MA (2018) Effect of hallucinogens on unconditioned behavior. *Curr Top Behav Neurosci* 36:159–199.
- Hasler F, Bourquin D, Brenneisen R, Bär T, Vollenweider FX (1997) Determination of psilocin and 4-hydroxyindole-3-acetic acid in plasma by HPLC-ECD and pharmacokinetic profiles of oral and intravenous psilocybin in man. *Pharm Acta Helv* 72:175–184.
- Hong IK, Chung ST, Kim HK, Kim YB, Son YD, Cho ZH (2007) Ultra fast symmetry and SIMD-based projection-backprojection (SSP) algorithm for 3-D PET image reconstruction. *IEEE Trans Med Imaging* 6:789–803.
- Jørgensen LM, Weikop P, Villadsen J, Visnapuu T, Ettrup A, Hansen HD, Baandrup AO, Andersen FL, Bjarkam CR, Thomsen C, Jespersen B, Knudsen GM (2016) Cerebral 5-HT release correlates with [11C]Cimbi36 PET measures of 5-HT_{2A} receptor occupancy in the pig brain. *J Cereb Blood Flow Metab*:1–10.
- Keller SH, Svarer C, Sibomana M (2013) Attenuation correction for the HRRT PET-scanner using transmission scatter correction and total variation regularization. *IEEE Trans Med Imaging* 32:1611–1621.
- Köhler O, Krogh J, Mors O, Benros ME (2016) Inflammation in Depression and the Potential for Anti-Inflammatory Treatment. *Curr Neuropharmacol* 14:732–742.
- Kornum BR, Knudsen GM (2011) Cognitive testing of pigs (*Sus scrofa*) in translational biobehavioral research. *Neurosci Biobehav Rev* 35:437–451.
- Leth-Petersen S, Gabel-Jensen C, Gillings N, Lehel S, Hansen HD, Knudsen GM, Kristensen JL (2016) Metabolic Fate of Hallucinogenic NBOMes. *Chem Res Toxicol* 29:96–100.
- Liao Y, Smyth GK, Shi W (2014) FeatureCounts: An efficient general purpose program for assigning sequence reads to genomic features. *Bioinformatics* 30:923–930.
- Löscher W, Witte U, Fredow G, Ganter M, Bickhardt K (1990) Pharmacodynamic effects of serotonin (5-HT) receptor ligands in pigs: stimulation of 5-HT₂ receptors induces malignant hyperthermia. *Naunyn Schmiedebergs Arch Pharmacol* 341:483–493.
- Ly C et al. (2018) Psychedelics Promote Structural and Functional Neural Plasticity. *Cell Rep* 23:3170–3182.
- MacLean KA, Johnson MW, Griffiths RR (2011) Mystical Experiences Occasioned by the Hallucinogen Psilocybin Lead to Increases in the Personality Domain of Openness. *J Psychopharmacol* 25:1453–1461.
- Madsen MK, Fisher PM, Burmester D, Dyssegaard A, Stenbæk DS, Kristiansen S, Johansen SS,

- Lehel S, Linnet K, Svarer C, Erritzoe D, Ozenne B, Knudsen GM (2019) Psychedelic effects of psilocybin correlate with serotonin 2A receptor occupancy and plasma psilocin levels. *Neuropsychopharmacology* 44:1328–1334.
- Martin DA, Nichols CD (2016) Psychedelics recruit multiple cellular types and produce complex transcriptional responses within the brain. *EBioMedicine* 11:262–277.
- McCarthy DJ, Chen Y, Smyth GK (2012) Differential expression analysis of multifactor RNA-Seq experiments with respect to biological variation. *Nucleic Acids Res* 40:4288–4297.
- Nichols DE (2016) Psychedelics. *Pharmacol Rev* 68:264–355.
- Quednow BB, Komater M, Geyer MA, Vollenweider FX (2012) Psilocybin-induced deficits in automatic and controlled inhibition are attenuated by ketanserin in healthy human volunteers. *Neuropsychopharmacology* 37:630–640.
- R Core Team (n.d.) R: A Language and Environment for Statistical Computing.
- Rho M, Wesselingh S, Glass J, McArthur J, Choi S, Griffin J, Tyor W (1995) A potential role for interferon- α in the pathogenesis of HIV-associated dementia. *Brain Behav Immun* 9:366–377.
- Ritchie ME, Phipson B, Wu D, Hu Y, Law CW, Shi W, Smyth GK (2015) Limma powers differential expression analyses for RNA-sequencing and microarray studies. *Nucleic Acids Res* 43:e47.
- Ross S, Bossis A, Guss J, Agin-Liebes G, Malone T, Cohen B, Mennenga SE, Belser A, Kalliontzi K, Babb J, Su Z, Corby P, Schmidt BL (2016) Rapid and sustained symptom reduction following psilocybin treatment for anxiety and depression in patients with life-threatening cancer: A randomized controlled trial. *J Psychopharmacol* 30:1165–1180.
- Sigurgeirsson B, Emanuelsson O, Lundeberg J (2014) Sequencing degraded RNA addressed by 3' tag counting. *PLoS One* 9.
- Sureau FC, Reader AJ, Comtat C, Leroy C, Ribeiro MJ, Buvat I, Trébossen R (2008) Impact of image-space resolution modeling for studies with the high-resolution research tomograph. *J Nucl Med* 49:1000–1008.
- Tang H, Mayersohn M (2018) Porcine prediction of pharmacokinetic parameters in people: A pig in a poke? *Drug Metab Dispos* 46:1712–1724.
- Tyls F, Páleníček T, Horáček J (2014) Psilocybin - Summary of knowledge and new perspectives. *Eur Neuropsychopharmacol* 24:342–356.
- Tylš F, Páleníček T, Kadeřábek L, Lipski M, Kubešová A, Horáček J (2015) Sex differences and serotonergic mechanisms in the behavioural effects of psilocin. *Behav Pharmacol*:1.
- U.S. Department of Health and Human Services, Food and Drug Administration C for DE and R (2005) Guidance for Industry - Estimating the Maximum Safe Starting Dose in Initial Clinical Trials for Therapeutics in Adult Healthy Volunteers.
- Vandesompele J, Preter K De, Pattyn F, Poppe B, Roy N Van, Paepe A De, Speleman F (2002) Accurate normalization of real-time quantitative RT-PCR data by geometric averaging of multiple internal control genes. *Genome Biol* 3:1–30.
- Villadsen J, Hansen HD, Jørgensen LM, Keller SH, Andersen FL, Petersen IN, Knudsen GM, Svarer C (2017) Automatic delineation of brain regions on MRI and PET images from the pig. *J*

Neurosci Methods 294:51–58.

Vollenweider FX, Vollenweider-Scherpenhuyzen MFI, Bähler A, Vogel H, Hell D (1998) Psilocybin induces schizophrenia-like psychosis in humans via a serotonin-2 agonist action.

Neuroreport 9:3897–3902.

Wang L, Nie J, Sicotte H, Li Y, Eckel-Passow JE, Dasari S, Vedell PT, Barman P, Wang L, Weinshiboum R, Jen J, Huang H, Kohli M, Kocher JPA (2016) Measure transcript integrity using RNA-seq data. BMC Bioinformatics 17:1–16.

Wang L, Wang S, Li W (2012) RSeQC: Quality control of RNA-seq experiments. Bioinformatics 28:2184–2185.

Ye J, Coulouris G, Zaretskaya I, Cutcutache I, Rozen S, Madden TL (2012) Primer-BLAST: a tool to design target-specific primers for polymerase chain reaction. BMC Bioinformatics 13.

Yu G, Wang LG, Han Y, He QY (2012) ClusterProfiler: An R package for comparing biological themes among gene clusters. Omi A J Integr Biol 16:284–287.

Declarations of co-authorship

GRADUATE SCHOOL OF HEALTH AND MEDICAL SCIENCES
UNIVERSITY OF COPENHAGEN



PHD-THESIS DECLARATION OF CO-AUTHORSHIP

The declaration is for PhD students and must be completed for each conjointly authored article. Please note that if a manuscript or published paper has ten or less co-authors, all co-authors must sign the declaration of co-authorship. If it has more than ten co-authors, declarations of co-authorship from the corresponding author(s), the senior author and the principal supervisor (if relevant) are a minimum requirement.

1. Declaration by	
Name of PhD student	Lene Lundgaard Donovan
E-mail	lene.donovan@nru.dk
Name of principal supervisor	Gitte Moos Knudsen
Title of the PhD thesis	Epigenetic and pharmacological investigations of the pig brain In vivo and in vitro studies of [11C]Martinostat and psilocybin

2. The declaration applies to the following article	
Title of article	Imaging HDACs in Vivo: Cross-Validation of the [11C]Martinostat Radioligand in the Pig Brain
Article status	
Published <input checked="" type="checkbox"/>	Accepted for publication <input type="checkbox"/>
Date: 09 July 2019	Date:
Manuscript submitted <input type="checkbox"/>	Manuscript not submitted <input type="checkbox"/>
Date:	
If the article is published or accepted for publication, please state the name of journal, year, volume, page and DOI (if you have the information).	Molecular imaging and biology 2019 10.1007/s11307-019-01403-9

3. The PhD student's contribution to the article (please use the scale A-F as benchmark)	
Benchmark scale of the PhD-student's contribution to the article	
A. Has essentially done all the work (> 90 %) B. Has done most of the work (60-90 %) C. Has contributed considerably (30-60 %) D. Has contributed (10-30 %) E. No or little contribution (<10 %) F. Not relevant	
1. Formulation/identification of the scientific problem	C
2. Development of the key methods	B
3. Planning of the experiments and methodology design and development	B
4. Conducting the experimental work/clinical studies/data collection/obtaining access to data	B
5. Conducting the analysis of data	B
6. Interpretation of the results	B
7. Writing of the first draft of the manuscript	A
8. Finalisation of the manuscript and submission	A
Provide a short description of the PhD student's specific contribution to the article. Lene took part in nearly all the PET scans used in the present study, she produced all the in vitro data, and she conducted all the data analysis. She drafted the manuscript and finalized it for publication.	

Latest update of the declaration: December 2018

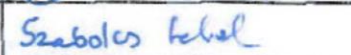
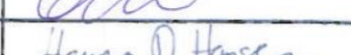
4. Material from another thesis / dissertationⁱⁱ

Does the article contain work which has also formed part of another thesis, e.g. master's thesis, PhD thesis or doctoral dissertation (the PhD student's or another person's)? Yes: No:

If yes, please state name of the author and title of thesis / dissertation.

If the article is part of another author's academic degree, please describe the PhD student's and the author's contributions to the article so that the individual contributions are clearly distinguishable from one another.

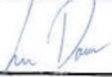
5. Signatures of the co-authorsⁱⁱⁱ

	Date	Name	Title	Signature
1.	17-Feb-2020	Janus Magnussen	M.Sc.	
2.	17-Feb-2020	Agnete Dyssegaard	M.Sc.	
3.	17-Feb-2020	Szabolcs Lehel	PhD	
4.	17-Feb-2020	Jacob Hooker	PhD	
5.	26/2/2020	Gitte Knudsen	DMSc.	
6.	17-Feb-2020	Hanne Hansen	PhD	
7.				
8.				
9.				
10.				

6. Signature of the principal supervisor

I solemnly declare that the information provided in this declaration is accurate to the best of my knowledge.
 Date: 26/2/2020
 Principal supervisor: 

7. Signature of the PhD student

I solemnly declare that the information provided in this declaration is accurate to the best of my knowledge.
 Date: 17-Feb 2020
 PhD student: 

Please learn more about responsible conduct of research on the [Faculty of Health and Medical Sciences' website](#).



PHD-THESIS DECLARATION OF CO-AUTHORSHIP

The declaration is for PhD students and must be completed for each conjointly authored article. Please note that if a manuscript or published paper has ten or less co-authors, all co-authors must sign the declaration of co-authorship. If it has more than ten co-authors, declarations of co-authorship from the corresponding author(s), the senior author and the principal supervisor (if relevant) are a minimum requirement.

1. Declaration by	
Name of PhD student	Lene Lundgaard Donovan
E-mail	lene.donovan@nru.dk
Name of principal supervisor	Gitte Moos Knudsen
Title of the PhD thesis	Epigenetic and pharmacological investigations of the pig brain In vivo and in vitro studies of [11C]Martinostat and psilocybin

2. The declaration applies to the following article	
Title of article	Effects of a single dose of psilocybin on behaviour, brain 5-HT _{2A} receptor occupancy and gene expression in the pig.
Article status	
Published <input type="checkbox"/>	Accepted for publication <input type="checkbox"/>
Date:	Date:
Manuscript submitted <input type="checkbox"/>	Manuscript not submitted <input checked="" type="checkbox"/>
Date:	
If the article is published or accepted for publication, please state the name of journal, year, volume, page and DOI (if you have the information).	

3. The PhD student's contribution to the article (please use the scale A-F as benchmark)	
<u>Benchmark scale of the PhD-student's contribution to the article</u>	
A. Has essentially done all the work (> 90 %) B. Has done most of the work (60-90 %) C. Has contributed considerably (30-60 %) D. Has contributed (10-30 %) E. No or little contribution (<10 %) F. Not relevant	
1. Formulation/identification of the scientific problem	B
2. Development of the key methods	B
3. Planning of the experiments and methodology design and development	A
4. Conducting the experimental work/clinical studies/data collection/obtaining access to data	B
5. Conducting the analysis of data	B
6. Interpretation of the results	B
7. Writing of the first draft of the manuscript	A
8. Finalisation of the manuscript and submission	A
Provide a short description of the PhD student's specific contribution to the article. Lene planned and conducted all the in vivo experiments, she planned and facilitated the in vitro experiments, and she analyzed most of the data. Lene drafted the manuscript.	

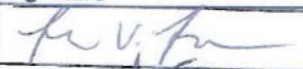
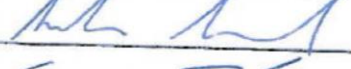
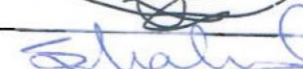
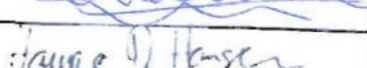
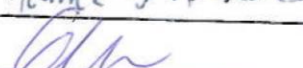
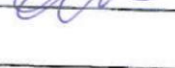
4. Material from another thesis / dissertationⁱⁱ

Does the article contain work which has also formed part of another thesis, e.g. master's thesis, PhD thesis or doctoral dissertation (the PhD student's or another person's)? Yes: No:

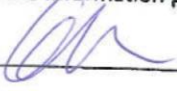
If yes, please state name of the author and title of thesis / dissertation.

If the article is part of another author's academic degree, please describe the PhD student's and the author's contributions to the article so that the individual contributions are clearly distinguishable from one another.

5. Signatures of the co-authorsⁱⁱⁱ

	Date	Name	Title	Signature
1.	26/2/2020	Jens Vilstrup Johansen	M.Sc.	
2.	25/02/2020	Nidia Fernandez Ros	B.Sc.	
3.	26/2/2020	Elham Jaber	PhD	
4.	26/2/2020	Kristian Linnet	Prof.	
5.	26/2-20	Sys Stybe Johansen	Ass.prof.	
6.	26/02/2020	Brice Ozenne	PhD	
7.	26/2/2020	Shohreh Issazadeh-Navikas	Prof.	
8.	25/2/2020	Hanne Demant Hansen	PhD	
9.	26/2/2020	Gitte Moos Knudsen	DMSc	
10.				

6. Signature of the principal supervisor

I solemnly declare that the information provided in this declaration is accurate to the best of my knowledge.
 Date: 26/2/2020
 Principal supervisor: 

7. Signature of the PhD student

I solemnly declare that the information provided in this declaration is accurate to the best of my knowledge.
 Date: 26/2/2020
 PhD student: 

Please learn more about responsible conduct of research on the [Faculty of Health and Medical Sciences' website](#).